# Design and Simulation of MEMS based Inertial Electromagnetic Harvester

Adnan Murtaza Danish

NUST201261230MCEME35512F

Supervisor

Dr. Muhammad Mubasher Saleem

DEPARTMENT OF MECHATRONICS ENGINEERING

COLLEGE OF ELECTRICAL & MECHANICAL ENGINEERING

NATIONAL UNIVERSITY OF SCIENCES AND TECHNOLOGY

ISLAMABAD

August, 2016

# Design and Simulation of MEMS based Inertial Electromagnetic Harvester

Adnan Murtaza Danish

NUST201261230MCEME35512F

A thesis submitted in partial fulfillment of the requirements for the degree of

MS Mechatronics Engineering

Thesis Supervisor:

Dr. Muhammad Mubasher Saleem

Thesis Supervisor's Signature:_____

DEPARTMENT OF MECHATRONICS ENGINEERING

COLLEGE OF ELECTRICAL & MECHANICAL ENGINEERING

NATIONAL UNIVERSITY OF SCIENCES AND TECHNOLOGY, ISLAMABAD

August, 2016

## Declaration

I certify that this research work titled "*Design and Simulation of MEMS based Inertial Electromagnetic Harvester"* is my own work. The work has not been presented elsewhere for assessment. The material that has been used from other sources it has been properly acknowledged / referred.

Signature of Student

Adnan Murtaza Danish

NUST201261230MCEME35512F

## Language Correctness Certificate

This thesis has been read by an English expert and is free of typing, syntax, semantic, grammatical and spelling mistakes. Thesis is also according to the format given by the university.

Signature of Student

Adnan Murtaza Danish

NUST201261230MCEME35512F

Signature of Supervisor

## Copyright Statement

## Acknowledgements

I am extremely thankful to my Creator Allah Subhana-Watala and Prophet (S.A.W.W) that you guided me throughout this work at every step and for every new thought which You setup in my mind to improve it. Indeed, I could have done nothing without your priceless help and guidance. Whosoever helped me throughout the course of my thesis, whether my parents or any other individual was Your will, so indeed none be worthy of praise but You.

I am profusely thankful to my beloved parents who raised me when I was not capable of walking and continued to support me throughout in every department of my life.

I would also like to express special thanks to my honorable supervisor Dr. Muhammad Mubasher Saleem for his too much help throughout my thesis and his guidance at every step was too much beneficial for me. I can safely say that I haven't get any guidance and devotion in such depth from anyone else in my entire phase of study.

I would also like to pay special thanks to Dr. Khalid Ashraf for his tremendous support and cooperation. Each time I got stuck in something, he came up with the solution. Without his help I wouldn’t have been able to complete my thesis. I appreciate his patience and guidance throughout the whole thesis.

I would also like to thank Dr. Umar Shahbaz Khan, Dr. Mohsin Islam Tiwana and Lt. Col Dr. Adnan for being on my thesis guidance and evaluation committee and express my special Thanks to them for their help.

Finally, I would like to express my gratitude to all the individuals who have rendered motivation and valuable assistance to me.

*Dedicated to my Father & Mother*

*and Michel Faraday for inventing principle of Electromagnetic Induction and Nicola Tesla for his work on wireless transmission of electricity.*

## Abstract

Due to the advent in low power wireless electronics, devices are becoming compact and power requirements have reduced to the levels of microwatts. So intensive research is being carried on to scavenge energy from ambient sources found in environment to power portable electronics and ultra-low power wireless sensors by external sources**.** This thesis investigates the development of one of the technique of harvesting electrical energy from vibrations based on the Faraday's law of electromagnetic induction. Focus was to design a harvester completely compatible with MEMS fabrication techniques, can work on multiple frequencies and to take advantage of magnetic flux distribution of an array of permanent magnets in the specific direction (also called Active side) by using Halbach Array of magnets. The micro fabricated coils connected in series with each other are placed towards an Active side. Finally, the proposed design resulted in a maximum output voltage of 18mV with a maximum power of 0.53nW at a resistive load of 98kΩ and frequency of 40.7Hz.

.

# Table of Contents

## List of Figures

## List of Tables

## List of Parameters

| Name | Expression | Value | Description |
|---|---|---|---|
| Lmx | 8[mm] | 0.008 m | Total x length of magnets |
| Lmy | 5[mm] | 0.005 m | Total y length of magnets |
| f | 48.9[Hz] | 48.9 Hz | Frequency |
| T | 1/f | 0.02045 s | Period |
| Br | 1.4[T] | 1.4 T | Remanent flux density in PM |
| dis | 30[um] | 3E−5 m | Distance (gap) between magnets and coils |
| Lcx | Lmx/4 | 0.002 m | x-length of coil |
| Lcy | Lmy | 0.005 m | y-length of coil |
| xc | Lmx/2 | 0.004 m | x-coordinate of coil border (half length in x direction) |
| yc | Lmy/2 | 0.0025 m | y-coordinate of coil border (half length in y direction) |
| Nc | 52 | 52 | Number of turns in each real coil |
| Ntotal | Nc*8 | 416 | Total number of turns |
| c | Lmy/16 | 3.125E−4 m | Width of each magnet |
| fac | 2 | 2 | Factor of nominal frequency for filter |
| omegan | 2[rad]*pi*f | 307.25 rad/s | Nominal frequency |
| omegac | fac*omegan | 614.5 rad/s | Cut-off angular frequency (for filter) |
| RC | 98[kohm] | 98000 Ω | Resistance of coils |
| LC | 0.00353[H] | 0.00353 H | Inductance of coils |
| RF | RC | 98000 Ω | Resistance in filter |
| CF | 1/(RF*omegac) | 1.6606E−8 F | Capacitance in filter |
| RL | RC | 98000 Ω | Resistance of load |
| CL | 1/(LC*omegan^2) | 0.0030009 F | Capacitance of load |

# Chapter 1. INTRODUCTION

Electrical energy has become the key resource in development of any nation. Since the dawn of industrial age humans are constantly searching for the reliable energy sources. As the time passed relying on electrical energy has become more and crucial as well as a constant threat to the earth's ecology. Therefore, a race of renewable power sources has been started. Many natural resources have been employed to extract energy like solar, wind, water and thermal. But these energy providers are bulk in size, expensive and need constant maintenance. So to power up low consumption devices like low power electronic circuits in remote areas such sensor networks, different energy harvesting techniques were proposed so far.

## 1.1 Energy Harvesting

The term, Energy harvesting was used in literature to describe the process of photosynthesis in plants due to sunlight. Now this term readily used for extracting energy from ambient resources like solar radiation, motion of natural of artificial objects and thermal processes in nature [1].
Energy harvesting is basically a process of harnessing environmental sources to generate electricity on micro level. This energy can be efficiently utilize in sensors and other low power circuits which require the power of few micro watts [2]. Energy harvester have many uses from military applications to wearable and medical devices.

### 1.1.1 Background

The basis of energy harvesting is directly derived from Faraday's Law of electromagnetic induction in 1831 [3]. This law of electromagnetic induction provides the possibility to convert mechanical energy in electrical energy. Energy harvesting system works on the principle of change of flux in the coil of a harvester when it oscillates due to the ambient motion from environment. The induced voltage and energy will then be supplied to attached load. Energy harvesters find their applications in many devices and can be used on several vibrating sources. Electro Magnetic Micro Harvesters will be discussed in detail in later sections.

## 1.2 Micro Energy Harvesters

Micro Energy harvesters are considered as one of the best wireless power suppliers. They have the same importance as that of wireless communication because of the several reasons like portability, no need of replacement of batteries, reduced installation cost and continuous supply of power to remote locations. Previously in such applications batteries were used as power supplier but due to their several disadvantages, efforts are being made to replace batteries by micro energy harvesters. Also an increase in mobile electronic devices is giving rise to the need of wireless sources of power Due to this reason, mechanical vibrations are getting considerable amount of interest of researchers as a source of power supply. Since environment supply an ample amount of vibrations, these vibrations can be converted into useful amount of electrical energy by using self-contained and maintenance free energy harvesters. A common example of this phenomenon is the utilization of continuous vibrations during the operation of a large range of industrial machinery such as electrical motors, compressors, turbines etc. Micro Level vibration energy harvesters can be installed on these machines to power up the sensors which can monitor condition and health of the machine. Another common example of this type of usage is in the automotive industry for automatic monitoring of tire pressure[4] [5].

### 1.2.1 Types of Micro Energy Harvester

In this thesis, vibration-based energy harvesters are of major consideration. These type of micro generator consist of inertial mass attached to the spring. This inertial mass vibrates in to and fro motion relative to frame when subjected to vibration. This motion of inertial mass crosses the magnetic flux and generate electricity as a result. Based on the above discussion, micro energy harvesters can broadly categorize in three types;

1) Piezoelectric Energy Harvesters
2) Electrostatic Energy Harvesters
3) Electromagnetic Energy Harvesters

#### 1.2.1.1 Piezoelectric Energy Harvesters

The piezoelectric energy harvesters are of much interest from the last two decades. Piezoelectric energy harvesters work on the principle of strain generation in piezoelectric materials such as PZT or PVDF. In principle, when vibration from environment deform the piezoelectric material, a

potential difference will be generated across the terminals. The produced potential difference forms a damping force which is proportional to relative velocity in the structure made of piezoelectric material. This property of voltage generation when subjected to strain, is due to sudden charging within the crystals, polycrystalline ceramics and piezoelectric polymers.

The most basic design of piezoelectric harvester is like cantilever beam mentioned in literature [6]. It is manufactured by depositing thin layer of piezoelectric material on micro fabricated cantilever beam with lump mass at the free end of the beam. The lumped mass controls the frequency of the beam when subjected to vibration. Figure 1.1 depicts how piezoelectric harvester works in principle [7].

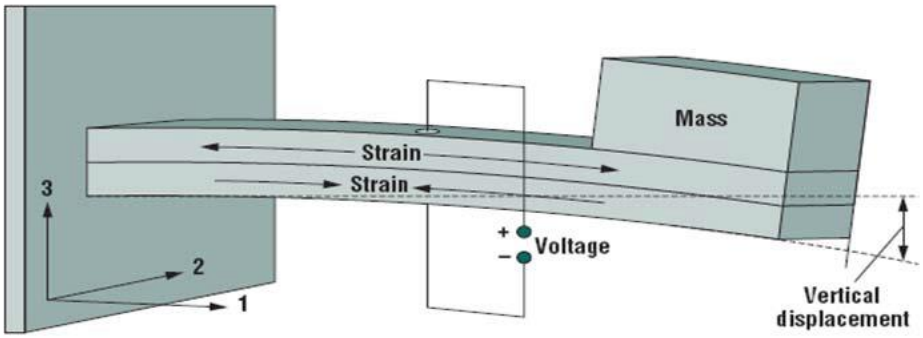


Figure 1.1: Conceptual design of Piezoelectric Energy harvester [7].

There are two type of operations that can be performed on a piezoelectric harvester. From Figure 1.1 it is clear that force can be either applied along with axis 3 and axis 1. The generated output voltage will obtain across the face perpendicular to axis 3 and a simple resistive load can be applied to estimate the amount of power or optionally a storage capacitor can also be used in cases where data need to be received and transmitted for few moments and this cycle continues [8]. Also composite beam piezoelectric harvesters are most commonly used and are of much interest due to their wide no of applications and effectiveness [9].

However piezoelectric generators are very difficult to manufacture using standard MEMS fabrication methods. These devices perform on very low vibration and they are vulnerable to mechanical defects like creep and fatigue over accidental or repetitive/cyclic loading and voltage breakdown at high frequencies [10]. Also piezoelectric harvesters may suffer from charge leakage at low operating frequencies [11] along with the issues of high internal resistance, low output current and low power density make them less suitable. [12][13][14].

### 1.2.1.2 Electrostatic Energy Harvesters

An electrostatic energy harvester works on the principle of gap variation between two conductive plates resulting in the change of capacitance. The gap is filled with some dielectric, in most cases air. The capacitance between two plates changes with when the conductive plates moves relative to each other due to vibration. This results in increase in stored energy in the harvester [15]. Also electrostatic transducers are much suitable at low frequencies and their integration with microelectronics is also feasible.

In electrostatic energy harvesters, configuration of capacitance of the system will decide to be a voltage source or a current source. In either of the case, one parameter either voltage or current is kept as constant. Keeping the charge constant across the capacitor, the device will act as voltage source. In this condition an additional charge source is required to keep the charge constant. However, if the potential difference is kept constant then the device will act as charge source. In this case, an additional voltage source will be required to keep the voltage constant. There are three mechanical configurations to use the capacitance as energy.

In-Plane overlap conversion

In-Plane gap closing conversation

Out-of-plane gap closing conversation

All these conversations can be seen in figure below

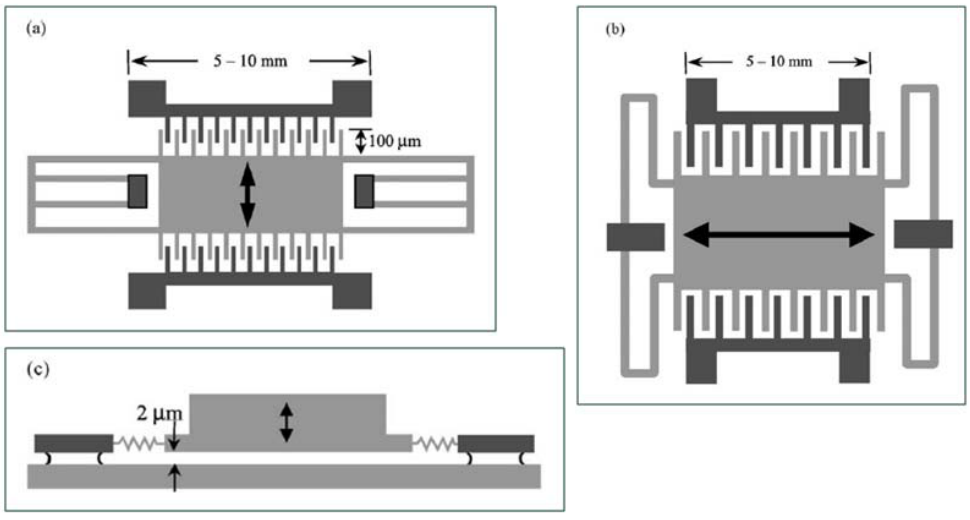


Figure 1.2: (a) In-Plane Overlap. (b) In-Plane Gap Closing. (c) Out-of-Plane Gap Closing [16].

But electrostatic harvesters are effective at microscale when they are employed for actuation purposes but their results are poor when used as generators [17] Another issue of electrostatic harvesters is their preliminary requirement of an additional source of voltage to pre-charge [15], however in many harvesters this problem is over-come by the usage of electrets [18]. Also electrostatic harvesters are much feasible for the use at low frequencies and low stiffness applications due to their low losses [10] [19].

#### 1.2.1.3 Electromagnetic Energy Harvesters

Electromagnetic Micro Energy Harvesters (EMEHs) works on the principle of Faraday's Law of Electromagnetic Induction. According to Faraday's Law when a conductor moves in a magnetic flux, a potential difference will be created on the ends of inductor.

EMEHs produce electricity due to the motion of coil in the magnetic field of a permanent magnet. Normally, coil could be a wounded wire over an insulator or just planer wires over an insulator. When EMEH is supplied by some vibration from an ambient source, either the coil or magnets move relative to each other, voltage will be induced across the ends of the coil. In the simplest configuration, either the magnet of the coil is suspended close to each other. The spring is attached to frame. When vibration occurs either magnet or coil moves relative to the frame of EMEH. Mechanically it is a mass spring system which is also vulnerable to mechanical damping due to air resistance, material stiffness and relative inertias. However electrical damping also occurs as a result of current passing through the inductor. Further information related to EMEHs will be discussed in detail in Chapter 2 of this reports. Detailed literature review supported with schematic and models has been discussed.

The advantage of EMEH over other discussed MEHs is that it doesn't require separate voltage source like electrostatic harvesters nor it is subjected to creep and fatigue like in piezoelectric energy harvesters. EMEHs provides higher energy densities. They are less vulnerable to damages that's results due to sudden spike in vibration pattern or excessive loadings. Due to parallel spring configuration no mechanical stops should be needed. Mechanical stops in MEMS fabrication is a critical issue [20].

### 1.2.2 Advantages and Disadvantages

#### 1.2.2.1 Advantages

a. Can generate voltage < 1 volt even on very smaller size.
b. Can perform over longer period of time than conventional batteries
c. Can be manufactured using standard MEMS fabrication technology
d. Can perform on very low to very high frequencies

#### 1.2.2.2 Disadvantages

a. No standardization so far in this technology
b. No specific measure of parameters
c. Very few commercially available energy harvesters

### 1.2.3 Application of Micro Energy Harvesters

a. Wireless sensor networks
b. Bio Medical Implants
c. Condition and Health monitoring of Machinery
d. Human Powered Devices
e. Wearable Gadgets
f. Health Monitoring in Humans
g. Structural Monitoring

## 1.3 Motivation

Micro Electro Mechanical Systems (MEMS) is the emerging technology of this age. Even in its dawn, MEMS find its path in almost every field of technology, from medical sciences to robotics to energy generation systems. It has been three decades, since the initiation of this technology, still a lot of vacuum is prevailing to fill by the researchers. MEMS is the future of every technology and it's just matter of years that MEMS can be seen in every walk of life.

One of the remarkable application of MEMS are micro level energy harvesters. These harvesters provide very low power but can easily be used to power up sensors, condition monitoring systems

and wireless electronics. They have found to be a very good replacement of conventional batteries and can be installed on remote locations. They harvest energy from ambient energy sources from environment thus require no maintenance or replacement over longer time. Observing these benefits, there is a huge need to work on such EMEHs, which will accordingly lead to some reliable solution for such applications.

## 1.4 Methodology

The course of this research will start with detail literature survey. During the literature review, main focus will be on exploring different mechanism of energy harvesting and types of electromagnetic energy harvesters (EMEHs). After having complete understanding of EMEHs, focus will come down to developing a novel mechanism for Electromagnetic Energy Harvesting and establish state-of-art.

Once the conceptual design will be cleared up, a complete design will be modeled in as a solid model. This task will comprise of creating a solid model for representation of complete design and a simplified model that will be used for Finite Element simulation. Afterward a thorough electromagnetic simulation will be performed in finite element software suite. Derived results will be analyzed and compared with literature. If the results will not up to the mark, few design provisions will be adapted, more preferably changing in magnetic array. In the end final model with complete analysis of novel Electromagnet Energy Harvester will be represented. Figure 1.3 provides comprehensive layout of research activities.

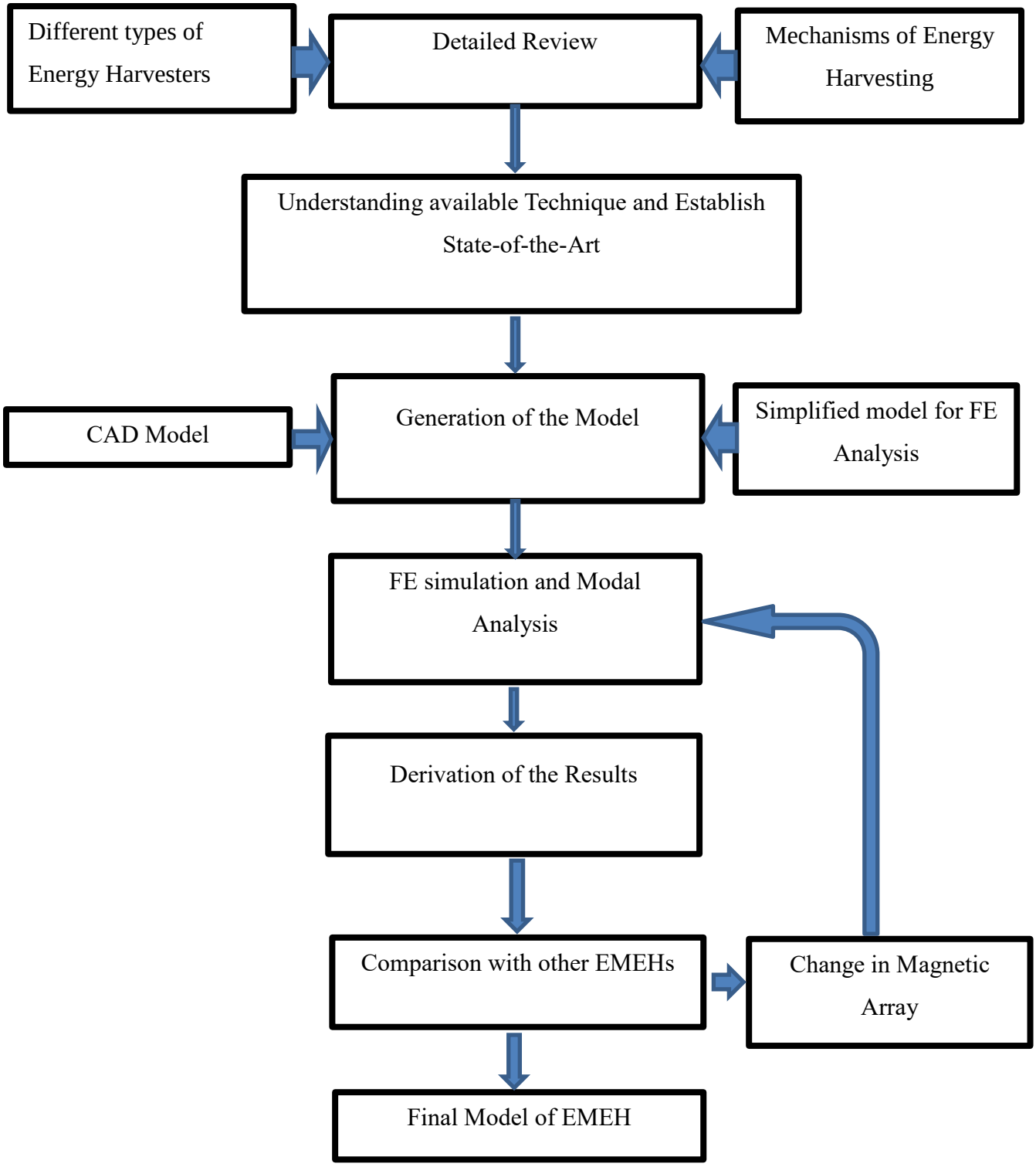


Figure 1.3: Flowchart of Research Activities

# Chapter 2. Literature Review

Supply of power through wireless devices are of prime importance and very good replacement of batteries. From the years, significant amount of research has been done in this regard. Energy harvesters are very promising devices in providing wireless technology. Energy harvesters worked on the principle of extracting energy from ambient vibrating source. Energy harvesters finds various application in remote energy consumptions devices like medical implants, wearable computing etc. [21] [21]

Studies indicate that utilization of wireless energy supply system in many applications like medical, industry and military. Usage of such devices minimize the need of external power supplies and batteries. These energy harvesters scavenge energy from the atmosphere ambient sources like temperature, light and vibrations. Vibration is the most promising source in this regard. Because it comes in many forms with abundance like human movement, vehicular motion and seismic vibrations [22].

This study discusses the energy harvesting system based on up-frequency concept. This system generates the electricity through the electromagnetic induction using mechanical movement of the coil in the magnetic field. System consist of top and bottom resonating plates connected with soft springs which damps the ambient vibrations from the source. Operating frequency of the system is between 10-100 Hz ambient frequencies. Simulation results of the system reported the maximum output voltage 6mV and power of 120nW however on micro implementation generates the power of 3.97 µW at 25 Hz ambient frequency [21]. Figure 2.1 indicates the working model of the said harvester.

Another study has been described by the same group of researchers and they successfully able to improve the previous design using a single cantilever at the frequency of 95Hz with the output voltage of 0.57 mV and power of 0.25 nW with the size of 8.5 x 7 x 2.5 mm2 [23].

Another research shows a slightly different approach using same concept of up-conversion of low frequencies. In this system power generation due to the planer motion by using magnet on the low frequency plane and the coils on the high frequency plane. Macro-scale prototype of the said system gives the output of 5.1 µW and the maximum voltage of 11.1mV. However on conversion

to micro electromechanical systems (MEMS), promised the power of 119 nW and output voltage of 15.2 mV with the size of 10 x 8.5 x 2.5 mm2 [22].

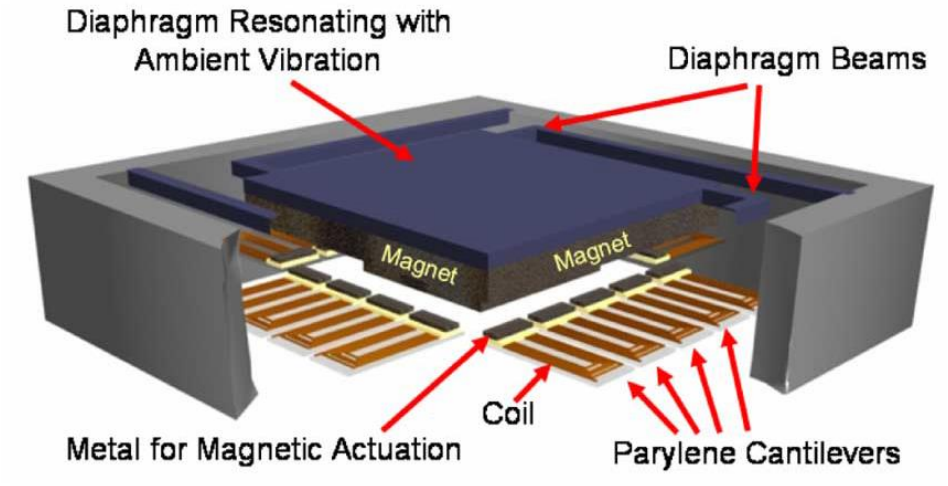


Figure 2.1: 3D model of Micro scale Generator[21]

A novel technique has been introduced by Zorlu et al. using the same concept of up-conversion method for low frequencies. In this study, a magnet has been mounted on a vibrating diaphragm and the coil has been place on a cantilever with hinge that first restrict the motion of cantilever and produce tension the beam and then get released with a jerk and starts vibrating. Figure 2.2 shows the schematic for the discussed EMEHs.

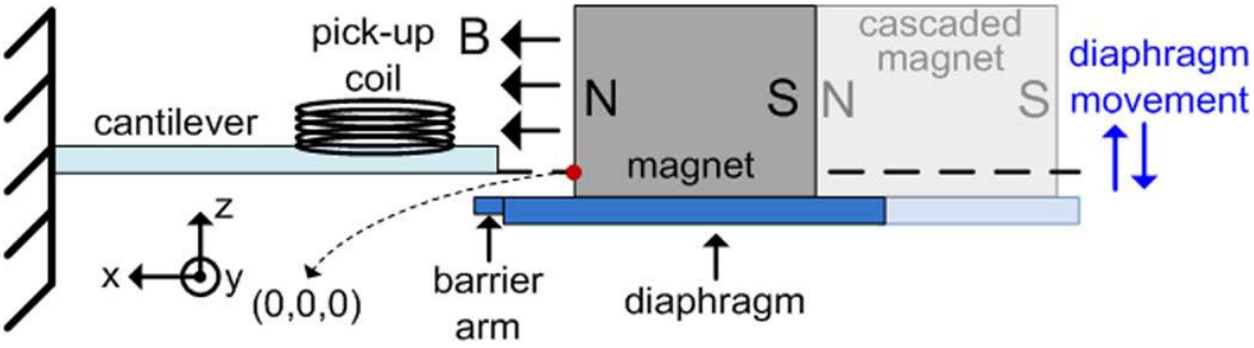


Figure 2.2: Electromagnetic Harvester using magnets mounted on diaphragm. [24]

This method converts the low ambient frequency into higher external frequencies with enhances the efficiency of the system. This method can also be adopted for the piezoelectric and electrostatic type of energy harvesters.

However, wearing of the tip of cantilever due to friction and cyclic collision is due which is the short coming in the design. This wearing of the tip is limiting factor of complete life of the

harvester. Resilience and durability of the cantilever tip can be enhanced by proper heat treatment or some coating technique. This energy harvester has been tested to give 88.6 mV and 544.7 µW with the power density of 184 µW /cm3. This has been achieved by up-converting the ambient frequency (>10 Hz) to 394 Hz. The volume of this harvester has been reported is 2.96 cm3 [24].

Another a relatively sophisticated vibration based energy harvesting system has been introduced by Arian et al. Proposed system has dual rail, high efficiency system. This system consists of an energy harvester and a PCB mounted with discrete diodes, two capacitors for external output storage and a custom powered ASIC. System converts the kinetic energy into electrical energy through an energy harvester, in which induced voltages from both coils which then rectifies in a bias generator network. Afterwards network converts and step-up the AC into two DC voltages which is saved in the capacitors which is then converted into Dual Rail DC and stored in the external capacitors. All this circuitry is compacted on a single PCB below the harvester module. This system is the size of C-type battery (16cm3). The size comparison can be seen in Figure 2.3. The power density of the system 6.06 micro W/cm3 at 8 Hz vibration. The system delivers the power of 54 µW [25].

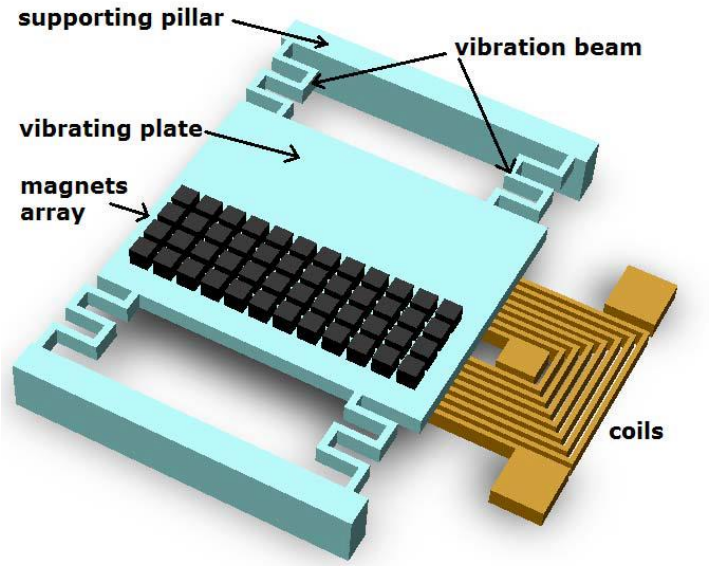


Figure 2.3: EMEH with a series coil harvester [14]

In 2001, a very simple micro level energy harvesting system has been designed. The working principle of this system is based on Faraday's Law. System consist of cantilever with the housing, a magnet has been placed on the beam which provides the magnetic field and a fixed coil. The coil

cuts the magnetic flux and converts mechanical energy into electrical energy. Operating frequency of this system was 320 Hz with the size of 240 mm3 and output power was 1mW. [26].

Another study indicates a simpler yet useful design of micro level energy harvester which can work on frequency range from 50-300 Hz. The magnetic generator uses Neodymium iron Boron (NdFeB) magnets fixed on a steel beam which can vibrate on different frequencies by just adjusting the length of the beam. Design of generator depicts that It can work on resonance frequencies which can be tuned easily to match the frequencies of the environment. This model has been prototyped and tested on a shaker table. However output power and voltages aren't disclosed in the literature [27].

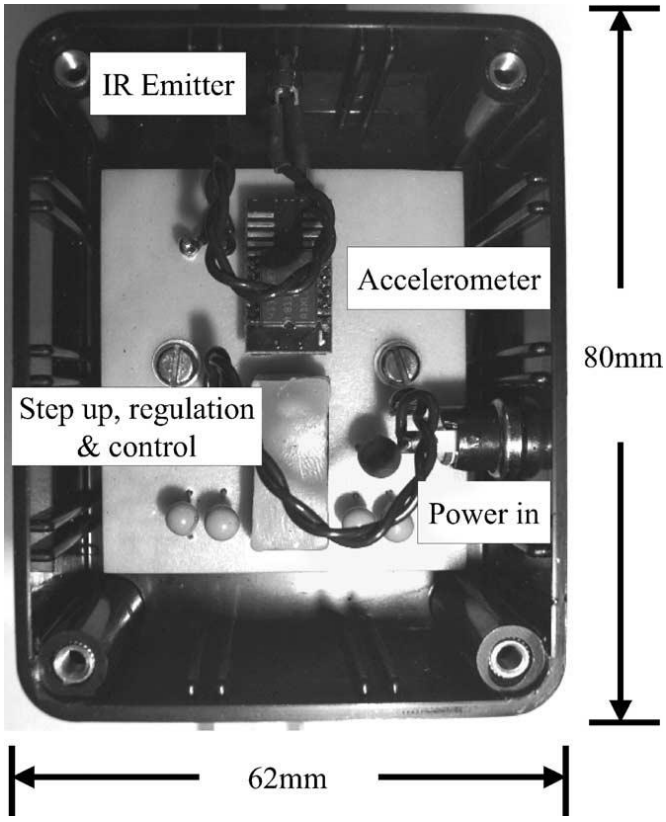


Figure 2.4: Layout of the prototype [27]

Another study proposed two prototype working on the same principle of harvesting energy from ambient vibration source for powering remote accessible sensors and their data transmission. One prototype is consisting of torus magnets and the coil is mounted on cantilever. Coil has been mounted to cut the magnetic field of magnets on vibration of cantilever. However the second prototype has four magnets with the same topology, shown in Figure 2.5. Later one has been tested

on top of engine block of 5-years Volkswagen Polo. The average power produced by the generator was 157 µW [28].

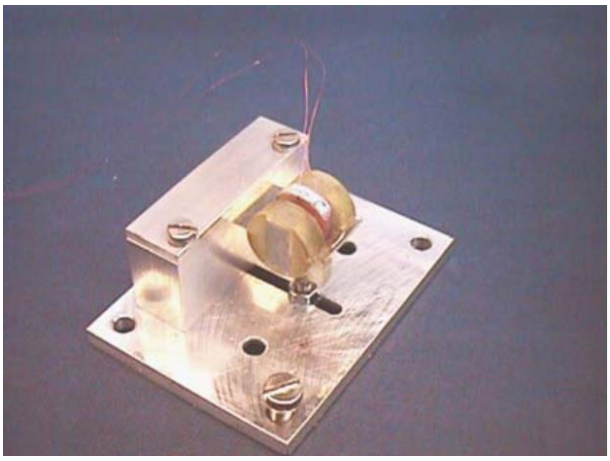

Figure 2.5: Prototype of cantilever based EMEH.

Researcher at University of Southampton, developed a cantilever based micromechanical energy harvester. This energy harvester can function on ambient frequencies as low as 50-60 Hz. The harvester design comprises of four magnets mounted on a cantilever producing constant magnetic flux through the coil as the cantilever vibrates. This energy harvester intent for an air compressor which generates ambient frequency of up to 60 Hz. In this study, first FE simulation has been performed using commercial FEA package. Later on experimental analysis has also been performed. This research paper then summarizes and compares the result of both simulation and experimental results, Experimental results are 25 % lower than the simulation results which mainly due to assembly tolerances in the actual device. Mean output voltage generated b said device is 87mV and power of 17.8 µW [29].

Another study highlights the usage of low power MEMS based energy harvesters. It has been stated that the current advances in Very Large Scale Integrated Circuits reduces the load of network sensors from mill watts to micro watts. This advancement can remove the batteries as a power source with micro level energy harvesters. These energy harvesters harness the energy from atmosphere using a vibration source. This research developed a theory based design and evaluate it using simulation of electromagnetic harvesters using electroplated micro magnets. Electromagnetic finite element solution has been utilized to calculate the voltage and power which is 55 mV and 70 µW respectively, also shown in **Error! Reference source not found.** [30].

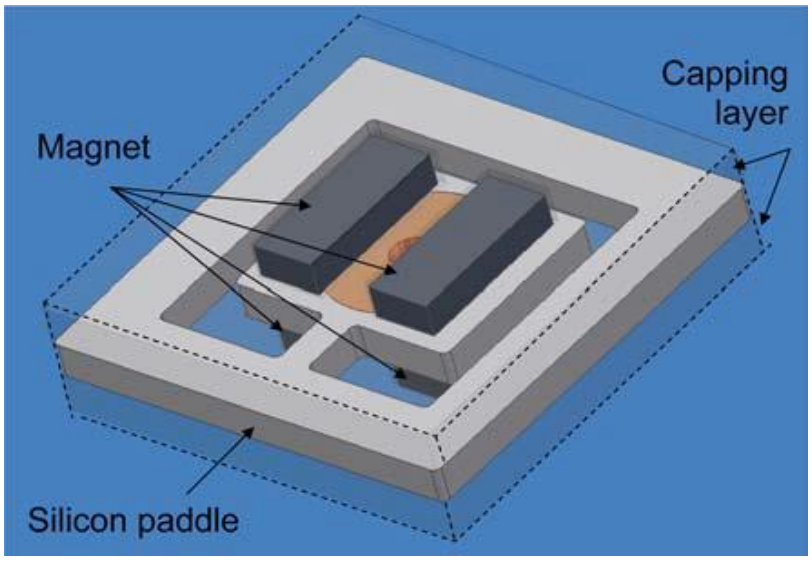


Figure 2.6: EMEH manufactured by Micro Machined Silicon [31]

Koukhareno et al. proposed a design of electromagnetic energy harvester in which the electromagnets are fixed however the coil is vibrating laterally. This design works on the principle of electromagnetic transduction method. This device operates at very high frequencies ranging from 1.6 - 9.5 kHz generating the peak voltage of 0.7 – 4.15 V and maximum output power of 104 nW [31] [32].

Torah et al. successfully design and implement a micro level energy harvester harnessing energy from ambient power source. This design has been tested and found sufficient to continuously support a radio-frequency (RF) based accelerometer. Power output of the system was 45 µW with a volume of approximately 150 mm3 [33].

Despite the designing, comparison studies has also been performed by several researchers [34], [35]. In the proposed paper, studies indicate that scaling has the significant effect on the power generation capabilities. Beeby et al. [35] study the effect of scaling from macro to micro level energy harvester power density and found that macro scale energy harvesters exhibit the power density of 2615 nW/mm3. However micro level energy harvester gives the power density of 47 nW/mm3. This study also indicates the difficulty in acquiring ample amount of electromagnetic coupling due to the reduction in size of generator.

Another study indicates the more promising development in the field of energy harnessing devices from environment. Beeby et al. developed a micro electromagnetic harvester with the volume of just 0.15 cm3. In the design phase the, some properties of the harvesters have been optimized to

attain more prominent and practical results. This design employ four laser sintered NdFeB magnets mounted on an etched cantilever using cyanoacrylate as bonding material. The circuit has also been coated with zinc which is used to couple the magnetic flux between top and bottom magnet. This harvester has capability to produce 46 µW utilizing the vibration frequency of 52 Hz. The power density of this generator is 307 µW/m3 [36].

Despite the last decade, in recent years, advancements in the MEMS technology give rise to next generation of vibration based energy harvesters. Tao et al. developed a novel mechanism, an adjustable lumped mass coil system in which the harvester can be tuned between frequencies using only 2 DOF configuration. That mechanism gets fabricated using micro machining on a silicon wafer using DRIE technique (double-sided deep reactive-ion etching).

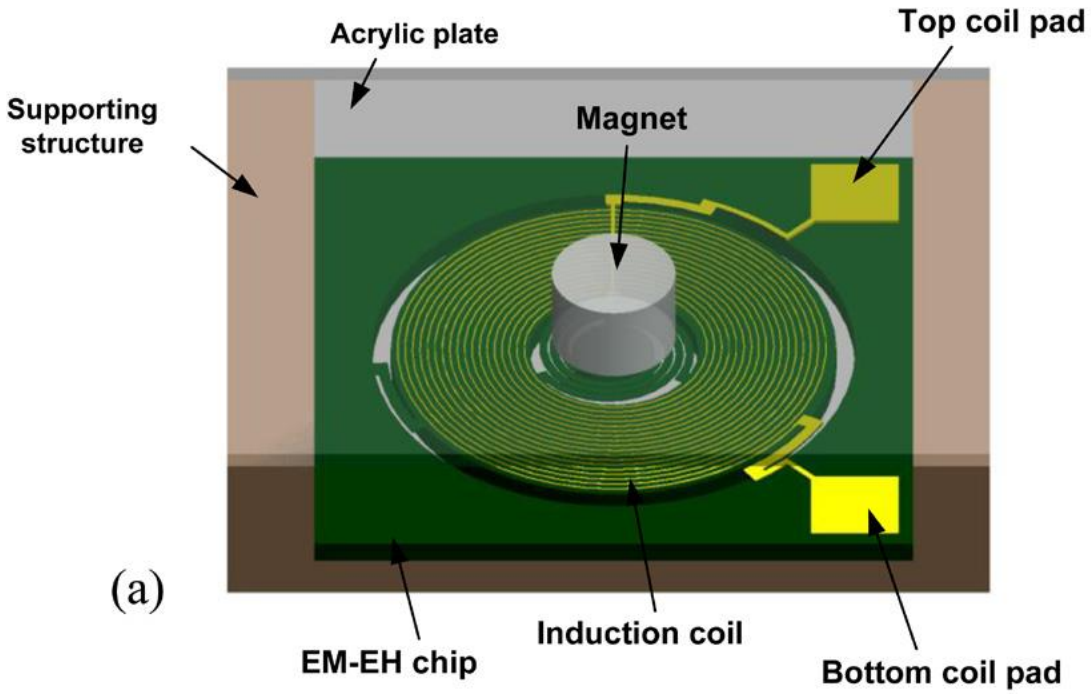


Figure 2.7: Two DOF Electromagnetic Harvester [37]

Usage of this fabrication technique results in very light weight energy harvester i.e. 0.12g. In this proposed research, configuration is in such a way that a permanent magnet is concentrically fixed in the center of a coil on a supporting plate. However the coil has been vibration around the magnet with both connectors are on either side of the coil (top and bottom side), as shown in Figure 2.7. Detailed finite element analysis and electromagnetic analysis has also been done. The power output of the said device is 0.96 nW with the power density of 2.30 x 10-7 W/ cm3 g2 [37].

Above discuss power outputs are seemingly more promising than the other related researches in recent year. In 2015, a research indicates the power output of 5.5 × 10−10 W using the frequency of 400 Hz with normalized power density of 6.1 × 10−11 W /cm3 g2 [38]. Few other research shows the power output of 5.5 × 10−9 W, 4.9 × 10−9 W, 6.6 × 10−9 W with the frequency of 840, 190 and 113 Hz respectively [23], [39], [40].

Yamaguchi et al. presents a novel electromagnetic vibration based energy harvester. Design optimization tools has also been employed to improve the performance of the harvester. In the proposed design the same NdFeB magnets fabricated on Si-Corrugated structure. For improving the harvester power generation rigorous FE analysis has been performed on the trench pitch. Parameters like space ratio and trench pitch has been optimized. On experimentation, stated design produce voltage of 2.65 mV and power of 7.60 nW [41].

In another presented design, a novel completely MEMS based harvester was fabricated in which magnets were sputtered in the silicon substrate trenches and the coils were fabricated on separate substrate and both substrates were then bonded. The coils connected in series were employed in this design. This harvester resulted in output power of 0.12nW but this device had an issue of oxidation of micro magnets [40]. So an improved version of the device was fabricated and the magnets were covered by a polyimide material to prevent the oxidation and the output power improved to 0.760nW [42].

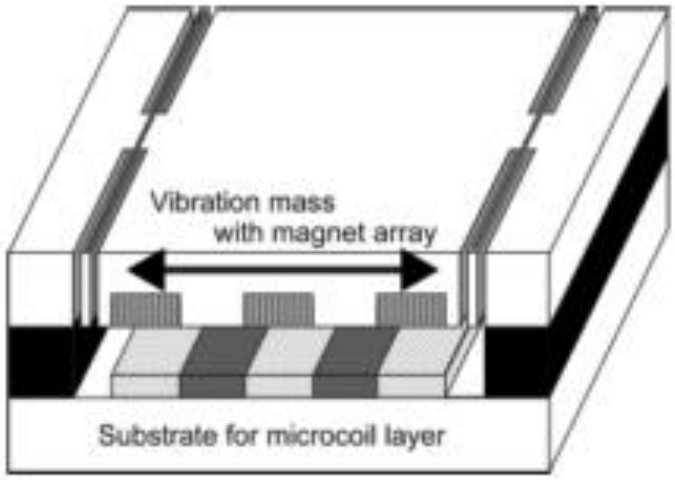


Figure 2.8: MEMS fabricated EMEH [42]

| S. No. | Year | REFERENCE | Frequency Hz | Dimensions | Base Acc., g | Voltage | Attached Load | Power | Coil Turns (T) & Resistance |
|---|---|---|---|---|---|---|---|---|---|
| 1. | 1995 | Williams & Yates [44] | 70, 330 | 5x5x1mm$^3$ | | | | 1uW, 0.1mW | |
| 2. | 1997 | Shearwood & Yates [45] | 4.4kHz | | | | 39Ω | 0.3uW | |
| 3. | 1998 | Rajeevan & Anantha [46] | 94 | | | 180mV-p | 10 Ω | 400 uW | |
| 4. | 2001 | Ching, Wong et al. [47] | 60 - 100 | 1cm$^3$ | | 2 - 4.4V p-p | 1000Ω | 200-830uW rms | |
| 5. | 2001 | El-Hami, Beeby et al. [26] | 320 | 240mm$^3$<br>10.9x3x5.2 | | | 0.28 Ω | 1mW/0.53mW-Rl | 0.28 Ω |
| 6. | 2001 | Williams, Yates et al. [48] | 0.1-10Mhz<br>4 MHz-p | 6mm = Lappx<br>0.7mm=Tappx | | Few mV | 39 Ω | 0.43 uW | 13T, 31 Ω |
| 7. | 2004 | Beeby et al. [49]<br>(2 Coil types, F & Bulk) | 100 Hz device<br>6.4, 12.6, 9.5k (B) | | | 0.38, 0.76, 0.57Vnl | | | 71T, 77 ohm (F)<br>309T, 109 ohm |
| 8. | 2004 | Jones, Beeby et al. [50] | A = 322 Hz | A= 0.84cm$^3$<br>B= 3.15cm$^3$ | | B=250mV | A = 0.6 Ω | A= 37-180uW<br>B= 3.9mW-p, 157uW-Avg | |
| 9. | 2005 | Beeby et al. [51] | 9.8, 7.1, 4.7 kHz | 100mm$^3$ | 1g | 9, 6.5, 4.3V | 20.4, 14.8, 9.8 | 0.5uW/2, 1.4,0.9mW | 600T |
| 10. | 2006 | Beeby et al. [52] | 350 Hz (fig-9) | | 0.3g | 16.9mV | 100 Ω | 2.85uW | 600T |
| 11. | 2006 | Xingping, Yi-Kuen [53] | 40 Hz | | | | | 35 mW | |
| 12. | 2006 | Koukharenko, Beeby et al. [31] | 1.6kHz, 9.5kHz | | 1g | 0.7V, 4.15V | 2 kΩ | 0.11mW, 3.35mW | 600T, 112 ohm |
| 13. | 2006 | Kulkarni, Beeby et al. [30] | 7.4kHz | 30mm$^3$ | 0.4g | A= 55mV<br>B= 950mV | A=7.75Ω<br>B=7.5 kΩ | A= 70uW<br>B= 85uW | A= 60T/ B= 250T<br>Optimised= 20T |
| 14. | 2006 | Saha, Beeby et al. [54] | A= 13.11Hz<br>B= 84Hz | | 0.07g<br>7.95g | Graph | Graph | Graph | 850T/18Ω<br>300T/3.65Ω |
| 15. | 2006 | Torah, Beeby et al. [29] | 56.6Hz | | 60mg | M1: 52 mVrms<br>M2: 120 mVrms | 9 Mohm | 1.7uW<br>17.8uW | 600T/100Ω |
| 16. | 2006 | Serre et al. [55] | 360 Hz | 11x11x2.127mm$^3$ | | | | 45nW/ *0.2uW* | 910Ω |
| 17. | 2007 | Beeby et al. [56] | 52 Hz | 0.15 cm$^3$ | 0.06g | 428 mVrms | 4 kohm | 46uW | 2300T |
| 18. | 2007 | Kulkarni, Beeby et al. [57] | 8.08kH & 9.83kHz | 6mm x 5.7mm | 0.39g&1g | | 52.7 ohm | A=148, B=23nW | A=600T / B=65T |
| 19. | 2007 | Torah, Beeby et al. [33] | 43 – 109 Hz | 150mm$^3$ | 0.03-0.07g | 450mVrms | 4 kohm | 45uWrms | 2300T/1.6 kΩ |
| 20. | 2007 | Sari, Balkan, Kulah [58] | 3.3-3.6 kHz | 14x 12.5x8mm$^3$ | | 50 (E) / 20mV | 250 ohm | 0.5uW | 580 Ω |
| 21. | 2008 | Hohlfeld, Vullers, Boeck [59] | 5 Hz | 1cm$^2$ | | 500 mV | | 100 uW | |
| 22. | 2008 | Kulkarni, Beeby [60] | A= 808 Hz<br>B= 9837 Hz<br>C= 60 Hz | A= 106mm$^3$<br>B= 106mm$^3$<br>C= 150mm$^3$ | 0.39g<br>1g<br>0.9g | | B=52.7 ohm<br>C=110 ohm | A= 148nW<br>B= 23nW<br>C= 584nW | A=600T/112 Ω<br>B=65T/55 Ω<br>C= 2 times of coil B |

| | | | | | | | | | |
|---|---|---|---|---|---|---|---|---|---|
| 23. | 2008 | Kulah, Najafi [61] | 1-100Hz (due to multi-cantilevers) | 4mm$^2$ | | 76mV | 300 ohm | 3.97 uW @ 25 Hz | |
| 24. | 2008 | Saha et al. [62] | 8 Hz | 12.7 cm$^3$ | 0.03g | | 7.3 kohm | 14.55uW-2.6mW | 1000T/800 Ω |
| 25. | 2008 | Soliman et al. [63] | 90-100HZ | 0.299cm$^3$ | 0.1g | 49.3mV | 2.7 ohm | | 22T/ 1.2 Ω |
| 26. | 2008 | Torah, Beeby et al. [64] | 52 Hz | 150mm$^3$ | 0.06g | 931mVrms | 15 kohm | 58uW | 2800T/2.3 kΩ |
| 27. | 2008 | Zhang et al. [65] | 20 Hz | 22x16x2.5mm$^3$ | | 1.36V | | 3.1uW | 66,133T/147,263 Ω |
| 28. | 2008 | Serre et al. [66] | 120 Hz | 15x15mm memb. | | ¬200mV | 100 ohm | ¬55uW | 100 Ω |
| 29. | 2009 | Ayala, Beeby [67] | | | | | | | |
| 30. | 2009 | Bouendeu et al. [68] | 98 Hz | 1.45cm$^3$ | 1g | 0.27, 0.25V | 40 ohm | 356 µW | 2 * 10.7 Ω |
| 31. | 2009 | Brian Dick et al. [69] | 43.8 Hz | 27cm$^3$ | 2.3mg (fig-4) | 0.9Vrms (fig-4) | | 0.55mW (fig 6) | 2090T/225 Ω |
| 32. | 2009 | Fondevilla, Serre et al. [70] | 344 Hz | 1.35cm$^3$ | | 100mV (fig-5) | 105 ohm | 50uW | 52T, 100 Ω |
| 33. | 2009 | Hadas, Ondrusek, Singule [71] | 17 Hz | | 0.1g - 0.5g | 4Vrms (fig-5) | | 3mW - 26mW | |
| 34. | 2009 | Hatipoglu, Urey [72] | 46 Hz | 30x11.7mm$^3$ | 15g | 200mV | 100 ohm | 0.4mW | |
| 35. | 2009 | Mack, Wallrabe [73] | | | 6.12g | 12.5mV | 30Ω / 25T each core | | |
| 36. | 2009 | Marioli et al. [74] | 102 Hz | | 1g | 183.2mV | 76 ohm | 290uW (Best) | 27.1 Ω |
| 37. | 2009 | Wang et al. [75] | A=94.5 Hz B=55 Hz | 0.13cm$^3$ | A=0.5g B=1.52g | 42.6mVp-p B=18mV | | A=0.7µW B=0.61µW | A=300T/163 Ω B=60T (2layers) / 33Ω |
| 38. | 2009 | Wang, Arnold [76] | 530 Hz | 14.3mm$^3$ | 1g | 13.2Vrms | | 23pW (Best one) | Resistivity=1.89 |
| 39. | 2009 | P Wang et al. [77] | 280 Hz | 9x7x5mm$^3$ | 1.02g | 142.5mV | 81 Ω or 1MΩ? | 17.2µW | 2 coils*(30T, 40.4Ω) |
| 40. | 2010 | Z Wang et al. [78] | 25 Hz | L=9mm, D=20mm | | 2.32 Vp-p | 200 Ω | | 600T |
| 41. | 2010 | J. Park, Bang, Y. Park [79] | 54 Hz | 1x1x0.6cm$^3$ | 0.57g | 68.2mV | 18.1 Ω | 115.1µW | 183T, |
| 42. | 2010 | B. Yang, C. Lee [80] | 40-80Hz (Type II) | 1.5x1.5x1.2cm$^3$ | 1.9g | 9mV | 50 ohm | 0.4 uW | 12Layers*10T |
| 43. | 2010 * | Sari, Balkan, Kulah [81] | 50-200Hz | 8.5x7x2.5mm$^3$ | | 13.5mV (total) | | 20*0.25nW | 20Cantilevers*6T/150Ω |
| 44. | 2010 | Turkyilmaz, Kulah, Ali [82] | Magnet: 114Hz Coil diaph.: 2kHz | 10x8.5x2.5mm$^3$ | | 15.2mV | | 119nW | 92T |
| 45. | 2010 | Zhu, Beeby et al. [83] | 67.6Hz - 98 Hz | | 0.06g | 8.1 V | | 61.6µW-156.6µW | 6950T |
| 46. | 2011 | Emre Tan Topal. [84] | 120 Hz | 0.25cm$^3$ | | 7.2mVp-p | | 1.45µW | |
| 47. | 2011 | Galchev, Kim, Najafi [85] | 10Hz - 65Hz | 2.12cm$^3$ | 1g | | 220 Ω | 163p/13.6avg µW | 1200T/ 220Ω |
| 48. | 2011 * | C. Cepnik [43] | 361 Hz | 0.46 cm$^3$ | 0.01g | 10.4mV | 167.8Ω | 0.62 µW | 137.5Ω |

| | | | | | | | | | | |
|---|---|---|---|---|---|---|---|---|---|---|
| 49. | 2011 * | Q. Yuan, X. Sun et al. [86] | 64 Hz | 5x5x1mm³ | | 7.5µV | 2 *1.3Ω | | | |
| 50. | 2011 | X. Xing, X. Sun et al. [87] | 42 Hz | 29.3cm$^3$ | 5g | 2.52V | 2.5 Ω | | 20.84mW/cm$^3$ | |
| 51. | 2011 | E. Bouendeu et al. [88] | 132 Hz | 8 cm$^3$ | 1g | Single coil= 1.1V<br>Series= 4.49V<br>Parallel= 1.07V | 1200 Ω<br>6 kΩ (series)<br>500Ω (parallel) | 1 coil: 108µW<br>2 coils:404µW (series)<br>& 422µW (parallel) | 2100T/500 Ω | |
| 52. | 2011 | Zorlu, E.T.Topal, Kulah [24] | 2.96 cm$^3$ | | | 88.6 mV | 544.7µW | | | |
| 53. | 2011 | Dayal, Dwari, Parsa [89] | 108 Hz | | Close loop: 2.5g (fig-18) | Both Open & Close Loop= 3.3V | 1 kΩ | Open loop:10.8mW<br>Close loop:19.5mW | | 25<br>(T<br>(s<br>& |
| 54. | 2011 * | C. Cepnik, U. Wallrabe [90] | | 19.8x15.1x3mm$^3$ | 1.01g | 1.56mVrms | 24.9 mΩ | 12 µWavg | 9.2mΩ | |
| 55. | 2011 | Bouendeu et al. [91] | 78.43 Hz | 20x20mm$^2$ (appx) | 1g | 0.8(load voltage) | 1200 Ω | 315.37 µW | 675.1Ωinternal | |
| 56. | 2011 | Foisal, Lee, Chung [92] | 9 Hz | 14x48mm$^2$ | | 3.16V @ 9Hz<br>4.53V @ 14Hz | 97 Ω | 1.18mW | 1500T/96.502 Ω | |
| 57. | 2011 | Jiang, Masaoka et al. [40] | 115 Hz | 0.1cm$^3$ | 1.19g | 2 mV | | | 1.2kΩ | |
| 58. | 2011 | J.C Park, J.Y Park [93] (PDMS Springs used) | 53 Hz | 1x1x0.6cm$^3$ | 0.4g | 201mVp-p | 100 Ω | 115.1 µW | 183T/ 13.5Ω-Dc | |
| 59. | 2011 | Galchev et al. [94] | 1 - 40 Hz | 43(i) / 63(ext.) cm$^3$ | 0.01-0.10 | | | 0.46-0.72 µW | | |
| 60. | 2011 | Q. Yuan, S. Sun et al. [86] | 64 Hz | 5x5x1 mm$^3$ | | 7.5µV | | | | |
| 61. | 2011 | E. Sardini, M. Serpelloni [95] | FR4: 102 Hz<br>Latex: 41 Hz | 8.6cm$^3$ | 1g | FR4:183.2mV<br>Latex:378mV | 76 Ω | FR4: 290 µW<br>Latex: 153 uW | Inductor:280T/ 22.51Ω, L=24µH/ C=9.5pF | |
| 62. | 2011 | Zhang et al. [96] | 350 Hz | 14x13x0.4mm$^3$ | | 0.27mV | 3.90 kΩ | 2pW | 2 Coils*20T/ 4.77kΩ | |
| 63. | 2011 | W Pang, L. Wei, C. Lufeng [97] | 242 Hz | 12x11x? mm$^3$ | 0.5g | 28mV | | 0.55 µW | 26T | |
| 64. | 2011 | F. Khan, Sassani, Stoeber [98] | 371 Hz (Best) | 12x12x7 mm3 | 13.5g | | 7.5Ω (best o/p) | max: 23.56µW(pg-40) | 21T/ 7.5Ω | |
| 65. | 2012 | S.E Joe, M.S Kim, Y.J Kim [100] | 8 Hz | | Near to 0.5g | | | 430 µW | | |
| 66. | 2012 * | P. Wang, X. Dai et al. [101] | 280.9 Hz | 9x7x5mm$^3$ | 0.8g | 157.5mV | 1 MΩ | 21.7úW | 2 Coils in series (Ω not given) | |
| 67. | 2012 | K. Tao, G. Ding, P. Wang, Z Yang, Y. Wang [102] | 365 Hz | 20mm$^3$ | 1g | 20.9 µVp-p (open circuit) | | | 30T | |

| | | | | | | | | | |
|---|---|---|---|---|---|---|---|---|---|
| 68. | 2012 | V. Challa. David Arnold [103] | 5 kHz | | 1g,2g,3g,4g | 3.7-16µV | 1.5 Ω | 9.3, 37.5, 96, 171pW | 0.8µΩ |
| 69. | 2012 | H. Liu, B. W. Soon et al. [104] | 1285Hz (Best mode) | 10x8x0.45mm$^3$ | 1g | 3.5-3.6mV | 1.8 kΩ | 0.016 µW | 3 Coils*17T/640, 600,560Ω |
| 70. | 2012 | J. Chen, D. Chen et al. [105] | 235 Hz (Best mode) | | 172mVp-p | 90Ω | 10µW | 90Ω | |
| 71. | 2012 | Lee, Raman, Chung [106] | 12 Hz | | 0.2g | 2.32Vrms | 1.8 kΩ | 490 µW | 2000T |
| 72. | 2012 | Miki, Fujita et. al. [107] | 94.9 Hz | | 46 coils/ 5T | | 512 Ω | 760 pW | 46 Coils/5T |
| 73. | 2012 | S. Roundy et. al. [108] | | 37x37x3 mm$^3$ | | 3Vpeak(fig-8) | 20 Ω | 11 mJ | |
| 74. | 2013 | Tanaka, Fujita et. al. [109] | 595 Hz | | | 31.3mV | | 0.722 uW | |
| 75. | 2013 | K. Ashraf et. al. [110] | 10.3 Hz | 27.38 cm$^3$ | 50mg-1g | 7.92V | 3 kΩ | 20.9mW(5.02mW-avg) | |
| 76. | 2013 | Z. Li, M.D Han, H. X Zhang [14] | 48 Hz | 2.72mm$^3$ | | 0.98mv | 45 Ω | 0.015 µW | 8T |
| 77. | 2013 | D.H Bang, J.Y Park [111] | A= 36Hz, B=63Hz | 0.6mm$^3$ | A&B=0.3g | A&B=107&73mV | | A=29.02µW, B=23µW | A= 99Ω & B=55Ω |
| 78. | 2013 | H. Liu et. al. [112] | 840,1070,1490 Hz | 0.035cm$^3$ | 1g | Vmax=0.003 V | 626 Ω | 5.5nW, 0.5nW, 4.1nW | 626 Ω |
| 79. | 2013 | H. Lie et. al. [113] | 82 Hz | 0.032 cm$^3$ | 3g | Vmax=0.74mV | | 1.8nW | |
| 80. | 2013 | V. Pashaei, M. Bahrami [23] | 75 Hz | 0.64 cm$^3$ | | 67.4mV | | 46.6µW | 36T, 24.36 Ω |
| 81. | 2013 | Q. Zhang, E. Kim [114] | 290 Hz | 20x5x0.9mm$^3$ | | 30mV | 10.8 Ω | 2.6µW | 3*20T, 3*3.6Ω |
| 82. | 2014 | M. Han et. al. [115] | 64 Hz | 5x5x0.53mm$^3$ | 1g | 7.5 µV | | 0.3975nW | 1.9 Ω |
| 83. | 2014 | S. Chen, J. Wu, S. Liu [116] | 211Hz, 274Hz | 7.1x7x0.04mm$^3$ | 1.42g, 1.23g | 1&1.03mV (oc) | | 7.66nW, 7.43nW | 27 Ω |
| 84. | 2014 | M. Han et. al. [117] | 26.87 Hz | 10x10x10mm$^3$ | 0.5g | 3.82mV | | 0.75µW max | 2.5 Ω |
| 85. | 2014 | H. Liu et. al. [118] | 62.9 to 383.7 Hz | 6 x 6 mm$^2$ | 0.2g to 1g | 0.067 to 0.339mV | | | |
| 86. | 2014 | T. Shirai et. al. [119] | | 38x31x4 mm$^3$ | | 3.7V | | | |
| 87. | 2014 | K. Yamaguchi et al [120] | 400 Hz | 13.5x14x1.5 mm$^3$ | | | | 3.12 µW | |
| 88. | 2014 | Q. Zhang, E.S Kim [121] | 400 Hz | 51x11x0.4mm$^3$ | 6.4g | 1.02mV | 22 Ω | 0.55nW | 20T, 55Ω |
| 89. | 2015 | M. Bendame et. al. [122] | 12Hz max – (fig 26) | | 0.6g | 0.15V (fig-26) | | 12mW | 60T (1.75m), 3.6Ω |
| 90. | 2016 | K. Tao et. al. [37] | 326 Hz, 391 Hz | 290mm$^3$ | 0.12g | 3.6mV, 6.5mV | | 0.96nW | 57T, 12.7kΩ |
| 91. | 2016 | Q. Zhang et. al. [123] | A=250Hz B=75Hz | A= 0.2cm$^3$ B= 5.3cm$^3$ | A=1.5g B=5g | | A=0.7Ω B=190Ω | A=14.3µW B=1.04mW | A= 4*7T, 0.7Ω |

NOTE: Base Acceleration, g can be computed by using formula: $\mathbf{g = A * \omega^2}$

Table 2.1: Literature Review for Previous work done in the field of micro level harvesters.

# Chapter 3. Single Frequency Energy Harvester

As most of the harvesters found in literature work at a single frequency, so initially a harvester design was analyzed at a single frequency of 50 Hz. This chapter discusses the design and results of harvester operating at a single frequency.

## 3.1 Proposed Harvester Design (mention dimensions in image)

Energy Harvester initially designed for operating frequency of 50Hz comprises of sputtered NdFeB magnets having thickness of 20 µm and nickel substrate on which magnets are sputtered. Remanent flux density of NdFeB magnets is 1.4T. The magnets are arranged in halbach pattern, so that the maximum flux is concentrated in a single direction (discussed in next section). Springs are added adjacent to the nickel base supporting the magnets and these springs are fixed and subjected to the movement by the external vibrations. These magnets also serve as an inertial mass.

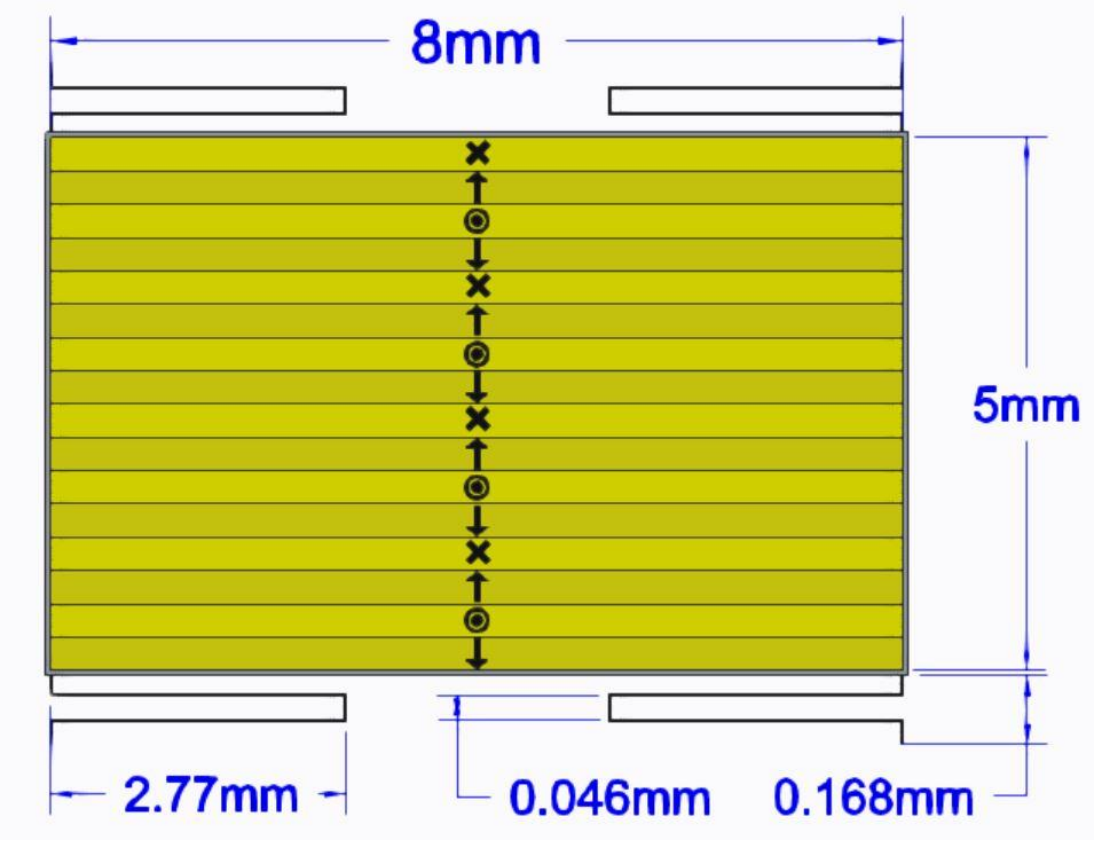


Figure 3.1: Harvester design for the single frequency

## 3.2 Operating Principle

The proposed harvester works on the principle of Faraday's law that when a magnet moves relative to coil or vice versa, it induces flux in the coils resulting in the voltage output. The movement is caused by the vibrations from the external source.

Mathematically it can be expressed as:

$$\text{Induced Voltage} = \text{EMF} = -N * \frac{d\emptyset}{dt} \tag{3.1}$$

Where,

N = No of turns

$\emptyset$ = BA = Magnetic flux

B = Magnetic field

A = Coils Area

The negative sign is due to the Lenz's law caused by eddy currents. The symbols used in the figure 3.1 shows the direction of polarity in accordance to the Halbach pattern.

## 3.3 Halbach Array

In simple arrangement of magnets, magnetic field are active on both sides of the magnet which has certain drawbacks as well as inefficient utilization of the magnetic flux. On contrary, Halbach array provides efficient and strengthen magnetic flux on active side of the magnet and other side remain quiet with very low or zero magnetic flux. Difference between simple magnetic array and Halbach array is shown in figure below.

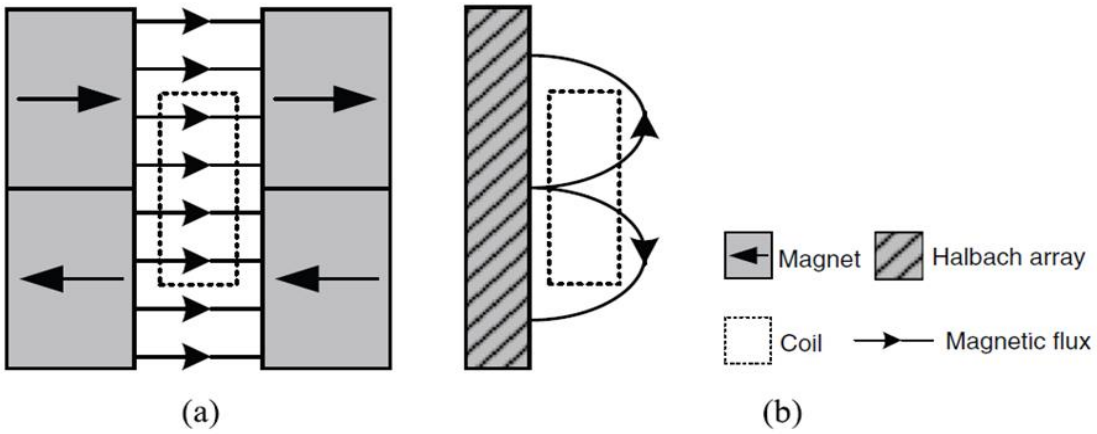


Figure 3.2: (a) Simple Magnetic Array. (b) Halbach Array [125]

The flux lines in a simple magnet travel from north to south and so they spread in all directions. Also the maximum flux is concentrated at the edges of the magnet and is less concentrated in the center portion of the magnets. Different orientations are found in literature and figure 3.2 (a) is one of them in which magnets are placed such that the maximum flux is concentrated in between the two pairs of magnets. Other reported orientations of magnets can be seen in [69][43] [123][42][14].

This approach has been utilized in the proposed design successfully. In later sections simulations results shows supremacy of halbach arrangement over simple arrangement. In the proposed design 16 planer magnets were used with main and transit magnets alternatively. Figure below indicates the implementation of halbach array in stepwise manner.

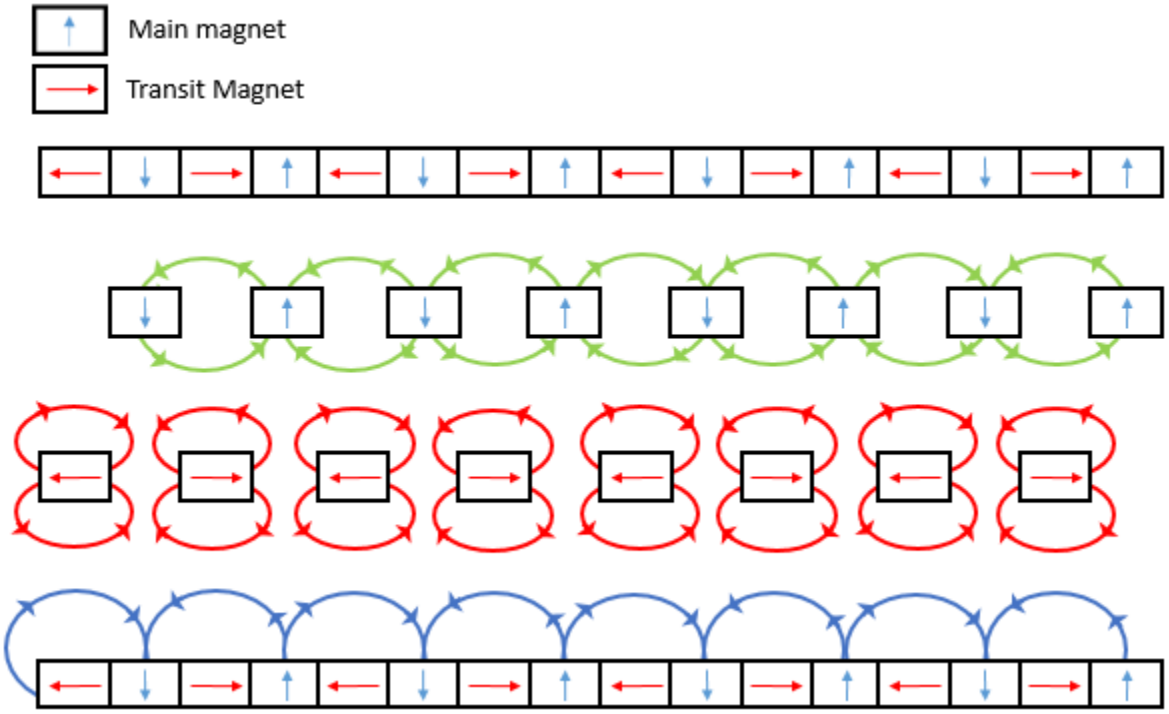


Figure 3.3: Halbach Array in Proposed Micro Energy Harvester

Figure 3.3 shows that how main and transit magnets cancel out the polarities and form the halbach array. It can also be seen that the maximum strength of magnetic flux is on the active side [125]. One more advantage of this arrangement is that if this device is used in electrical circuits, interference of electrical and magnetic field can be avoided.

## 3.4 Mathematical Modelling

The initial harvester model is designed to work for the vibrational frequency of 50 Hz which can be found in the tires of vehicles and also in the electric machinery.

The computed mass of the magnets and nickel base is 0.000013kg (Appendix A)

Using,

$$\omega_n = \sqrt{\frac{K}{m}} \tag{3.2}$$

Spring Constant is computed to be, $K_1 = 1.283$[N/m] at the required frequency of 50 Hz.

And for the design of springs, using the following equation,

$$K = \frac{2*E*t*w^3}{L^3} \tag{3.3}$$

The larger length of the spring comes out to be 2.75[mm]. The smaller length of 46[µm] is optimized such that the natural frequency of 50 Hz is obtained. The thickness and width of 20[µm] and [15µm] are standardized according to the METAL MUMPs process.

Frequency response at multiple smaller lengths of spring (stiffness) can be seen in the table:

| S. No. | Dimension of Smaller length (µm) | Frequency (Hz) |
|---|---|---|
| 1 | 20 | 55.155 |
| 2 | 40 | 51.21 |
| 3 | 46 | 50.53 |
| 4 | 50 | 50.89 |
| 5 | 100 | 48.84 |

Table 3.1: Optimization for 50 Hz frequency

Initially the damping for the single mass design was computed by using the relations of damping [27] [44] by considering the shear area but that resulted in high amplitudes of excitation which is not desirable. So Rayleigh damping was used to compute the next results. Details can be found in the chapter 4 and Appendix B.

## 3.5 Modal Analysis of Single Frequency Energy Harvester

In modal analysis, the dynamic behavior of structure under vibrational excitation is studied and mainly the natural frequencies that the device exhibit are observed. In the case of single frequency harvester, the first natural frequency is of our interest and in considered for the further analysis. Also the collective and single axis displacement can be observed. The proposed harvester is designed to move in ±y axis and the maximum displacement can be observed in this axis. Mainly these modes of vibrations help in suggesting the feasibility of the system when encountered with external vibration source.

During the modal analysis, we subjected Comsol Multiphysics for six frequencies. The damped modal analysis was carried out as can be seen in the figures because when damping is included, the software automatically returns the damped eigen values with real part depicting the natural frequency and the imaginary part showing the damping.

Below mentioned are the six natural frequencies of the said design, we consider the first natural frequency, remaining five are for the visual purpose and showing that they are not desirable due to the non-planer movement.

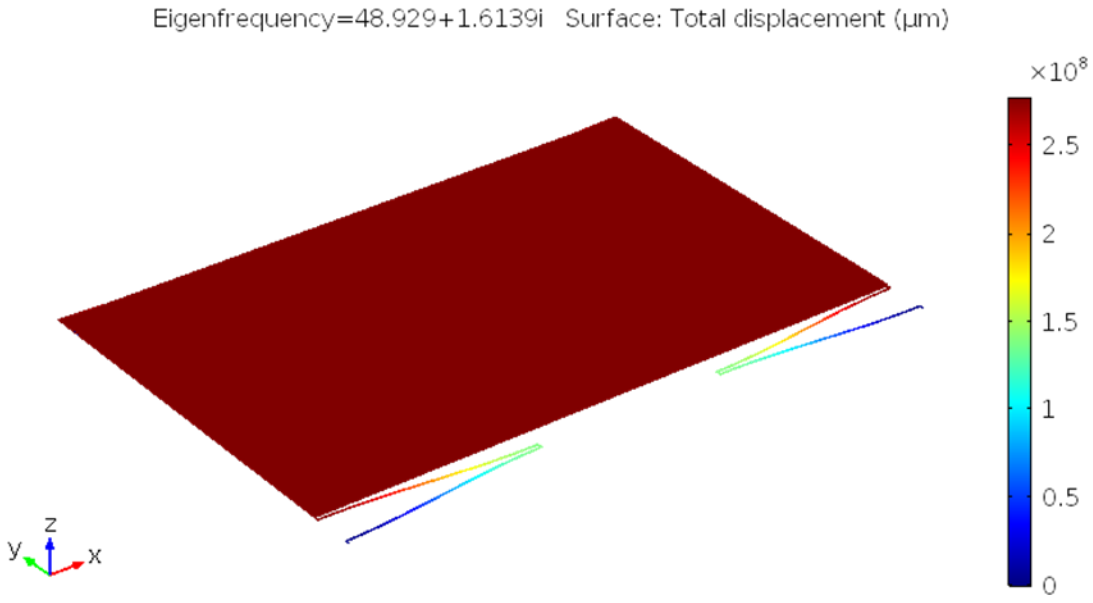


Figure 3.4: First Natural Frequency: (Planar movement)

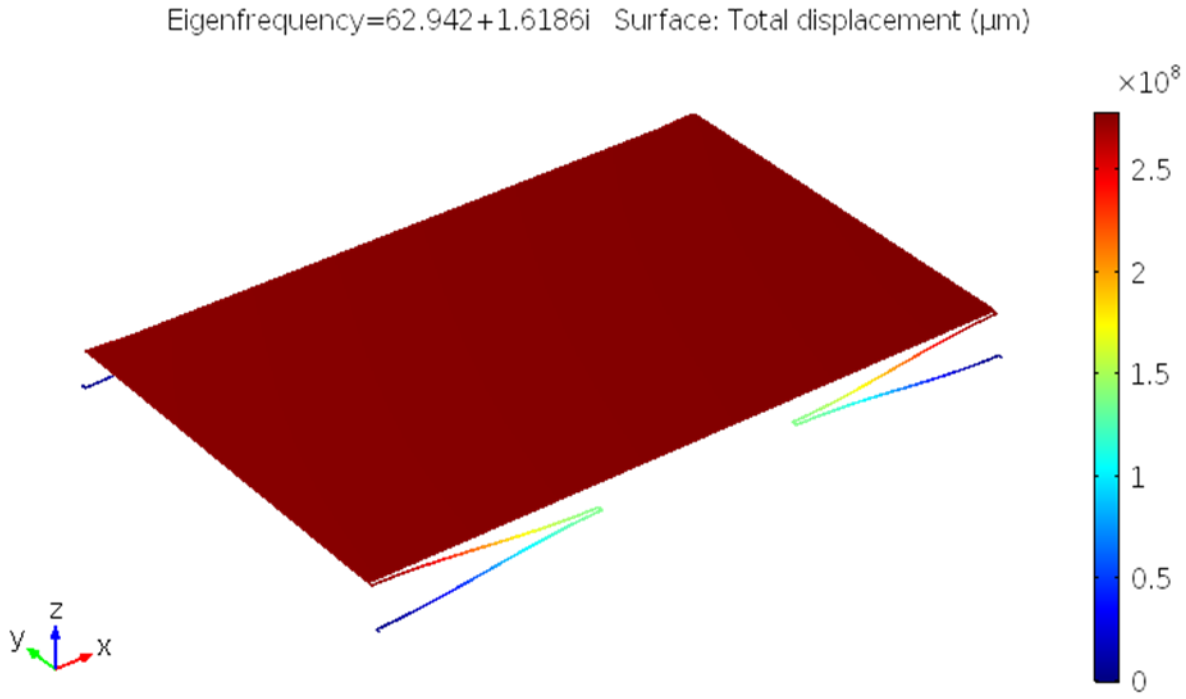


Figure 3.5: Second Natural Frequency

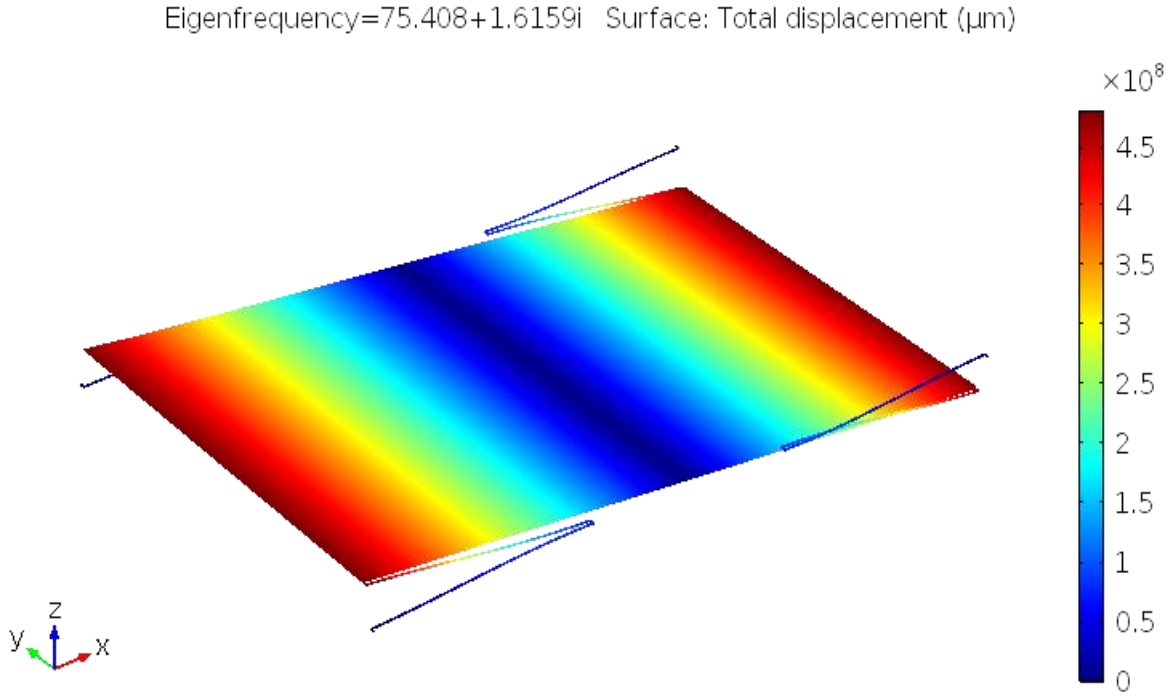

Figure 3.6 : Third Natural Frequency

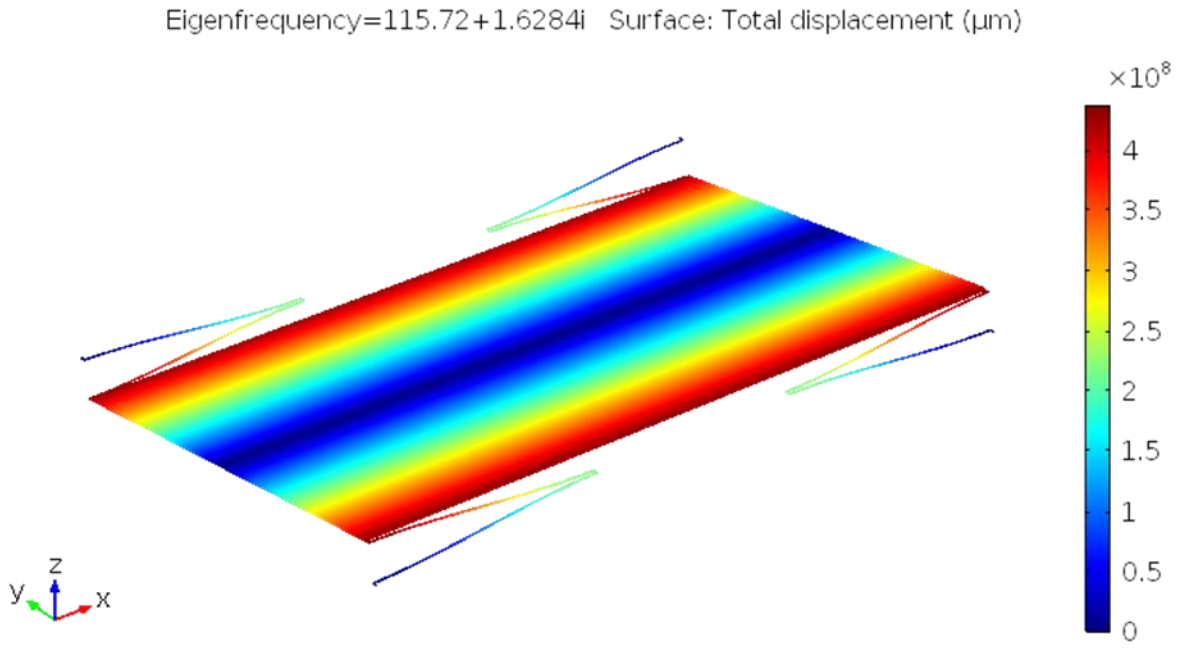


Figure 3.7: Fourth Natural Frequency

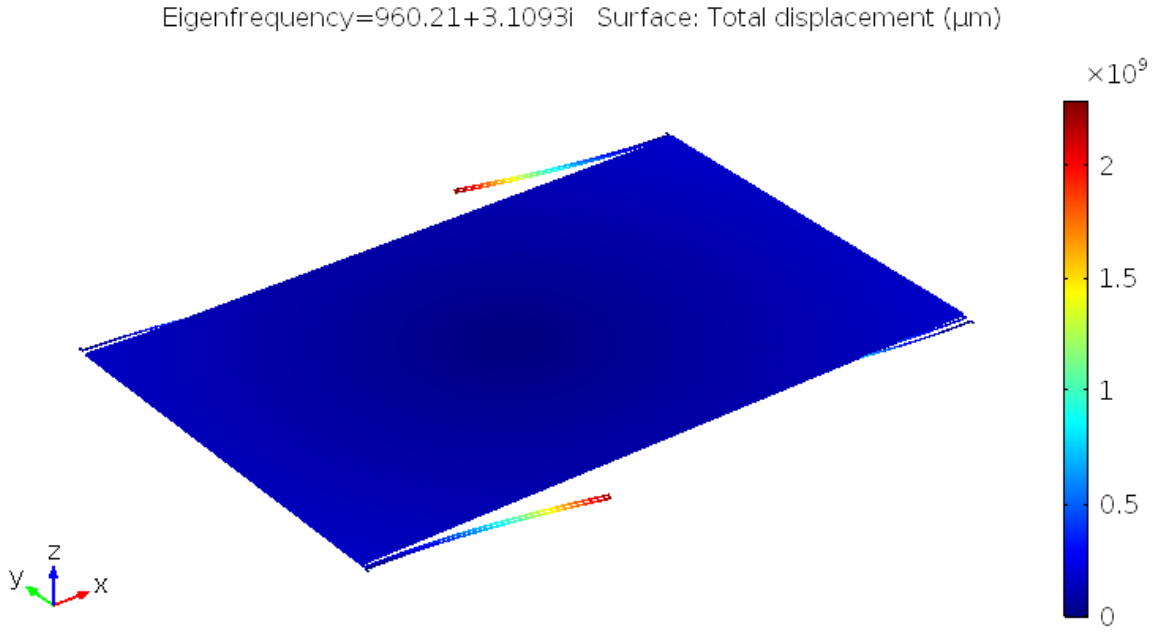


Figure 3.8: Fifth Natural Frequency

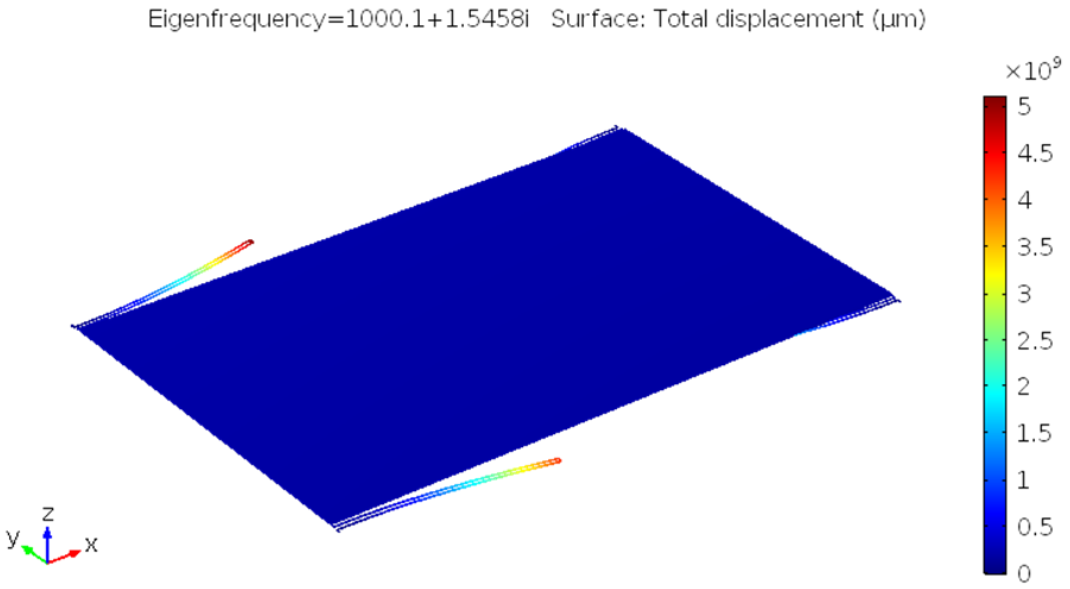


Figure 3.9: Sixth Natural Frequency

## 3.6 Harmonic Analysis of Single Frequency Energy Harvester

The purpose of harmonic study (also called frequency domain study) is to observe the behavior of the system under harmonic force. As the system is linear and the applied force is harmonic so the response of the system is also harmonic.

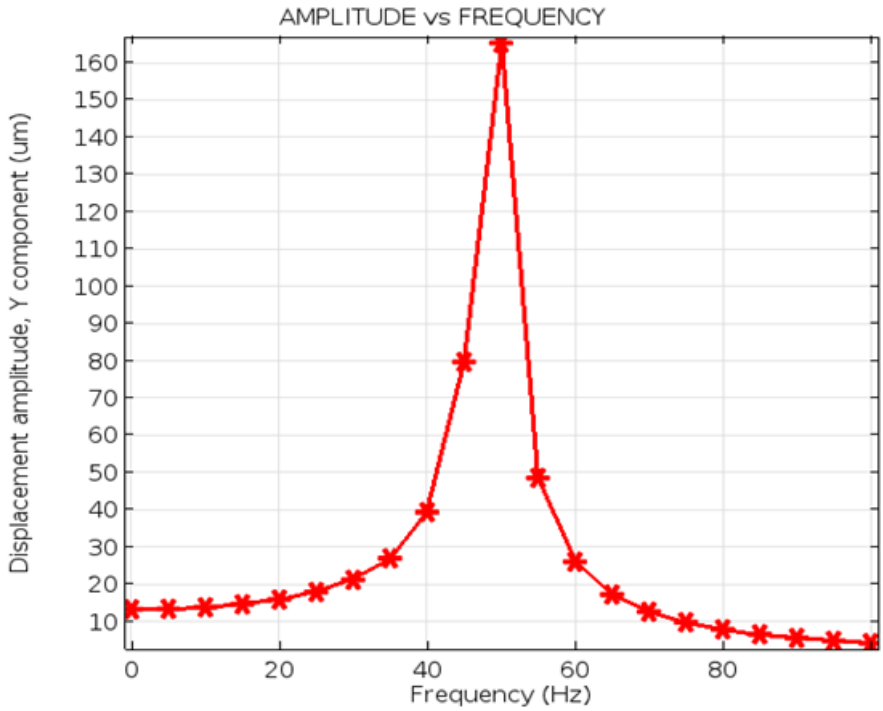


Figure 3.10: Single Mass: Harmonic Analysis

In the mentioned case for the single mass, the harmonic response shows a single peak showing the maximum displacement of the mass suspended with the springs at the first natural frequency of the system. The input force applied is volumetric with the value of 0.128g for this case. It also shows that as the damping is increased, the system gets slower. And at resonance and no damping, amplitude goes to infinity and there is no convergence at all for the simulation. Hence the plot shows that with damping, system can work at resonance or very near to it.

## 3.7 Electrical Design

This is layered mechanism, with each layer performing its role with relation to the above layer. The coils are placed underneath the magnets.

### 3.7.1 Coils

Coils are one of the important component of the harvester. In this design, voltage is induced in the coil by motion of magnets caused due to the vibration from ambient source and the output voltage is taken through the terminal pads of the coil. The coils are planer, micro fabricated with two layers. The coil layers are connected with each other through 4 Via holes each of $2.5E^{-3}$ $mm^2$ to maintain conductance and the Via holes are then filled by tungsten. The distance between the coils and magnets is kept 30µm. The standards adopted for coils are of MIMOS. Each coil faces two magnets i.e a single coil covers an area of 0.625mm x 8mm and the distance is kept symmetric from both ends. This orientation allows the maximum possible flux to interact with the coils. And all the coils are connected in series to achieve a good value of voltage. The thickness of each metal layer is 0.624um and 612µm respectively and a dielectric is used in between two layers so that both the layers are insulated without the interruption of flux lines. The inter turn gap between coil turns is kept 3µm and the width of each turn is also 3µm.

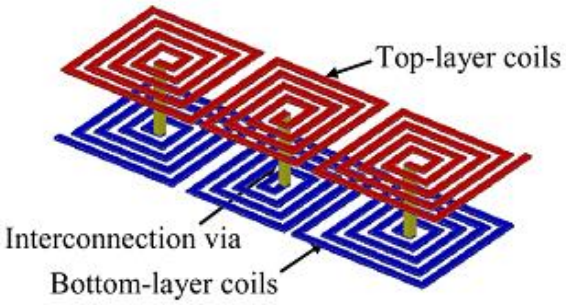


Figure 3.11: Schematic of Coils in Micro Energy Harvester

The calculated length of total coil wire is 6.668m with the resistance of 98KΩ. Design calculations related to coils are presented in Appendix A.

### 3.7.2 Circuitry

The following circuit is presented for our harvester model and it has been built up by using the spice model circuitry in Comsol Multiphysics. A low pass filter was also used to avoid the low frequency components. Nodes are defined in the image underneath.

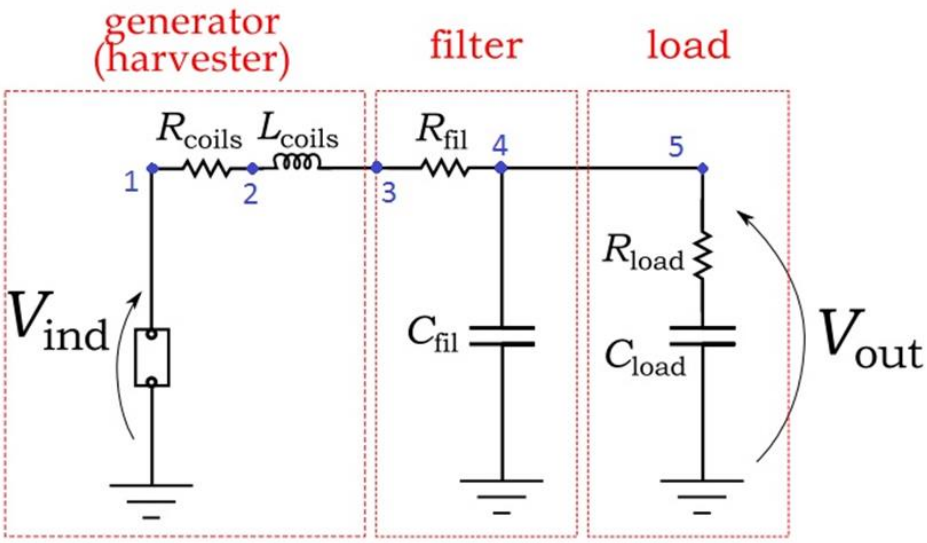


Figure 3.12: Circuit Diagram

| | | |
|---|---|---|
| Resistance of Coils | $R_{coils}$ | 98 kΩ |
| Inductance of Coils | $L_{coils}$ | 0.00353 H |
| Resistance for L.P Filter | $R_{fil.}$ | 98 kΩ |
| Capacitance for L.P Filter | $C_{fil.}$ | 1.624E-8 F |
| Resistance of Load | $R_{load}$ | 98 kΩ |
| Capacitance of Load | $C_{load}$ | 0.0028703 F |

Table 3.1: Circuit Parameters

Where,

$$C_{fil} = \frac{1}{R_f * \omega_c} \;\&\; \omega_c = 2 * \omega_n \tag{3.4}$$

$$C_{load} = \frac{1}{LC} * \omega_n^2 \;\&\; \omega_n = 2 * \pi * f \text{ [rad]} \tag{3.5}$$

## 3.8 Output Result for Single Frequency Energy Harvester

Simulation results indicate the following output results for the single frequency energy harvester.

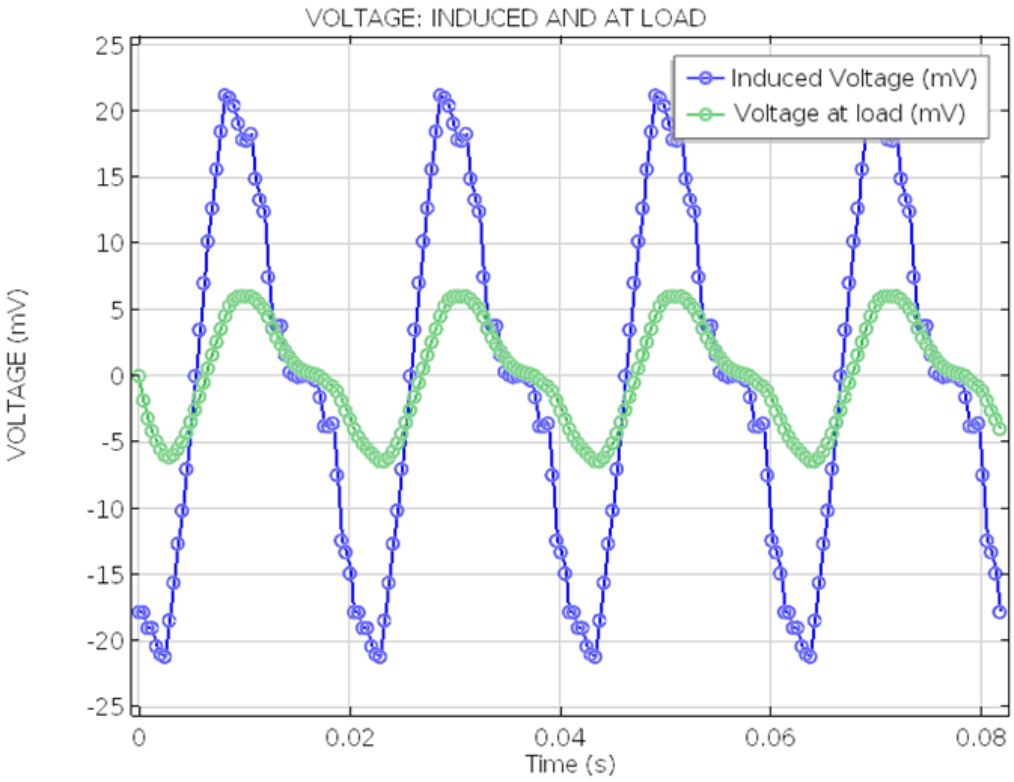


Figure 3.13: Induced and Load voltage of single mass at 48.92 Hz.

As can be seen from above results, a maximum voltage of 22mV is induced, indicated in blue lines represented by $V_{out}$ in the circuitry. As we know that the voltage drops when load is attached and it is represented by the green lines. In most of practical applications where continuous monitoring is not desirable like in tire pressure monitoring system, a capacitor is used for storage of charges and that output is delivered to the external sensor/s after the capacitor is full. And a power of 0.43nW can be extracted (figure 3.14) at a resistive load of 98kΩ, as it can be found in literature that the maximum power can be extracted when the load resistance is equal to the internal resistance [112].

However, the internal resistance can be decreased by using manufacturing standards of other foundry and using coils of gold which will result in an improved output.

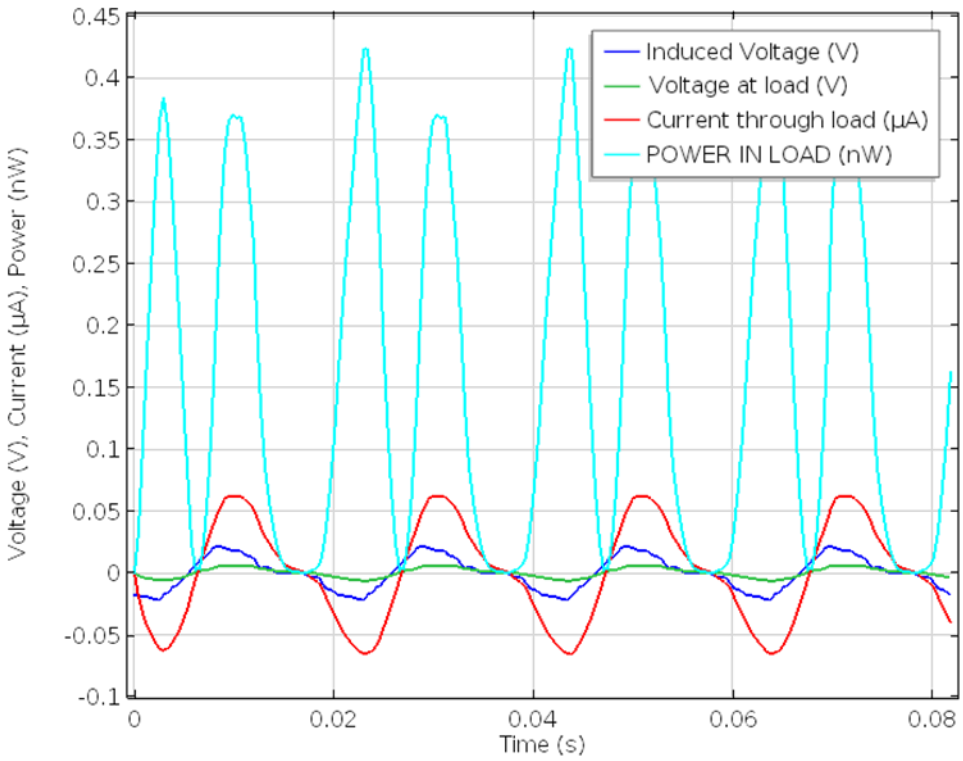


Figure 3.14: Induced voltage, Load voltage, Current drawn & Power

The above measurements are made at the first damped modal frequency of 48.92 Hz and its corresponding excitation amplitude is obtained from the interpolated function extracted from the harmonic analysis.

However, as we know that vibrations are not always of a single frequency, there may be some rise or down in the frequency of vibration source. Also possibly there are fabrication imperfections that rise during the fabrication process like springs which are intended to be of width 15 microns, may be their width is not of exact 15 microns, so it will directly influence the frequency of the device and it possibly will not work at the designed single frequency. So there is need for such a device which can work on a wide range of frequencies, although the peak power may effect but average power will always be greater.

# Chapter 4. Dual Mass Energy Harvester with wideband Energy Harvesting

This chapter includes the electromechincal design of the harvester. A novel approach has been utilized to carry out the design of the harvester.

## 4.1 Proposed Harvester Design

The proposed Micro Energy Harvester also works on the principle of Faraday's Law of electromagnetic induction. The main addition in this device is that an additional mass is added to it such that it harvests energy on a broad range of frequencies.

There are broadly two layers with in the harvester. Figure below shows the mechanical CAD model of said MEH.

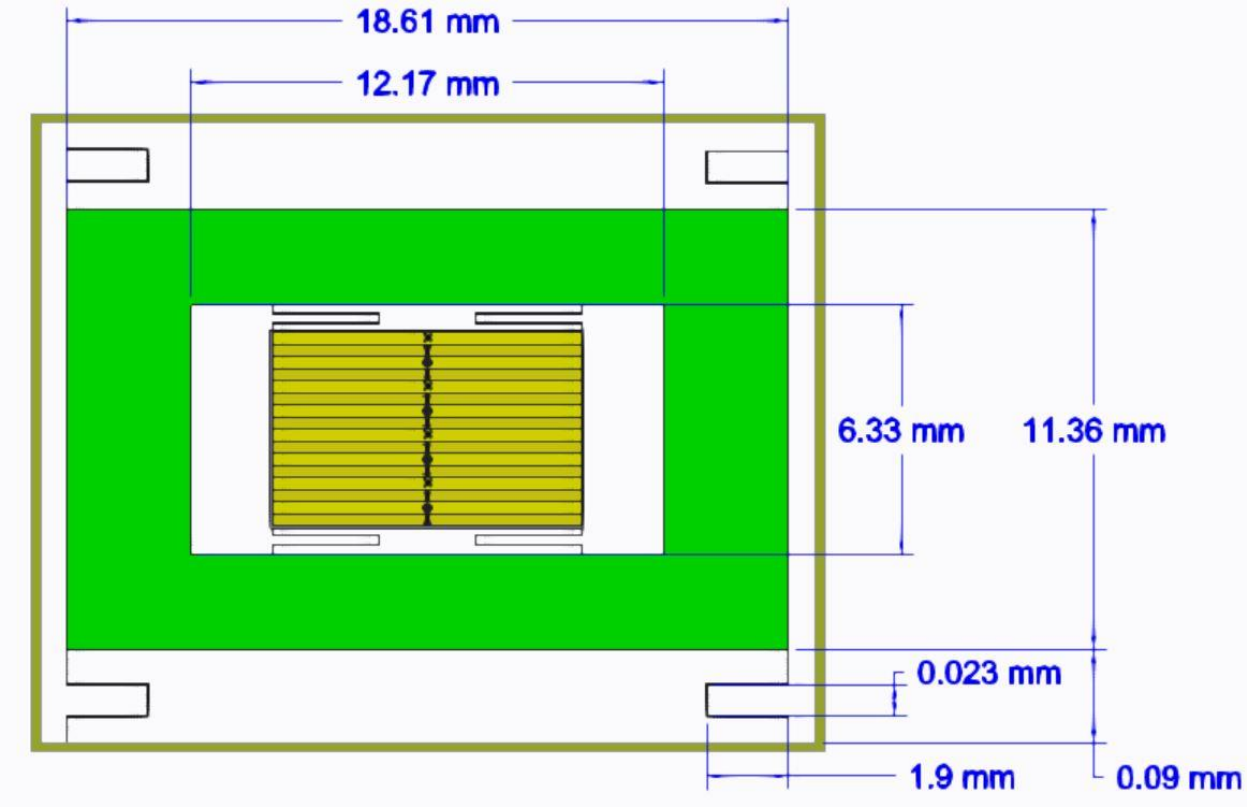


Figure 4.1: CAD model of proposed Micro Energy Harvester

Below figure shows the exploded view of harvester model in which the layers can be seen clearly. All of the shown parts will be discussed in the later sections in detail.

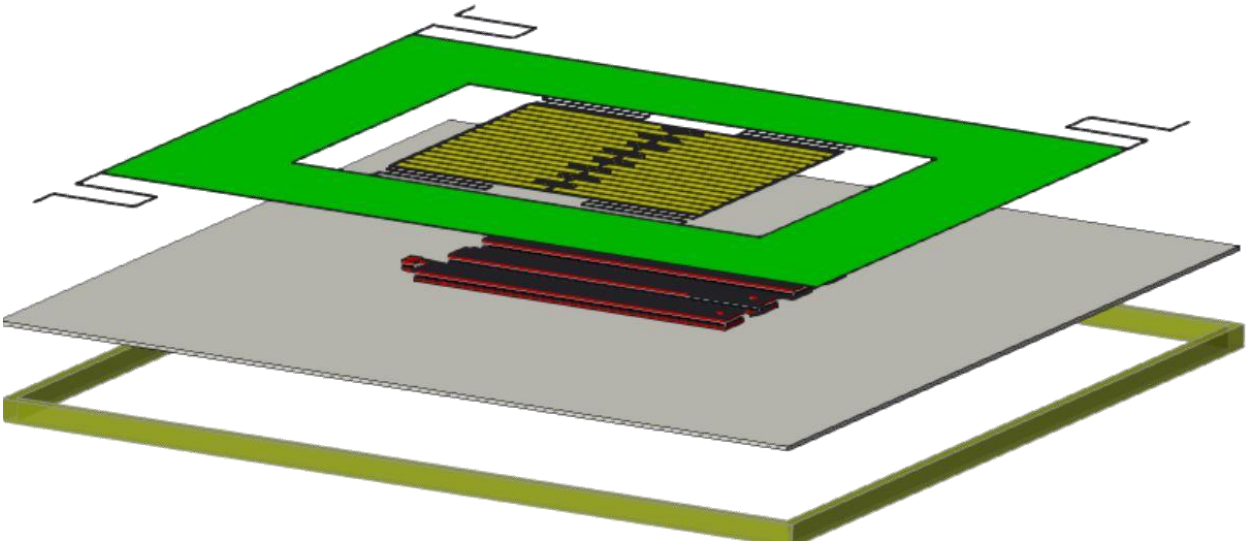

Figure 4.2: Exploded view of Micro Electromagnetic Harvester

### 4.1.1 Parts of Dual Mass Micro Electromagnetic Harvester

#### 4.1.1.1 Substrate:

Silicon substrate grown as the base of the harvester. It's a first layer in the harvester on which the aluminum coil has grown.

#### 4.1.1.2 Coils and Inner Mass:

The coil design and inner magnet design (also inner mass) is kept same and their details have already been discussed in section 3.7.1

#### 4.1.1.3 Outer Mass:

Dual mass system approach has been used while designing the proposed harvester. In principal, this design acts as absorber spring-mass configuration that can be connected to system subjected to unwanted oscillations. As a result, a resonance frequency will be generated between the

unwanted oscillations and spring-mass system [124]. This configuration helps the system to work on the wide band of frequencies.

## 4.2 Working Principle:

A comprehensible version of Dual mass system is shown in figure below with governing equations. It works such that the Mass M1(outer mass) acts as the drive mass and the Mass M2 (inner mass) acts as the absorber mass. Spring K1 is attached to the substrate and M2 is connected to M1 through Spring K2.

The inner mass, magnets behave as the absorber mass and are responsible for the voltage induction, as discussed in previous sections and the outer mass of nickel acts as the drive mass and is responsible for the wide bandwidth of the electromagnetic energy harvester.

$$m_1 x''_1 + c_1 x'_1 + k_1 x_1 + k_2 (x_1 - x_2) = F \quad (4.1)$$

$$m_2 x''_2 + c_2 x'_2 + k_2 (x_2 - x_1) = 0 \quad (4.2)$$

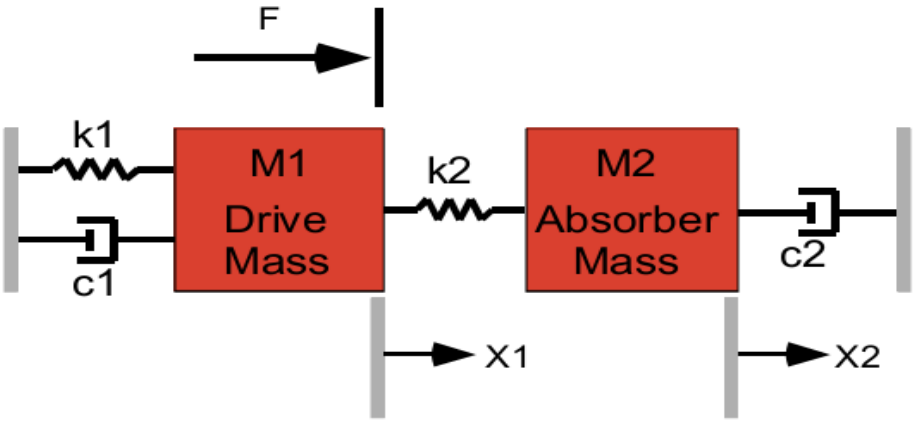


Figure 4.3: Dual Absorber Spring-Mass System [124]

Outer mass or inertial mass is attached to inner mass. Outer mass provides the inertia during the vibrations which makes this harvester to perform on multi bands of vibrations. This outer mass is attached to the casing with springs to provide oscillation. Calculations for outer mass and springs are given in Appendix A.

The amplitude and frequency phase response of the dual mass is shown below:

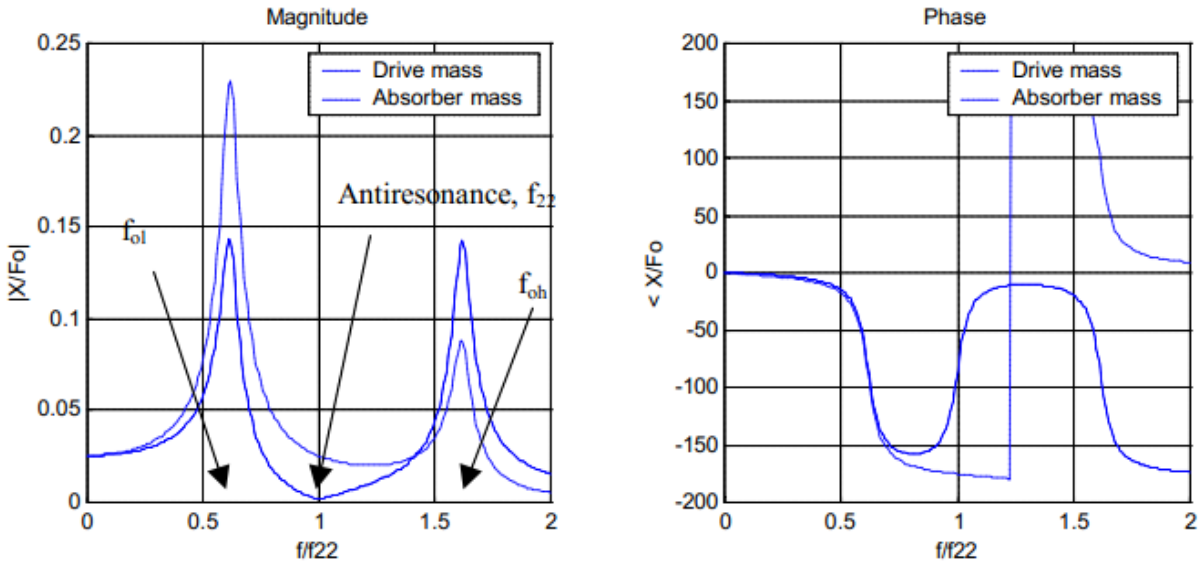


Figure 4.4: (a) Amplitude and (b) phase frequency response of dual mass design [124]

The frequencies $f_{ol}$ and $f_{oh}$ are the resonance frequencies and $f_{22}$ is the anti-resonance frequency. More the frequencies $f_{ol}$ and $f_{oh}$ are distant from eachother, more is the bandwidth of the frequencies.

$$\frac{\omega}{\omega_{22}} = \frac{f}{f_{22}} = \sqrt{\frac{1}{2}} \left\{ \frac{1}{\gamma^2} + (1+\mu) \pm \sqrt{\left[\frac{1}{\gamma^2} + (1+\mu)\right]^2 - \frac{4}{\gamma^2}} \right\}^{\frac{1}{2}} \tag{4.3}$$

The constants μ and γ control the separation between resonant frequencies and the gain respectively. Lesser the μ, less is the frequency separation between two peaks. The following values of μ and γ are used for our design.

$$\gamma = \frac{\omega_{inner\_mass}}{\omega_{outer\_mass}} = \frac{f_{inner\_mass}}{f_{outer\_mass}} = 0.8 \tag{4.4}$$

$$\mu = \frac{m_{inner\_mass}}{m_{outer\_mass}} = 0.5 \tag{4.5}$$

Figure 4.4 (a) and (b) shows separation between the two frequencies and out of phase and in phase response of the frequencies.

## 4.3 Optimization of g and damping values

Since the damping value calculated by the formulae mentioned in [27] [44] was not feasible giving high values of excitation amplitude, which is totally not desirable for us as it will cause the collision between inner and outer mass. So a procedure was adopted i.e. Design of Experiments Technique (DOE) which uses the central composite design to find the optimum values of g and damping.

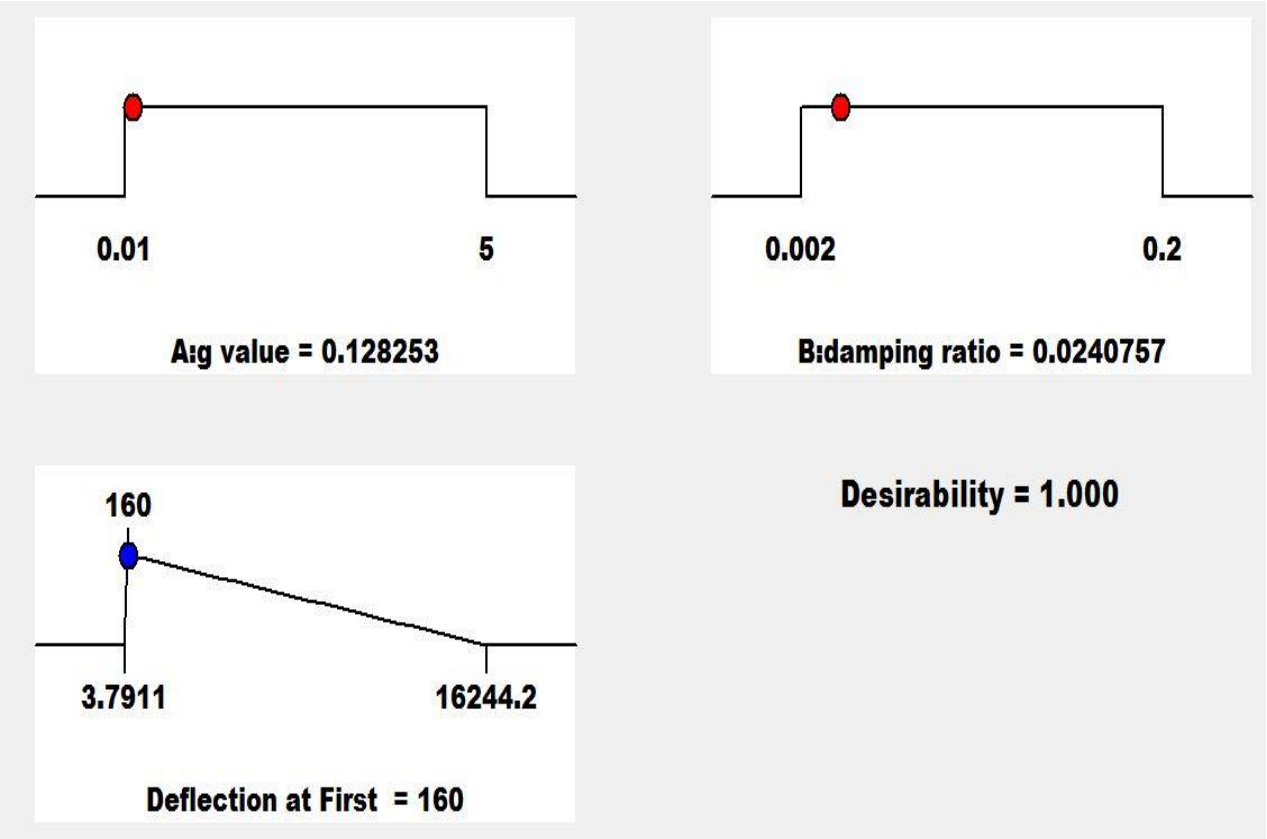


Figure 4.5: Optimization of g and damping value by DOE Technique

| S. No. | g ($m/s^2$) | ς Damping | Amplitude of 1st Peak (µm) | Amplitude of 2nd Peak (µm) | Amplitude at Centre of 1st & 2nd frequency (µm) |
|---|---|---|---|---|---|
| 1 | 0.255 | 0.0314 | 91.6614 | 35.2075 | 29.227 |
| 2 | 1.104 | 0.08403 | 91.661 | 35.29 | 29.228 |
| 3 | 0.6029 | 0.1815 | 251.616 | 92.309 | 70.3948 |
| 4 | 0.0253 | 0.018 | 65.5638 | 8.3667 | 3.1347 |
| 5 | 0.7664 | 0.0622 | 882.22 | 214.412 | 94.09 |
| 6 | 0.128 | 0.02407 | 158.06 | 70.187 | 15.178 |

Table 4.1: Different displacement values during optimization of g and damping

## 4.4 Manufacturing Sequence of Micro Energy Harvester

Manufacturing of the Micro Energy harvester starts with high-resistive silicon wafer which act as base which is manufactured using photolithography and deep reactive ion itching (DRIE). Right after that coils will be manufactured with aluminum using electroplating on the slicing base. This layer will be completed by developing bond using KMPR photoresist, patterned with photolithography.

For the second layer it starts with Silicon frame and high-aspect-ratio outer springs which are manufacture by DRIE and photolithography. Afterwards outer mass of nickel will develop using bulk micromachining. Again high-aspect-ratio springs will be developed using reactive ion etching. These spring will then be connected with inner mass. Inner mass comprises of high-resistive silicon wafer layer and magnet array. Silicon wafer layer will be manufactured using DRIE, with magnet molds created in it. NdFeB magnet array will develop using DC magnetron sputtering. Due to sputtering high performance magnetic properties will be achieved [40].

In the end, both layers can be bonded using already created KMPR photoresist by heating both layers under certain pressure. A manufacturing layout of proposed Micro Energy Harvester is presented in schema below.

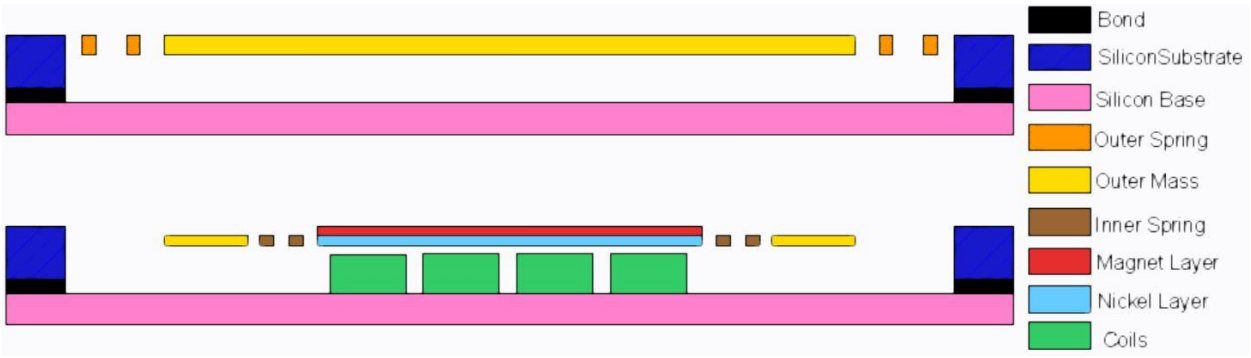


Figure 4.6: Manufacturing layout Scheme with cross-section

The cross-sections in figure 4.6 are taken from the locations as mentioned in the below mentioned figure.

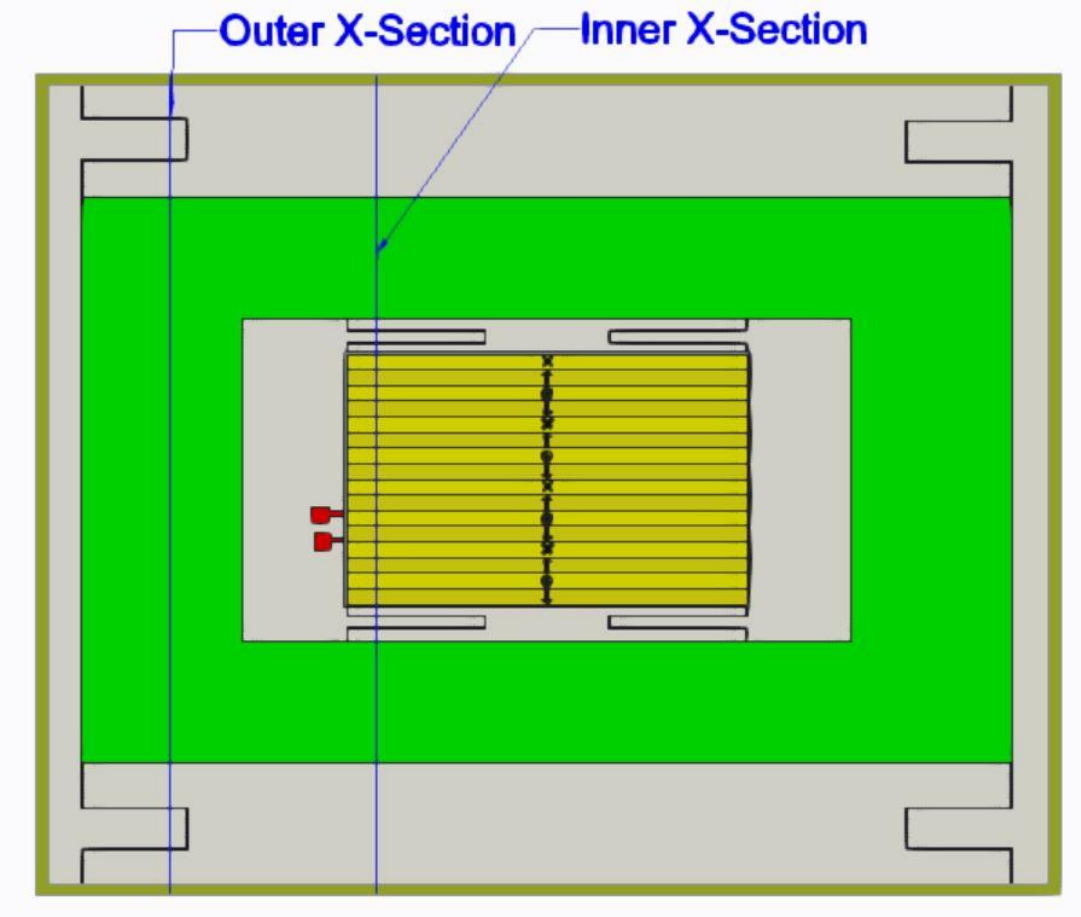


Figure 4.7: Dual Mass design representing the X-section at different lengths

# Chapter 5. Finite Element Simulation Approach

CAD models are primarily generated for the manufacturing and visualization purposes that is the reason modelers keep it detailed, even minute hinge is model. This detailed model is the “dream” of CAD modeler. Contrary it become “night mare” for the CAE personnel.

Finite Element Analysis performs calculations on nodes of an object. It has been observed from the studies and experience that number of complex geometry features are not required to perform an analysis [125]. Inclusion of those features not only increases the calculation cost but also produces some unnecessary results. So it has been widely advised by experts to simplify geometry as much as possible. But during this process extreme care should be taken not to omit the feature which is directly essential for the analysis.

There are some additional features in any model which are quite irrelevant for simulation and don’t play any role in results of analysis but increase the computation time and cost.

## 5.1 Geometry Formation:

Creating geometry in COMSOL is all about simplification of the CAD geometry. Complete geometry for the proposed system is shown in Figure 5.1 below.

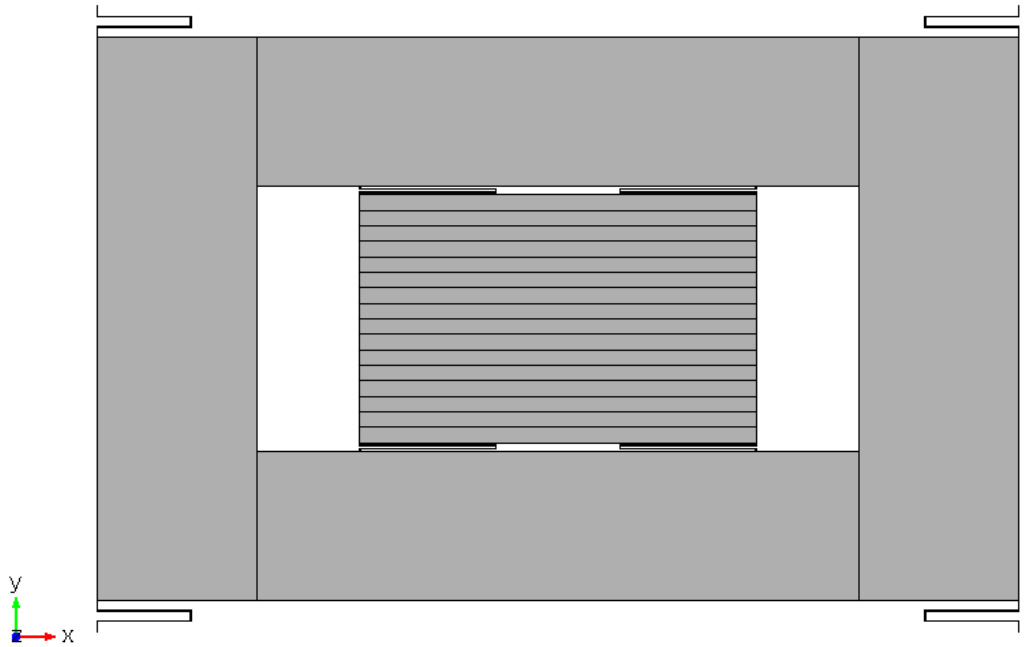


Figure 5.1: Model for Finite Element Analysis

Following are the steps which were taken in order to create a simplified model with the necessary features for the analysis.

## 5.2 Steps for modeling the system for FEA

1. It starts with the creation of block for base plate with the dimensions 8mm x 5mm x 0.02mm. Nickel was assigned to it as material property.

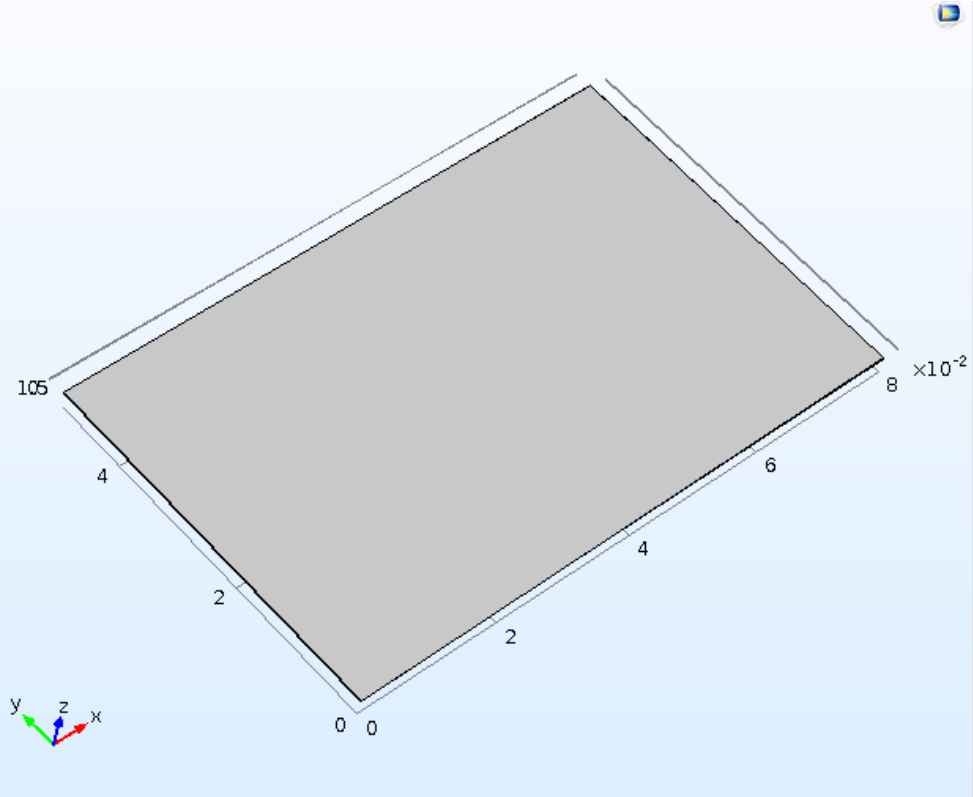


Figure 5.2: Base Plate of Nickel

2. After base, an array of 16 magnets was modeled, each magnet of dimension 8mm x 0.3125mm x 0.02mm. Magnetic properties assigned to this array has been discussed in details in later sections.

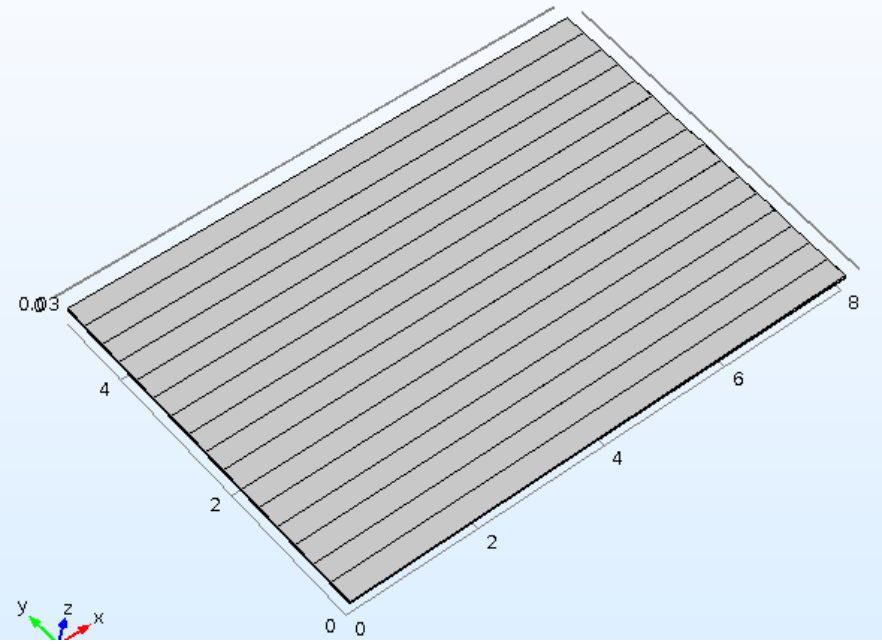


Figure 5.3: Array of 16 magnets

3. Springs were formed on the four sides of the nickel base plate & magnets resulting in the following geometry.

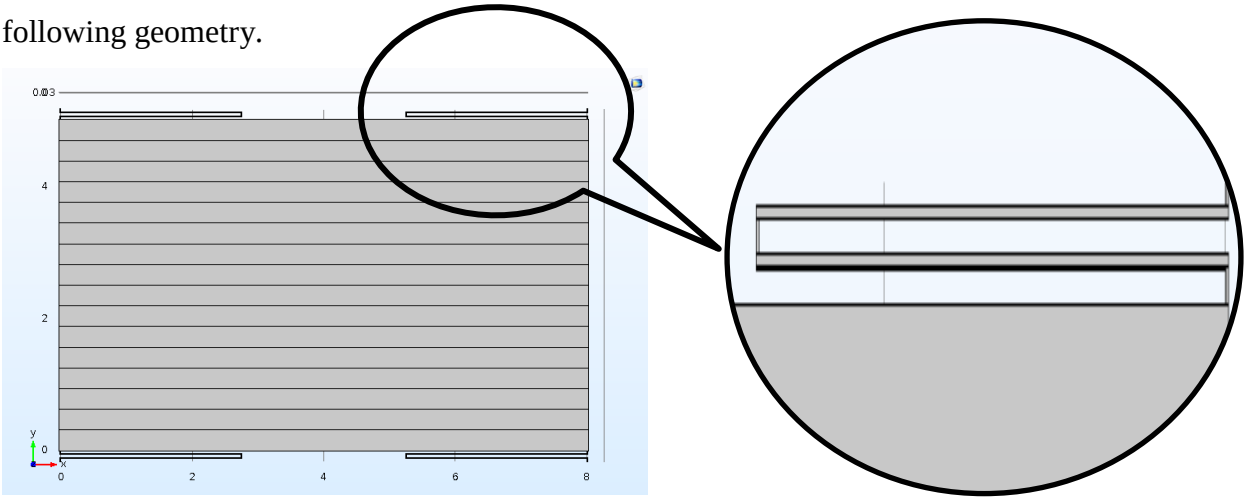


Figure 5.4: Spring Design for Inner Mass

Above geometry is also termed as inner mass in proposed harvester. Dimensions of springs connected to inner mass are as follows:

Smaller length: 0.046mm x 0.015mm x 0.02mm

Larger length: 2.758mm x 0.015mm x 0.02mm

The dimension and visibility of inner mass helps to create the geometry of outer mass.

4. Top and bottom blocks are buildup for outer mass each of dimension 12.172mm x 3mm x 0.02mm.

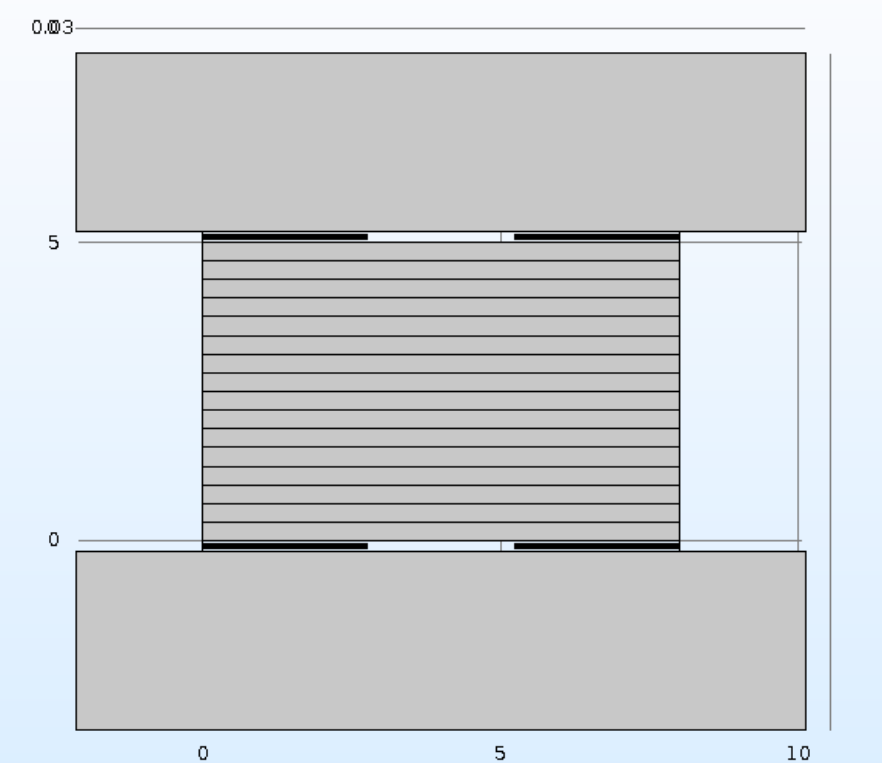


Figure 5.5: Step 1 of 2 of outer mass modeling

5. Then further two blocks are buildup, one each for top and bottom mass of dimensions 11.336mm x 3.221mm x 0.02mm, resulting in the following geometry.

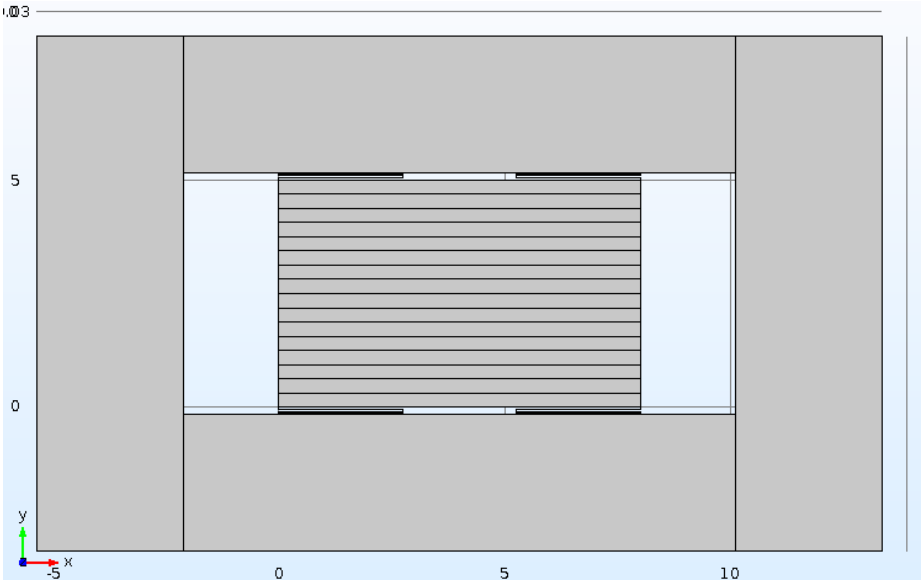


Figure 5.6: Step 2 of 2 of outer mass modeling

6. Finally the springs are formed connected to outer mass as follows:

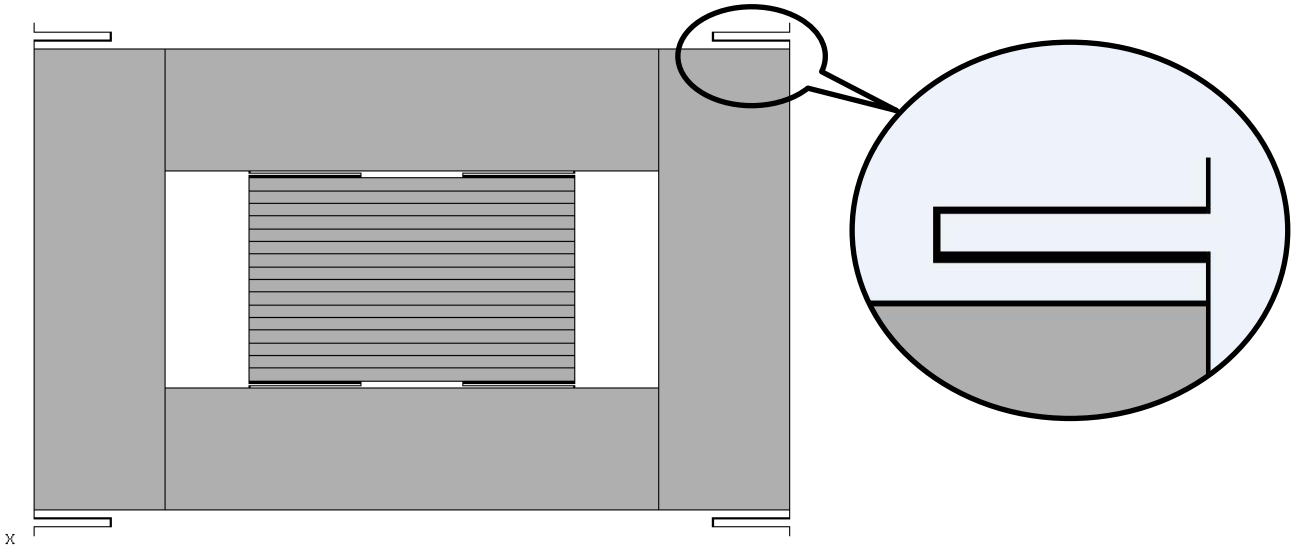

Figure 5.7: Springs of outer mass

Dimensions of springs connected to outer mass are as follows:

Smaller length: 0.0234mm x 0.01mm x 0.02mm

Larger length: 1.9002mm x 0.01mm x 0.02mm

Union option in Booleans and Partition is used to make sure that the faces of smaller and large lengths of springs attached to inner and outer mass are properly connected to each other. Both the inner and outer masses are designed to move in a single axis, y-axis by using the dual mass design approach discussed before and its calculations can be found in Appendix A.

## 5.3 Assigning Analysis Parameters

It is obvious that to perform analysis simplification the geometry to the maximum extent to avoid the computation complexities especially due to the deformation physics used in the simulations which is used to study the changes in physics when the geometry (represented by mesh in this case) changes due to imposed change in geometry externally (vibrations in this case).

For the analysis, it is known that inner mass (magnets) is responsible for the voltage induction, so for simplification and ease, the geometry was minimized by removing the springs and outer mass, as can be seen in the Figure 5.8.

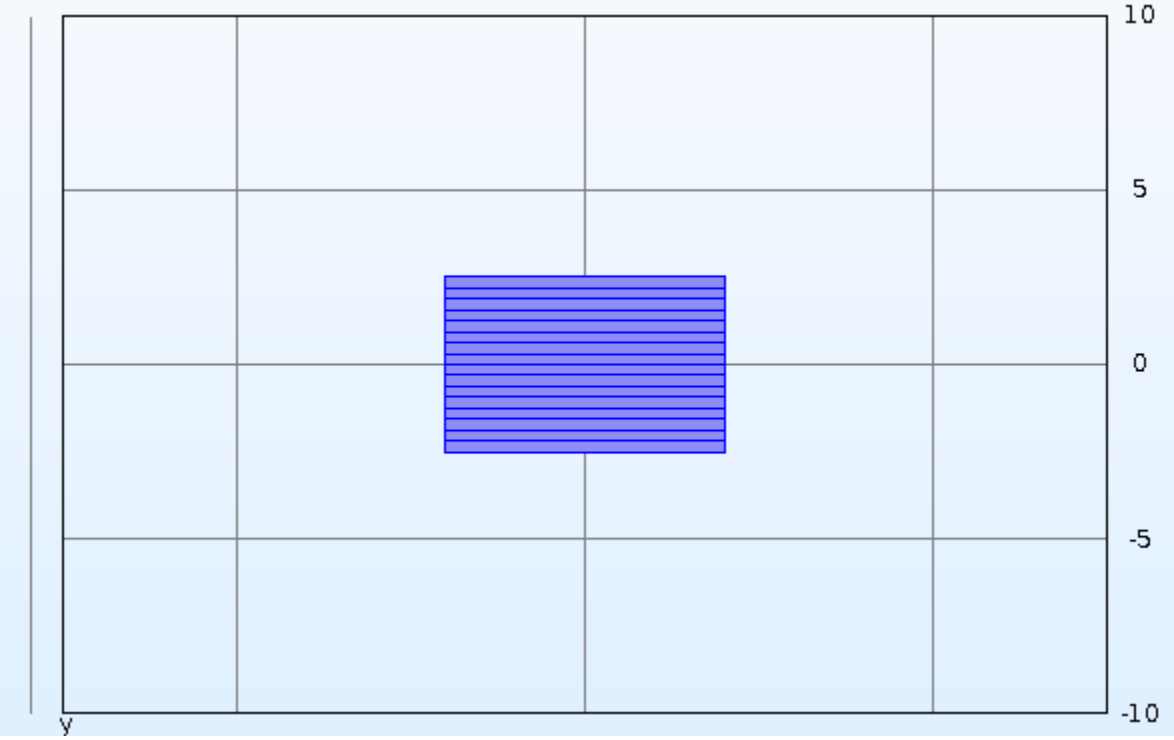


Figure 5.8: Magnets simplified for the analysis, with all the features removed.

The shaded portion in the Figure 5.8 are magnets.

### 5.3.1 Physics and Boundary Conditions:

Two physics are used in the analysis, Magnetic Fields, No Current and Deformed Geometry. The following boundary conditions and selections are used for the Magnetic Analysis:

1. Initially the magnets are centered w.r.t the origin.
2. The air block is defined enclosing the magnets. Magnets can be seen inside.

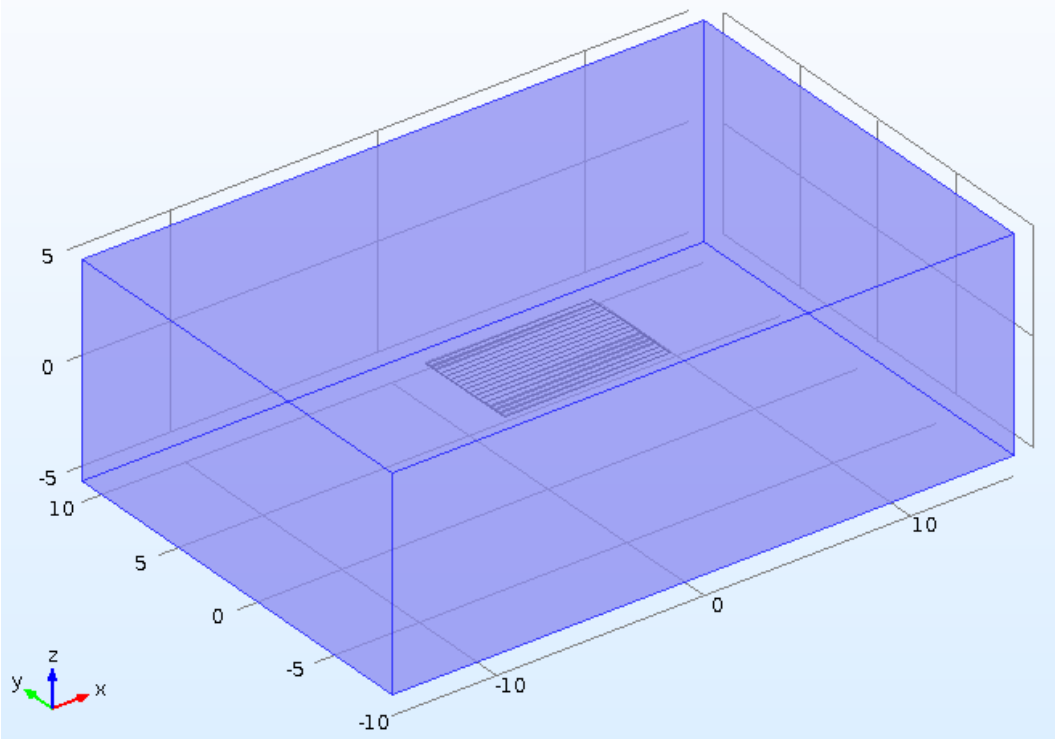


Figure 5.9: Boundary Condition for magnets

3. The coils area for four coils is defined (shaded portion) such that one coil is facing two magnets and the coils are symmetric from both ends.


Figure 5.10: Coil definition in analysis

3. The air block is partitioned from the center such that magnets are in one portion and the coils are in the other portion. It is done because magnets are moving and are given an input sinusoidal in deformed geometry whereas the coils are kept stationary, so they are in the other portion.
4. In the end to save the computation time, geometry is further reduced by using the Partition Objects option and finally we simulate the half portion of our geometry.

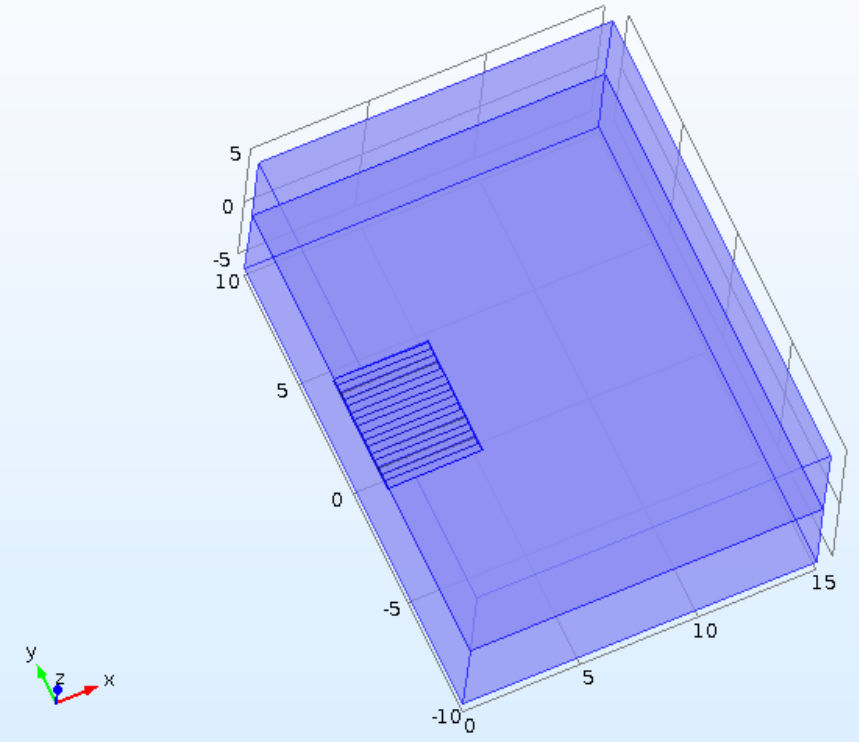


Figure 5.11: Centered Half Section for Computing optimization

5. The Form Assembly option is used instead of form Union at the end of geometry formation. Due to this Comsol deals geometry as a group of the geometry objects instead of treating all parts as a single geometry and pairs are formed.
6. The Zero Magnetic Scalar Potential is defined in magnetic field, no current (mfnc) physics and any edge is selected at the outer face of air box. It provides the boundary condition that depict zero magnetic potential on the boundary.
7. Magnets are assigned polarities in the Magnetic Flux Conservation option as follows:

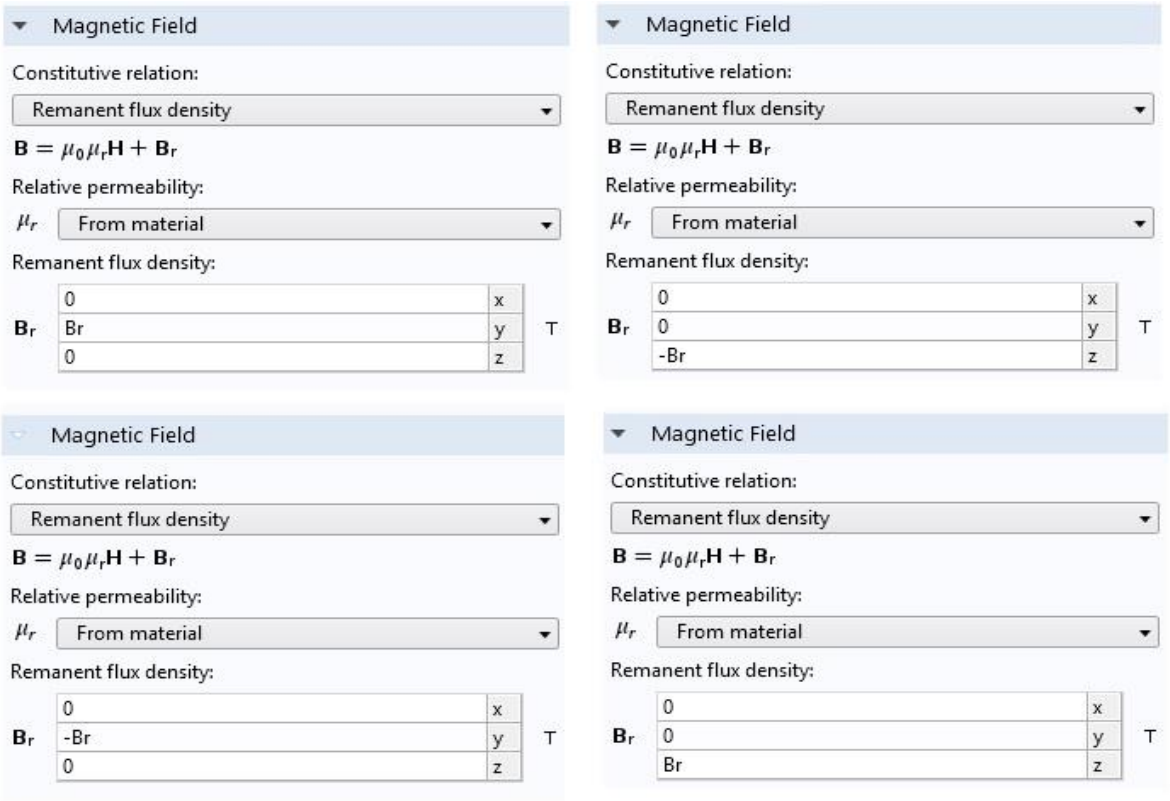


Figure 5.12: (a) (b) (c) (d) Definition of four different magnet polarities

8. The Figure 5.12 shows the assignment of polarities of magnets in four different directions for the Halbach Array. Br is the Remanent flux density and its value is defined as 1.4T in parameters. The negative sign reverses the polarity direction of magnet and finally the same pattern is used for the remaining twelve magnets.
9. In the deformed geometry physics, A*sin(2*pi*f*t) function is used as a vibrational input to our magnets in y direction.
10. The default value of 1.0E-6 of Relative repair tolerance is used.

### 5.3.2 Meshing:

Meshing is the discrete representation of geometry. There are four types of element types, TET, bricks, prisms, and pyramids. Free Tetrahedral mesh is used for the meshing of our geometry. Since magnets are of much interest, so they are meshed finely. Below mentioned are the meshes of our geometries.

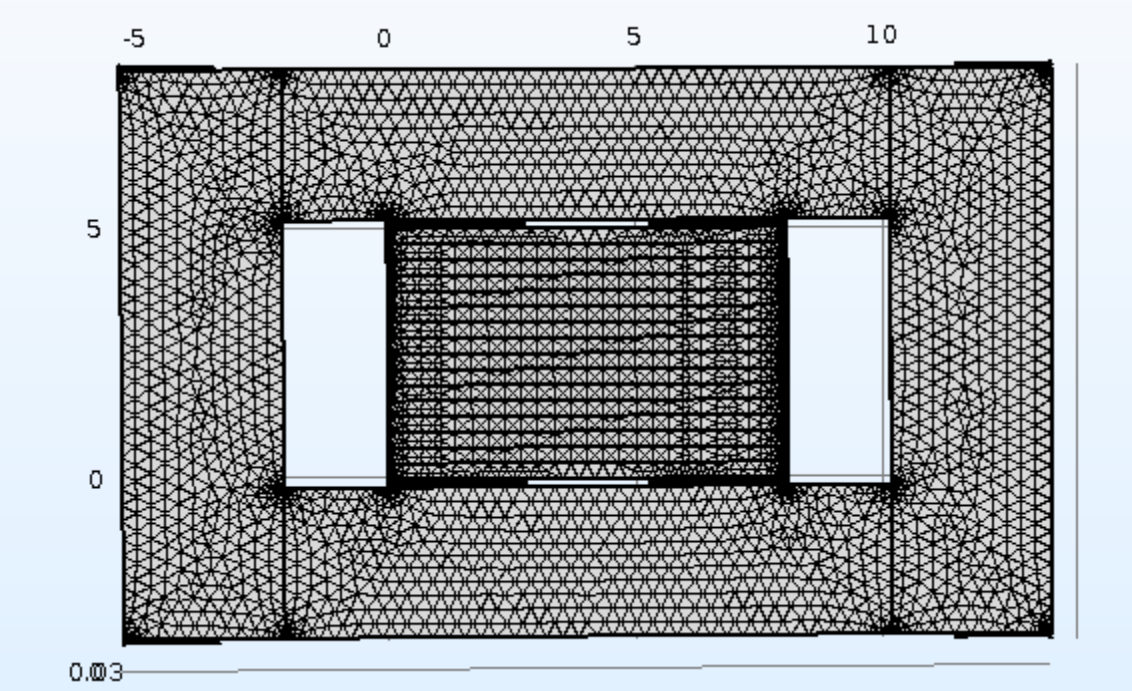


Figure 5.13: Tetrahedral meshing of the harvester model

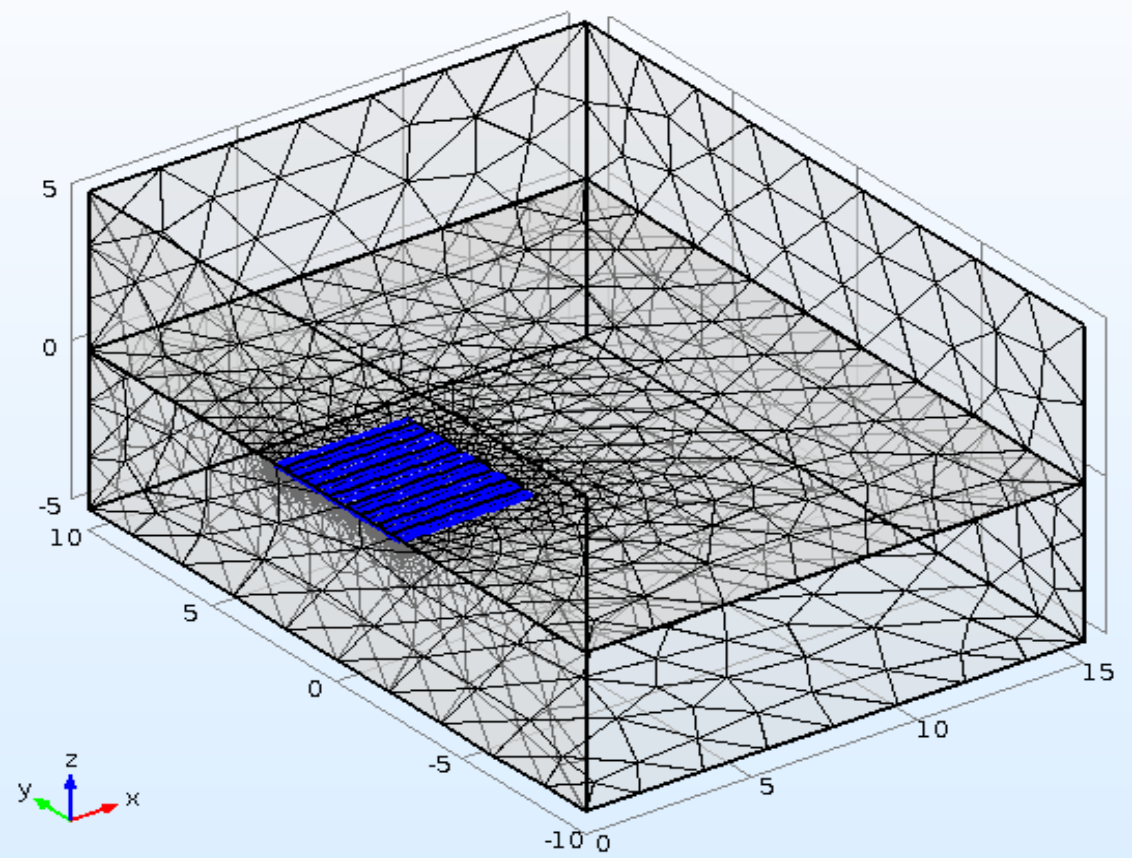


Figure 5.14: Meshing of bounded region (air)

# Chapter 6. Results and Discussion

In this section, first the results of magnetic analysis have been discussed. In the magnetic analysis flux density for Halbach magnetic array has been calculated. In further sections in this chapter modal, voltage and power output have been calculated.

## 6.1 Flux Density

Flux density is the density of magnetic lines in a specific region. Using Halbach array, flux density of the system has been enhanced which is shown in Figure 6.1. Contour plots indicate that due to halbach array flux density is maximum at the active side of the magnet. However it is very low on the quite side of the magnet.

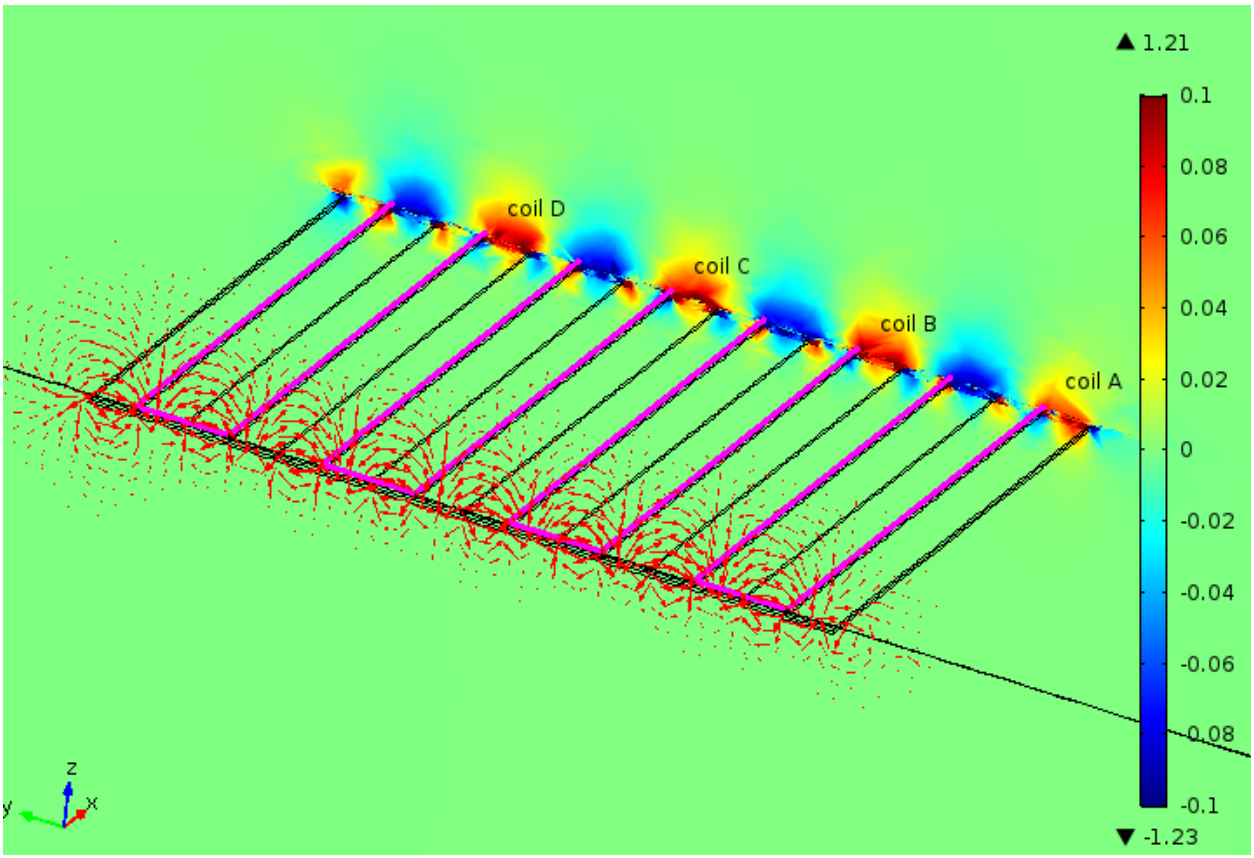


Figure 6.1: Isometric view of magnetic array and flux density.

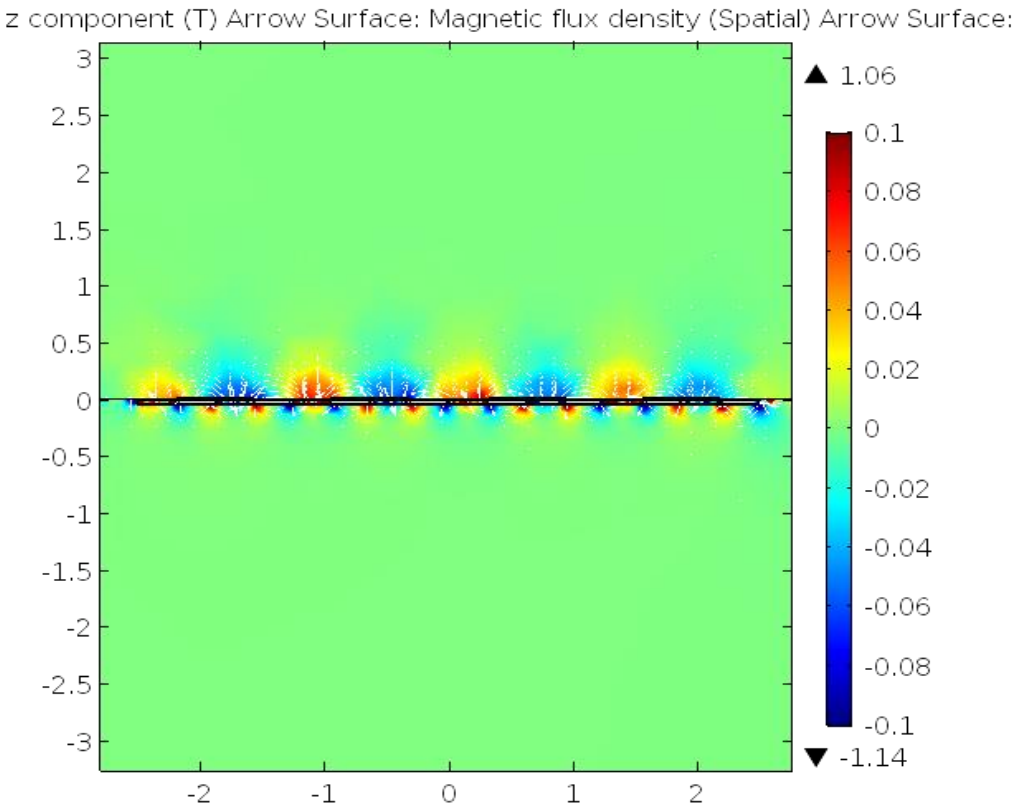


Figure 6.2: 2D – Z Component of Halbach Magnetic Flux Density Lines

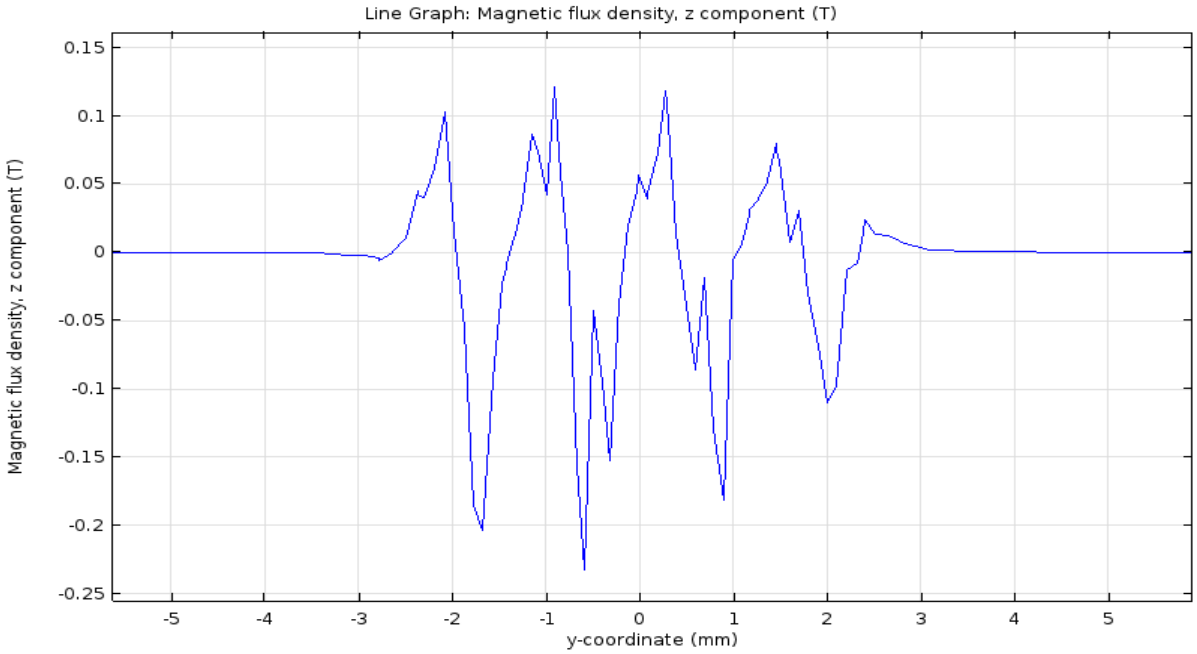


Figure 6.3: Flux density along coils at 20µm distance

It is clear from the Figure 6.3 that flux density is maximum at -2 mm to 2 mm in the y-coordinate which is 0.21 T

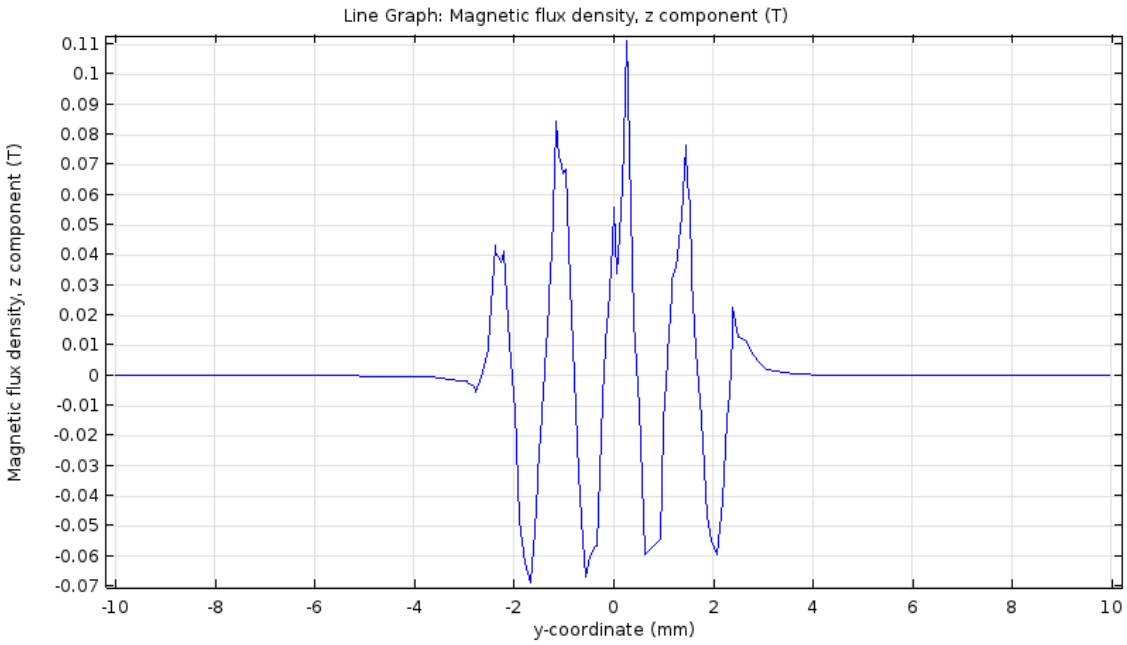


Figure 6.4: Flux density along coils at 30µm distance: (Case of Thesis)

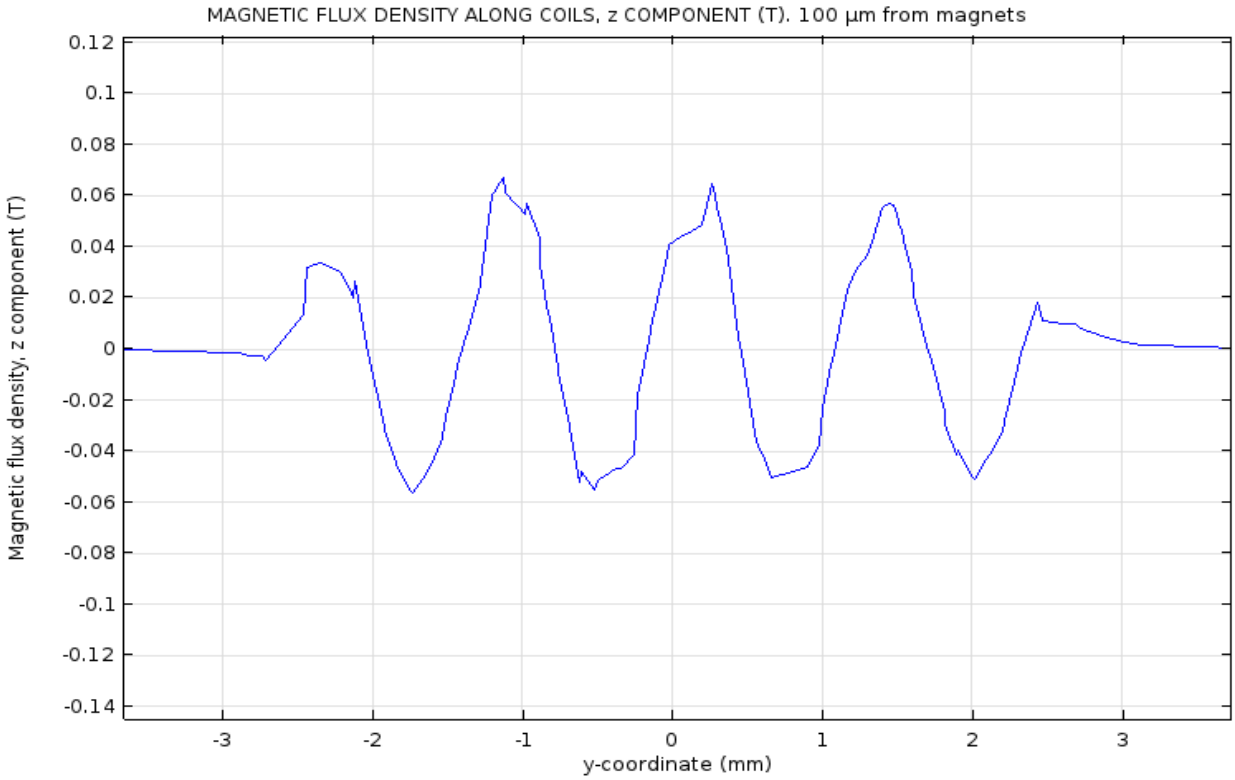


Figure 6.5: Flux density along coils at 100µm distance

However, increasing the distance between coils and magnets will result in weak flux density. This phenomena is shown in Figure 6.4 and Figure 6.5 at the distance of 30 µm and 100 µm respectively. It is important to note that Figure 6.4 is the case adopted in this thesis.

## 6.2 Modal Analysis

In modal analysis of double mass, natural frequency of the system has been carried out and first two modes have been taken into account which results in two peaks as discussed in previous section. These modes of vibrations help in suggesting the feasibility of the system when encountered with external vibration source.

### 6.2.1 Dual Mass

For dual mass, first two natural frequencies are of our interest. The results are displayed in the images underneath.

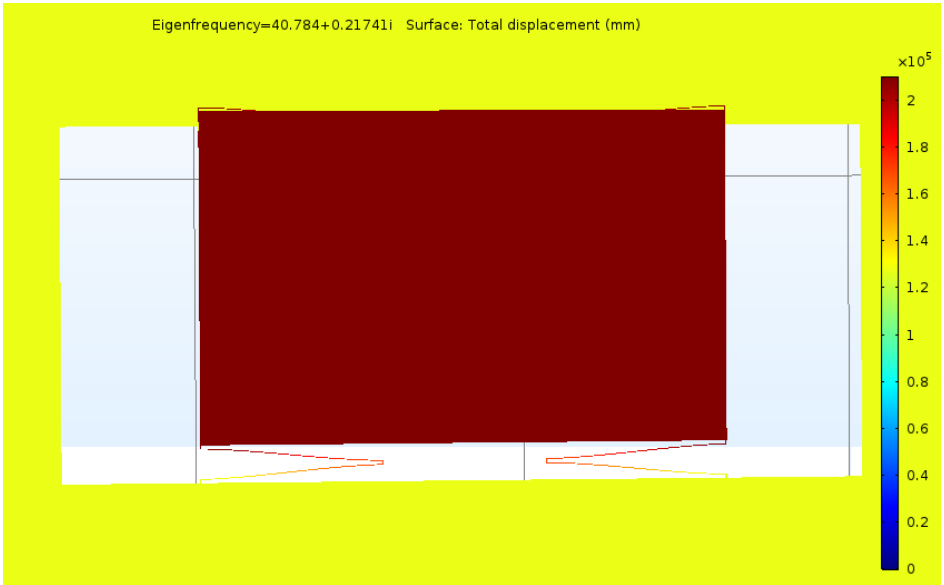

Figure 6.6: First Natural Frequency: (movement along y-axis)

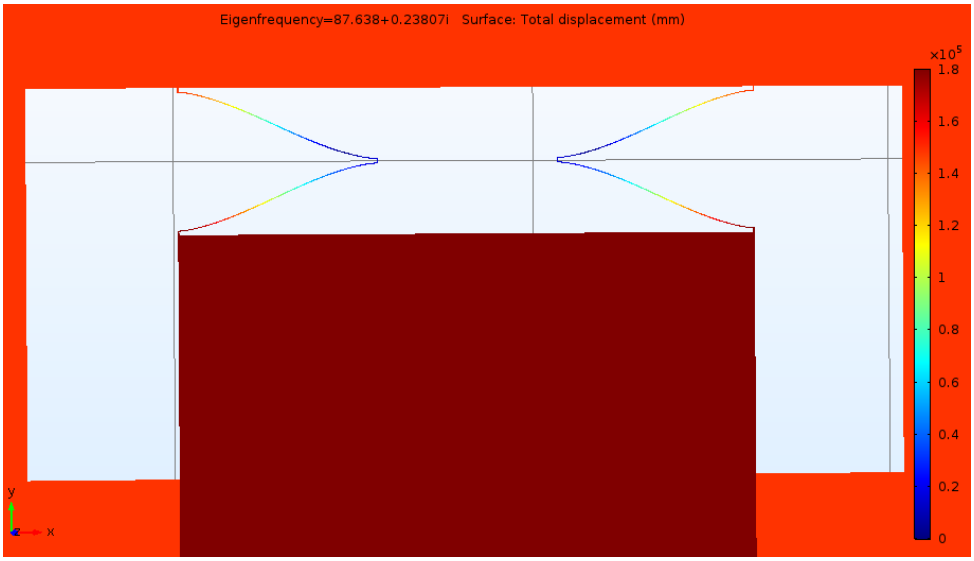


Figure 6.6: Second Natural Frequency

## 6.3 Harmonic Analysis

*Here we will observe the harmonic response of the dual mass design. In both cases, the force applied is volumetric with the value of 0.128 g. The Rayleigh Damping constants α and β are 0.02407.*

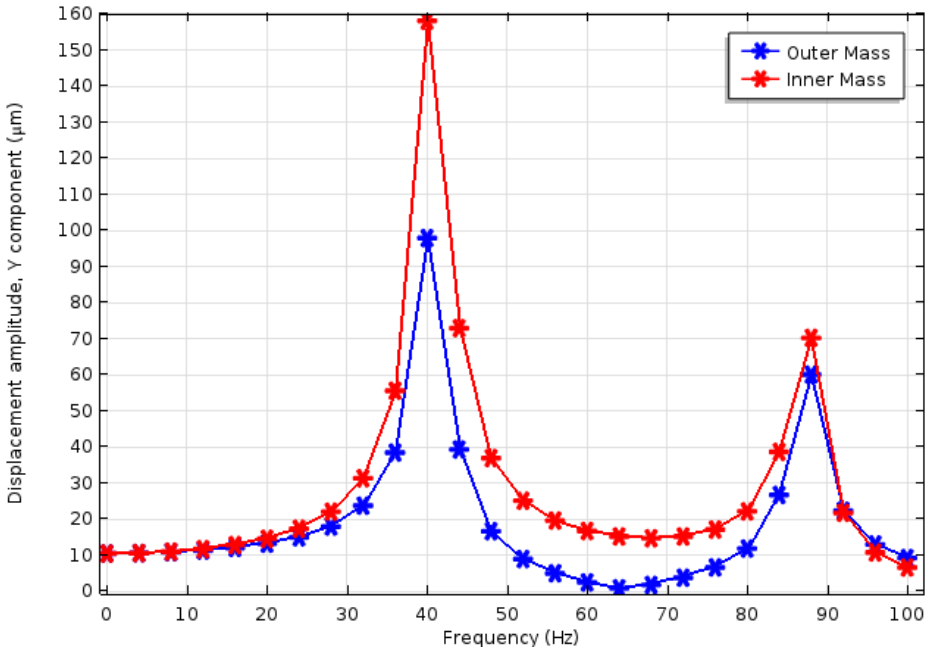


Figure 6.8: Dual Mass: Harmonic Analysis

Maximum amplitude can be seen at 40.7 Hz and 87.6 Hz.

## 6.4 Transient Analysis

Transient analysis indicate the displacement behavior of the system in any instance. In this study transient analysis has been performed on dual mass system only.

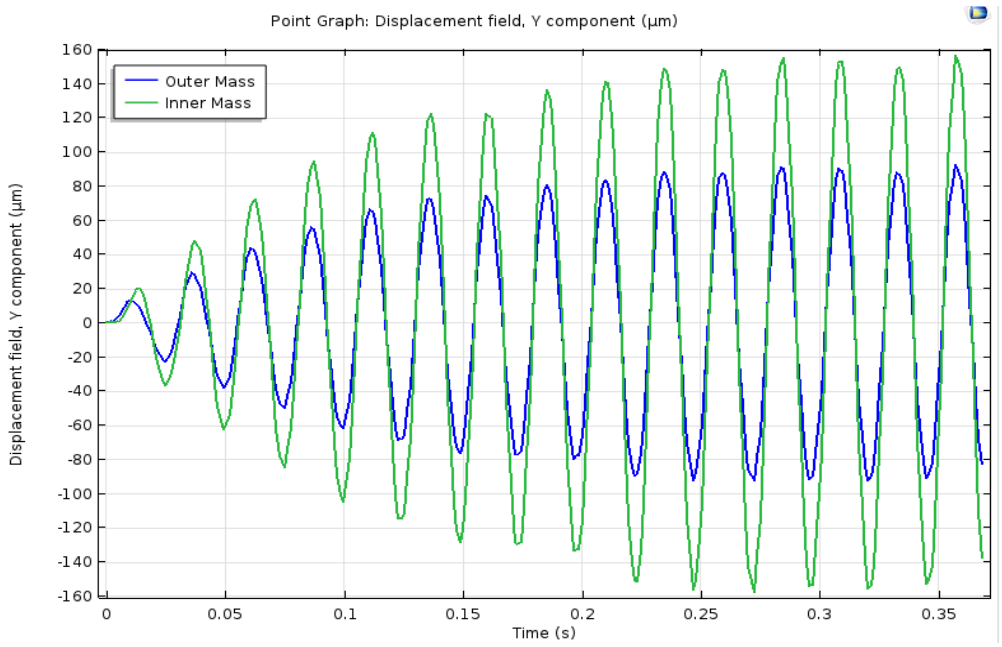


Figure 6.9: Transient Analysis of Dual Mass System

It can be seen that harvester become stable after 0.2 seconds and deliver output at constant rate.

## 6.5 Output Voltage

Voltage and Power results for the double mass are presented in the following chapter. All power calculations are done at a load resistance of 98kΩ which is equal to that of the coil resistance, as can be found from literature that the maximum power can be extracted when internal resistance is same to that of the external resistance. [112]

In dual mass system investigation, five different frequencies have been taken into consideration while calculating the output voltage and power.

**Case-I**: 40.7 Hz (First peak of harmonic Analysis)

As can be seen from below results, a maximum voltage of 18mV is induced and 0.3nW power can be extracted. The above measurements are made at the frequency of 40.7Hz and its corresponding excitation amplitude is obtained from the interpolated function extracted from the harmonic analysis.

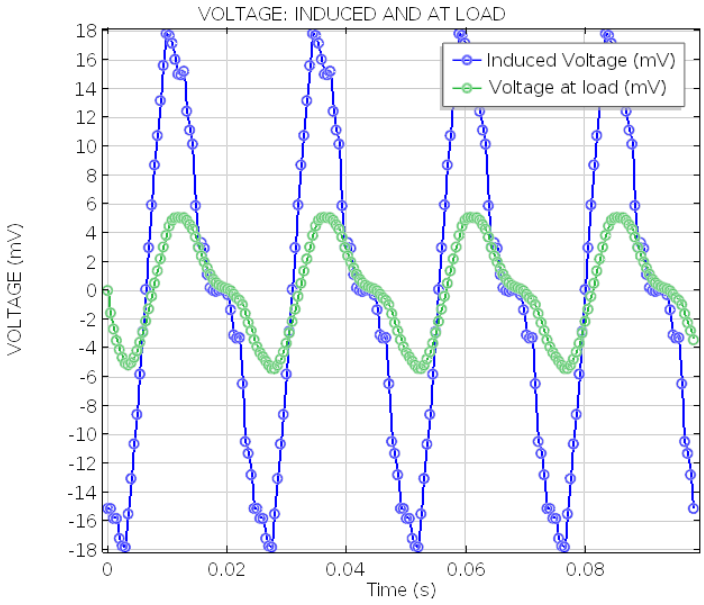


Figure 6.7: Dual Mass Induced and Load voltage of single mass at 40.7 Hz

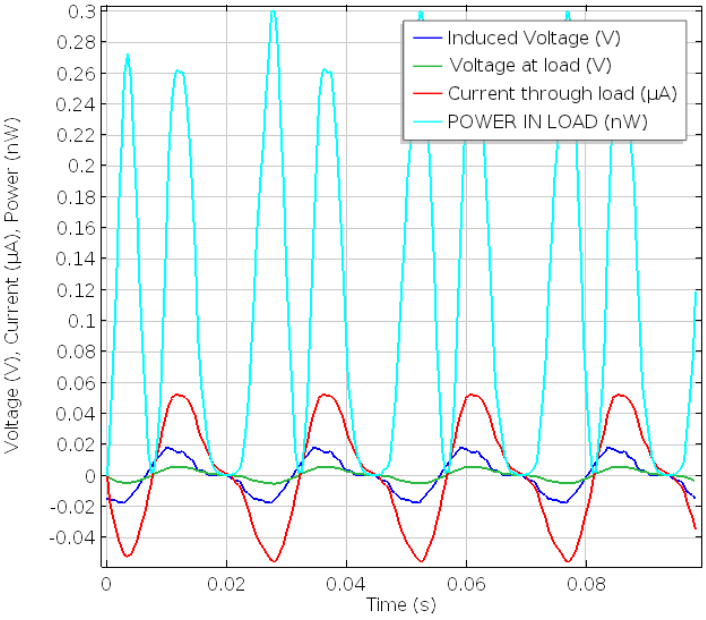


Figure 6.11: All parameters of dual mass system at 40.7 Hz.

**Case-II**: 87.6 Hz (Second peak of harmonic Analysis)

As can be seen from below results, a maximum voltage of 14.5mV is induced and 0.2nW power can be extracted. The above measurements are made at the frequency of 87.6Hz and its corresponding excitation amplitude is obtained from the interpolated function extracted from the harmonic analysis.

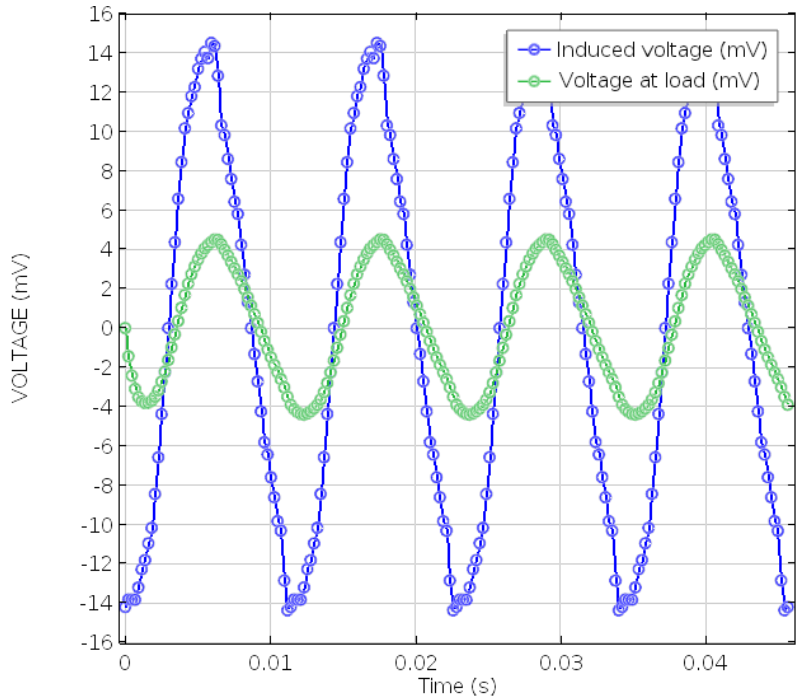


Figure 6.12: Dual Mass Induced and Load voltage of single mass at 87.6 Hz

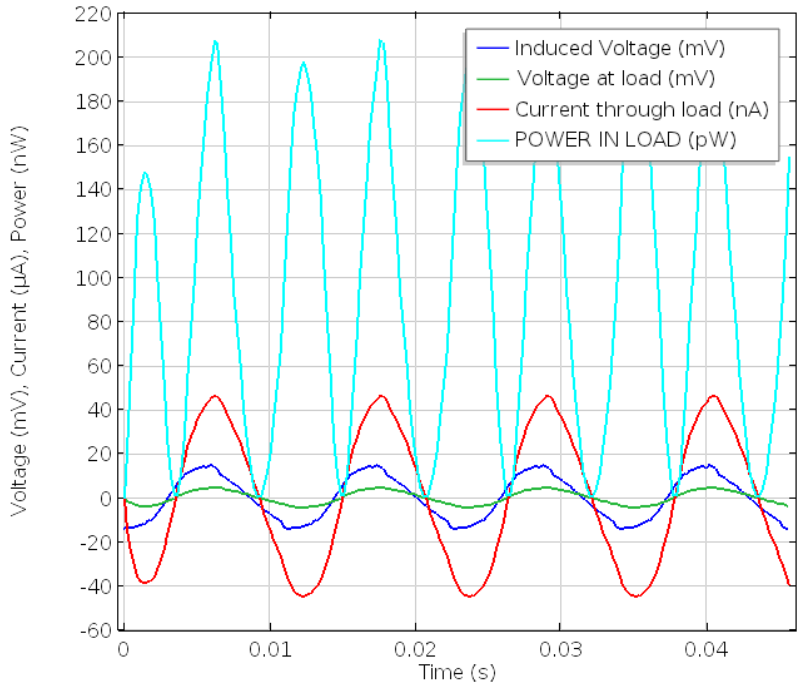


Figure 6.13: All parameters of dual mass system at 87.6 Hz.

**Case-III**: 100 Hz

As can be seen from above results, a maximum voltage of 1.5mV is induced and 4.84pW power can be extracted. The above measurements are made at the frequency of 100Hz and its

corresponding excitation amplitude is obtained from the interpolated function extracted from the harmonic analysis.

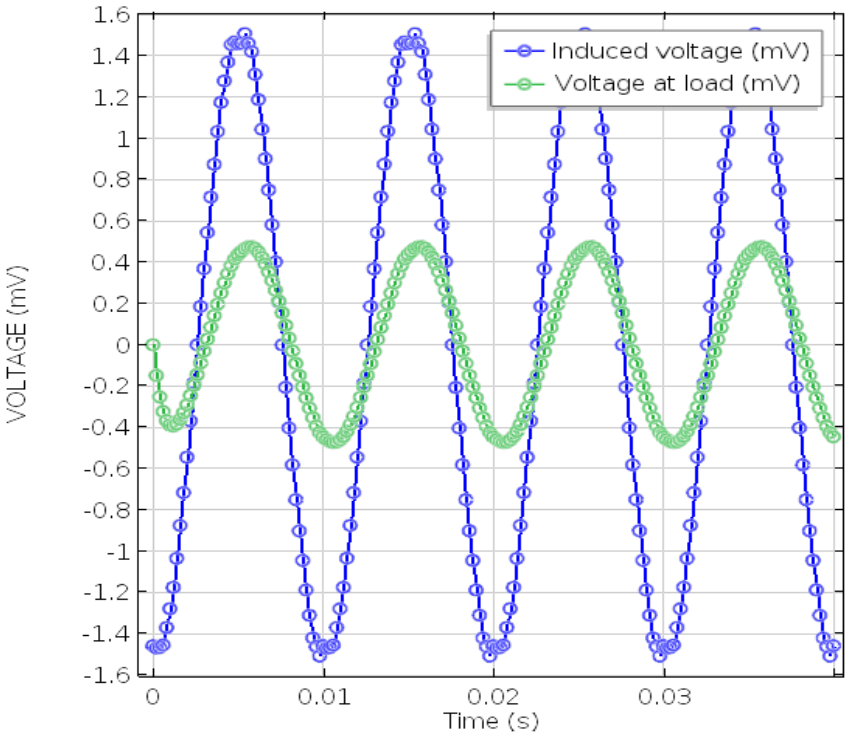


Figure 6.14: Dual Mass Induced and Load voltage of single mass at 100 Hz

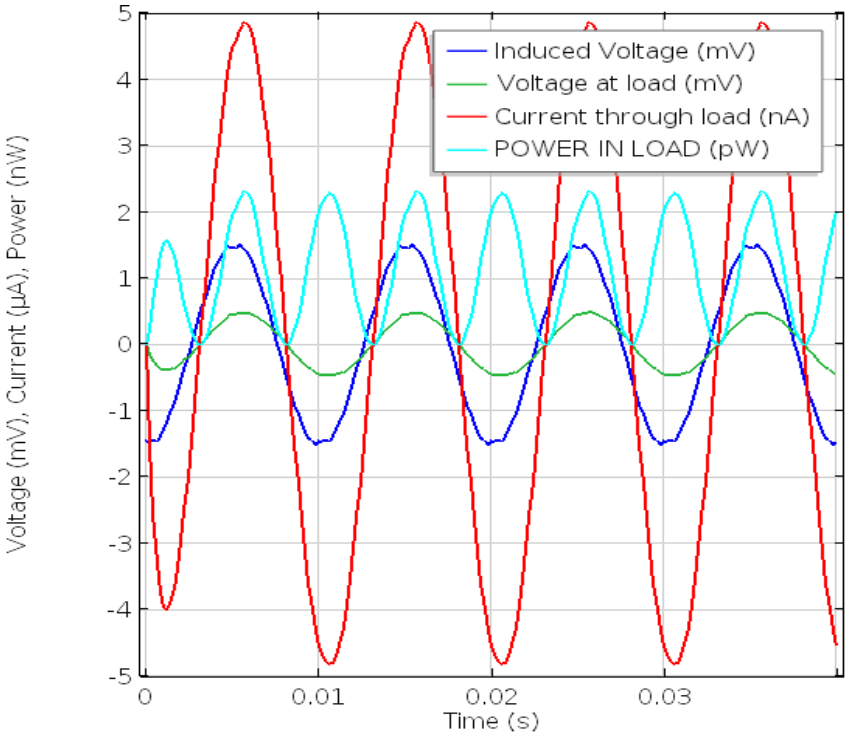


Figure 6.15: All parameters of dual mass system at 100 Hz.

**Case-IV**: 60 Hz

As can be seen from above results, a maximum voltage of 2.32mV is induced and 7.5pW power can be extracted. The above measurements are made at the frequency of 60Hz and its corresponding excitation amplitude is obtained from the interpolated function extracted from the harmonic analysis.

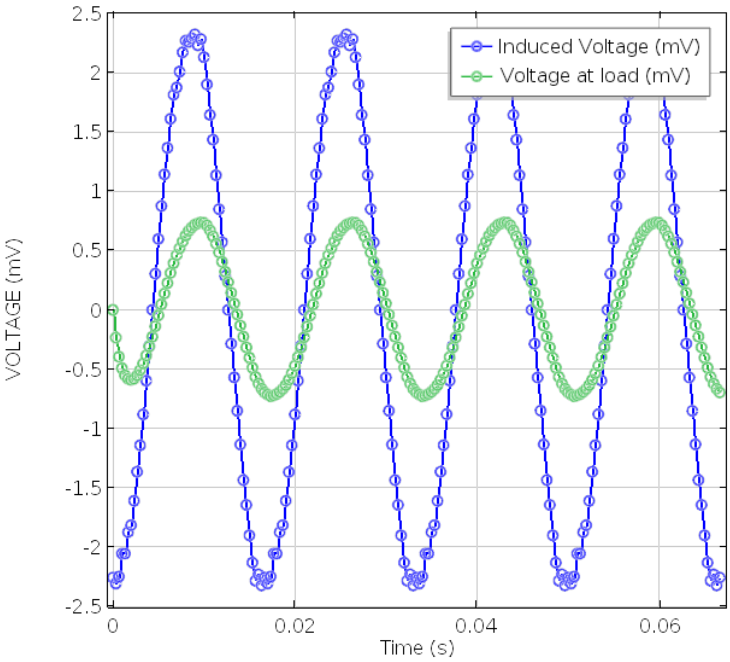


Figure 6.16: Dual Mass Induced and Load voltage of single mass at 60 Hz

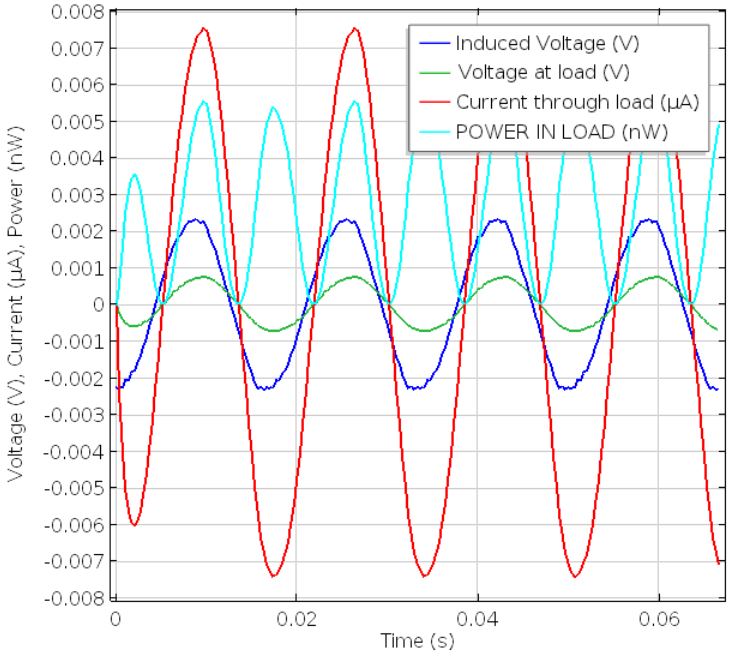


Figure 6.17: All parameters of dual mass system at 60 Hz.

**Case-V**: 20 Hz

As can be seen from above results, a maximum voltage of 0.67mV is induced and 0.215nW power can be extracted. The above measurements are made at the frequency of 87.6Hz and its corresponding excitation amplitude is obtained from the interpolated function extracted from the harmonic analysis.

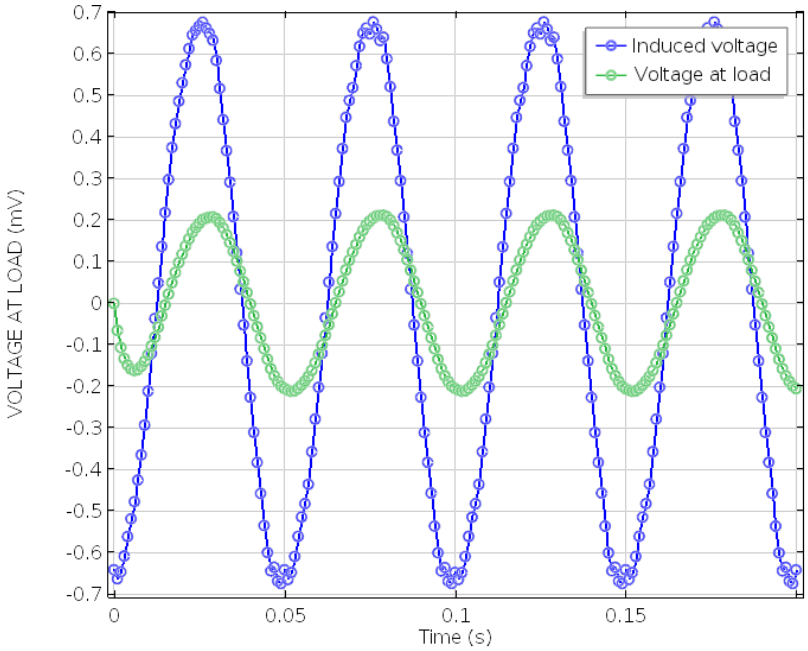


Figure 6.18: Dual Mass Induced and Load voltage of single mass at 20 Hz

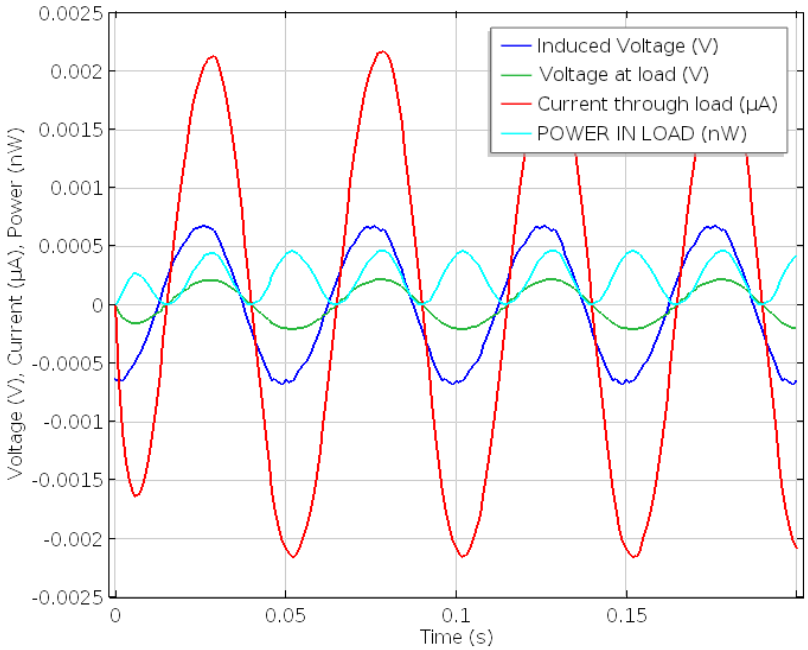


Figure 6.19: All parameters of dual mass system at 20 Hz.

## 6.6 Conclusion

As can be seen from the above results that using the dual mass approach, we can successfully harvest energy at multiple frequencies. Also the methodology adopted to widen the bandwidth is successfully implemented by using the dual mass approach, although this method reduces the peak power output but increases the average power output across its bandwidth. This can clearly be seen from the results. Also higher the frequency, more is the rate of change of flux and hence it is also an important parameter for the harvester design but in dual mass case, excitation amplitude is a dominating factor.

The output power is maximum at 40.7 Hz as expected due to the higher excitation amplitude. Then at the frequency of 80.7 Hz, we get the second maximum output where there is the second maximum value of excitation amplitude. If we consider the frequency of 60Hz between the two peaks obtained from harmonic analysis, we get the 3$^{rd}$ maximum output as this frequency lies in between the bandwidth area of harvester. And comparing the results to the frequencies other than the band between two peaks, 20Hz and 100 Hz, it can be seen that the output power is less as compared to peak frequencies due to the less gain values as compared to that of the 60Hz.

## REFERENCES


[1] W. Bertsch, J. R. Azzi, and J. B. Davidson, “Delayed light studies on photosynthetic energy conversion. I. Identification of the oxygen-evolving photoreaction as the delayed light emitter in mutants of Scenedesmus obliquus.,” *Biochim. Biophys. Acta*, vol. 143, no. 1, pp. 129–43, Jul. 1967.

[2] S. Khan, “Vibration-based electromagnetic energy harvesters for MEMS applications.,” University of British Columbia, Vancouver, 2011.

[3] M. Faraday, “Experimental Researches in Electricity,” *Philos. Trans. R. Soc. London*, vol. 122, no. January, pp. 125–162, 1832.

[4] Y. Leng, Q. Li, B. Hou, S. Liu, and T. Dong, “Wheel Antenna of Wireless Sensors in Automotive Tire Pressure Monitoring System,” in *2007 International Conference on Wireless Communications, Networking and Mobile Computing*, 2007, pp. 2755–2758.

[5] I.-H. Ho, J.-M. Chung, H.-C. Chen, and H.-W. Chiu, “A Battery-Less Tire Pressure Monitoring System,” in *VTC Spring 2009 - IEEE 69th Vehicular Technology Conference*, 2009, pp. 1–5.

[6] A. Khaligh, P. Zeng, and C. Zheng, “Kinetic Energy Harvesting Using Piezoelectric and Electromagnetic Technologies #x2014;State of the Art,” *Ind. Electron. IEEE Trans.*, vol. 57, no. 3, pp. 850–860, 2010.

[7] W. Ma, L. Rufer, Y. Zohar, and Man Wong, “Design and implementation of an integrated floating-gate electrostatic power micro-generator,” in *The 13th International Conference on Solid-State Sensors, Actuators and Microsystems, 2005. Digest of Technical Papers. TRANSDUCERS ’05.*, vol. 1, pp. 299–302.

[8] H. Search, C. Journals, A. Contact, M. Iopscience, S. Mater, and I. P. Address, “A piezoelectric vibration based generator,” vol. 1131, 2004.

[9] A. Paknejad, G. Rahimi, A. Farrokhabadi, and M. M. Khatibi, “Analytical solution of piezoelectric energy harvester patch for various thin multilayer composite beams,” *Compos. Struct.*, vol. 154, pp. 694–706, Oct. 2016.

[10] H. J. Jung and D. Song, “Which is better , electrostatic or piezoelectric energy harvesting systems”

[11] P. Miao, P. D. Mitcheson, a. S. Holmes, E. M. Yeatman, T. C. Green, and B. H. Stark,

"Mems inertial power generators for biomedical applications," *Microsyst. Technol.*, vol. 12, pp. 1079–1083, 2006.

[12] G. Poulin, E. Sarraute, and F. Costa, "Generation of electrical energy for portable devices," *Sensors Actuators A Phys.*, vol. 116, no. 3, pp. 461–471, Oct. 2004.

[13] T. Sterken, K. Baert, C. Vanhoof, R. Puers, G. Borghs, and P. Fiorini, "Comparative modelling for vibration scavengers," in *Proceedings of IEEE Sensors, 2004.*, pp. 1249–1252.

[14] Z. L. Li, M. D. Han, and H. X. Zhang, "A novel mems electromagnetic energy harvester with series coils," *National Key Laboratory of Science and Technology on Micro / Nano Fabrication , Institute of Microelectronics , Peking University , CHINA ABSTRACT* no. June, pp. 2245–2248, 2013.

[15] S. Meninger, J. O. Mur-Miranda, R. Amirtharajah, A. Chandrakasan, and J. H. Lang, "Vibration-to-electric energy conversion," *IEEE Trans. Very Large Scale Integr. Syst.*, vol. 9, no. 1, pp. 64–76, Feb. 2001.

[16] S. Roundy, P. K. Wright, and J. Rabaey, "A study of low level vibrations as a power source for wireless sensor nodes," *Comput. Commun.*, vol. 26, pp. 1131–1144, 2003.

[17] P. D. Mitcheson, S. Member, T. C. Green, and S. Member, "Maximum Effectiveness of Electrostatic Energy Harvesters When Coupled to Interface Circuits," pp. 1–14, 2012.

[18] N. Aga, N. Agasimani, C. D. Bhushanagoudra, A. Pawar, and S. Naduvinamani, "REVIEW on energy harvesting sources," vol. 12, no. 1, pp. 273–279, 2015.

[19] B. Dawoud, E. Amer, and D. Gross, "Experimental investigation of an adsorptive thermal energy storage," *Int. J. energy Res.*, vol. 31, no. August 2007, pp. 135–147, 2007.

[20] I. Sari, T. Balkan, and H. Kulah, "An electromagnetic micro energy harvester based on an array of parylene cantilevers," *J. Micromechanics Microengineering*, vol. 19, no. 10, p. 105023, Oct. 2009.

[21] H. Kulah and K. Najafi, "Energy Scavenging From Low-Frequency Vibrations by Using Frequency Up-Conversion for Wireless Sensor Applications," *IEEE Sens. J.*, vol. 8, no. 3, pp. 261–268, 2008.

[22] S. Turkyilmaz, H. Kulah, and A. Muhtaroglu, "Design and prototyping of second generation METU MEMS electromagnetic micro-power generators," *2010 Int. Conf. Energy Aware Comput. ICEAC 2010*, pp. 3–6, 2010.

[23] I. Sari, T. Balkan, and H. Kulah, “An Electromagnetic Micro Power Generator for Low Frequency Environmental Vibrations based on the Frequency Up-Conversion Technique,” *2009 IEEE 22nd Int. Conf. Micro Electro Mech. Syst.*, vol. 19, no. 1, pp. 14–27, 2010.

[24] Ö.¨Zorlu, E. T. Topal, and H. Külah, “A vibration-based electromagnetic energy harvester using mechanical frequency up-conversion method,” *IEEE Sens. J.*, vol. 11, no. 2, pp. 481–488, 2011.

[25] A. Rahimi, O. Zorlu, A. Muhtaroglu, and H. Kulah, “Fully Self-Powered Electromagnetic Energy Harvesting System With Highly Efficient Dual Rail Output,” *IEEE Sens. J.*, vol. 12, no. 6, pp. 2287–2298, Jun. 2012.

[26] M. El-hami, P. Glynne-Jones, N. M. White, M. Hill, S. Beeby, E. James, a. D. Brown, and J. N. Ross, “Design and fabrication of a new vibration-based electromechanical power generator,” *Sensors Actuators, A Phys.*, vol. 92, pp. 335–342, 2001.

[27] E. P. James, M. J. Tubor, S. P. Beeby, N. R. Harris, P. Glynne-Jones, J. N. Ross, and N. M. White, “An investigation of self-powered systems for condition monitoring applications,” *Sensors Actuators, A Phys.*, vol. 110, pp. 171–176, 2004.

[28] E. Minazara, D. Vasic, F. Costa, and G. Poulin, “Piezoelectric diaphragm for vibration energy harvesting.,” *Ultrasonics*, vol. 44 Suppl 1, no. 1–3, pp. e699–703, Dec. 2006.

[29] R. Torah, S. P. Beeby, M. J. Tudor, T. O’Donnell, and S. Roy, “Development of a Cantilever Beam Generator Employing Vibration Energy Harvestin,” no. 1, pp. 4–7, 2006.

[30] S. Kulkarni, S. Roy, T. O’Donnell, S. Beeby, and J. Tudor, “Vibration based electromagnetic micropower generator on silicon,” *J. Appl. Phys.*, vol. 99, pp. 2006–2008, 2006.

[31] E. Koukharenko, S. P. Beeby, M. J. Tudor, N. M. White, T. O’Donnell, C. Saha, S. Kulkarni, and S. Roy, “Microelectromechanical systems vibration powered electromagnetic generator for wireless sensor applications,” *Microsyst. Technol.*, vol. 12, pp. 1071–1077, 2006.

[32] C. R. Saha, T. O’Donnell, H. Loder, S. Beeby, and J. Tudor, “Optimization of an electromagnetic energy harvesting device,” *IEEE Trans. Magn.*, vol. 42, no. 10, pp. 3509–3511, 2006.

[33] R. N. Torah, M. J. Tudor, K. Patel, I. N. Garcia, and S. P. Beeby, “Autonomous low power microsystem powered by vibration energy harvesting,” *Proc. IEEE Sensors*, pp.

264–267, 2007.

[34] T. O'Donnell, C. Saha, S. Beeby, and J. Tudor, "Scaling effects for electromagnetic vibrational power generators," *Microsyst. Technol.*, no. April, pp. 26–28, 2007.

[35] S. P. Beeby, M. J. Tudor, R. N. Torah, S. Roberts, T. O'Donnell, and S. Roy, "Experimental COMPARISON of macro and micro scale electromagnetic vibration powered generators," *Microsyst. Technol.*, vol. 13, pp. 1647–1653, 2007.

[36] S. P. Beeby, R. N. Torah, M. J. Tudor, P. Glynne-Jones, T. O'Donnell, C. R. Saha, and S. Roy, "A micro electromagnetic generator for vibration energy harvesting," *J. Micromechanics Microengineering*, vol. 17, no. 7, pp. 1257–1265, 2007.

[37] K. Tao, J. Wu, L. Tang, X. Xia, S. W. Lye, J. Miao, and X. Hu, "A novel two-degree-of-freedom MEMS electromagnetic vibration energy harvester," *J. Micromechanics Microengineering*, vol. 26, no. 3, p. 035020, 2016.

[38] Q. Zhang and E. S. Kim, "Micromachined energy-harvester stack with enhanced electromagnetic induction through vertical integration of magnets," *J. Microelectromechanical Syst.*, vol. 24, no. 2, pp. 384–394, 2015.

[39] X. Dai, X. Miao, L. Sui, H. Zhou, X. Zhao, and G. Ding, "SPRINGS-Tuning of nonlinear vibration via topology variation and its application in energy harvesting," *Appl. Phys. Lett.*, vol. 100, no. 3, 2012.

[40] J. Yonggang, M. Shingo, F. Takayuki, U. Minoru, T. Tomohiko, F. Kouhei, H. Kohei, and M. Kazusuke, "imp. Fabrication of a vibration-driven electromagnetic energy harvester with integrated NdFeB/Ta multilayered micro-magnets," *J. Micromechanics Microengineering*, vol. 21, no. 9, p. 95014, 2011.

[41] K. Yamaguchi, Y. Tanaka, T. Fujita, N. Takehira, K. Sonoda, K. Kanda, and K. Maenaka, "Optimization and Experiment of Electromagnetic Energy Harvester by Using NdFeB Sputtered on High-aspect-ratio Corrugated Si," *J. Phys. Conf. Ser.*, vol. 557, p. 012056, 2014.

[42] S. Miki, T. Fujita, T. Kotoge, Y. G. Jiang, M. Uehara, K. Kanda, K. Higuchi, and K. Maenaka, "Electromagnetic energy harvester by using buried NdFeB," *Proc. IEEE Int. Conf. Micro Electro Mech. Syst.*, pp. 1221–1224, 2012.

[43] C. Cepnik, "a micro energy harvester with 3d wire bonded microcoils," *Graduate School Micro Energy Harvesting , Laboratory for Microactuators , Germany* pp. 665–668, 2011.

[44] C. B. Williams and R. B. Yates, “Analysis Of A Micro-electric Generator For Microsystems,” *Proc. Int. Solid-State Sensors Actuators Conf. - TRANSDUCERS ’95*, vol. 1, no. 0, 1995.

[45] C. S. R. B. Yates, “Development of an electromagnetic micro- generator,” *Electron. Lett.*, vol. 33, no. 22, pp. 1883–1884, 1997.

[46] V. P. Generation, R. Amirtharajah, and A. P. Chandrakasan, “Self-Powered Signal Processing Using,” *Commun. Soc.*, vol. 33, no. 5, pp. 687–695, 1998.

[47] N. N. H. Ching, H. Y. Wong, W. J. Li, P. H. W. Leong, and Z. Wen, “A Laser-micromachined Vibrational to Electrical Power Transducer for Wireless Sensing Systems,” *Inter.Conf. on Solid-state sensors and Actuators*, vol. 98, no. June, pp. 1–4, 2001.

[48] C. B. Williams, C. Shearwood, M. a. Harradine, P. H. Mellor, T. S. Birch, and R. B. Yates, “Development of an electromagnetic micro-generator,” *IEE Proc. - Circuits, Devices Syst.*, vol. 148, p. 337, 2001.

[49] S. P. Beeby, M. J. Tudor, E. Koukharenko, N. M. White, T. O’Donnell, C. Saha, S. Kulkarni, and S. Roy, “Micromachined silicon Generator for Harvesting Power from Vibrations,” pp. 2–5, 2004.

[50] P. G. Jones, M. J. Tudor, S. P. Beeby, and N. M. White, “An electromagnetic, vibration-powered generator for intelligent sensor systems,” *Sensors Actuators, A Phys.*, vol. 110, pp. 344–349, 2004.

[51] S. P. Beeby, M. J. Tudor, E. Koukharenko, N. M. White, T. O’Donnell, C. Saha, S. Kulkarni, and S. Roy, “Design and performance of a microelectromagnetic vibration powered generator,” *13th Int. Conf. Solid-State Sensors, Actuators Microsystems, 2005. Dig. Tech. Pap. TRANSDUCERS ’05.*, vol. 1, pp. 5–8, 2005.

[52] S. Beeby, M. Tudor, R. Torah, E. Koukarenko, S. Roberts, T. O’Donnell, and C. Saha, “Macro and Micro Scale Electromagnetic Kinetic Energy Harvesting Generators,” *J. Microsyst. Technol.*, no. April, pp. 26–28, 2006.

[53] X. Cao and Y. K. Lee, “Design and fabrication of mini vibration power generator system for micro sensor networks,” *Proc. IEEE ICIA 2006 - 2006 IEEE Int. Conf. Inf. Acquis.*, pp. 91–95, 2006.

[54] C. Saha, T. O’donnell, H. Loder, S. Beeby, and J. Tudor, “Optimization of an

electromagnetic energy harvesting device, IEEE Trans," *Magn. 42 (October (*, vol. 10, no. 10, pp. 3509–3511, 2006.

[55] A. P´erez-Rodr´ıguez, C. Serre, N. Fondevilla, C. Cereceda, J. R. Morante, E. J, and J. Montserrat, "electromagnetic inertial generator for vibrational energy scavenging compatible with si technology," *Eurosensors XIX (Barcelona, Spain)*, vol. 1, pp. 57–60, 2005.

[56] S. P. Beeby, R. N. Torah, M. J. Tudor, P. Glynne-Jones, T. O'Donnell, C. R. Saha, and S. Roy, "NPD: A micro electromagnetic generator for vibration energy harvesting," vol. 17, pp. 1257–1265, 2007.

[57] S. Kulkarni, E. Koukharenko, J. Tudor, S. Beeby, T. O'Donnell, and S. Roy, "Fabrication and test of integrated micro-scale vibration based electromagnetic generator," *Transducers Eurosensors '07 - 4th Int. Conf. Solid-State Sensors, Actuators Microsystems*, pp. 879–882, 2007.

[58] I. Sari, T. Balkan, and H. Kulali, "A wideband electromagnetic micro power generator for wireless microsystems," *Transducers Eurosensors '07 - 4th Int. Conf. Solid-State Sensors, Actuators Microsystems*, pp. 275–278, 2007.

[59] D. Hohlfeld, R. Vullers, and J. Boeck, "NOVEL DESIGN: An electromagnetic energy harvester for low frequency excitation," *Integr. Issues …*, 2008.

[60] S. Kulkarni, E. Koukharenko, R. Torah, J. Tudor, S. Beeby, T. O'Donnell, and S. Roy, "Design, fabrication and test of integrated micro-scale vibration-based electromagnetic generator," *Sensors Actuators, A Phys.*, vol. 145–146, pp. 336–342, 2008.

[61] H. Kulah and K. Najafi, "Energy Scavenging From Low-Frequency Vibrations by Using Frequency Up-Conversion for Wireless Sensor Applications," *Sensors Journal, IEEE*, vol. 8, no. 3, pp. 261–268, 2008.

[62] C. R. Saha, T. O'Donnell, N. Wang, and P. McCloskey, "Electromagnetic generator for harvesting energy from human motion," *Sensors Actuators, A Phys.*, vol. 147, pp. 248–253, 2008.

[63] M. S. M. Soliman, E. F. El-Saadany, E. M. Abdel-Rahman, and R. R. Mansour, "Design and modeling of a wideband MEMS-based energy harvester with experimental verification," *1st Microsystems Nanoelectron. Res. Conf. MNRC 2008 - Enabling Synerg. Accel. Excell. Grad. Student Res.*, pp. 193–196, 2008.

[64] R. Torah, P. Glynne-Jones, M. Tudor, T. O'Donnell, S. Roy, and S. Beeby, "Self-powered autonomous wireless sensor node using vibration energy harvesting," *Meas. Sci. Technol.*, vol. 19, p. 125202, 2008.

[65] M. Zhang, D. Brignac, P. Ajmera, and K. Lian, "A Low-Frequency Vibration-to-Electrical Energy Harvester Min," *Proc. SPIE*, vol. 6931, p. 69310S–69310S–12, 2008.

[66] Æ. Joan and R. Morante, "Design and implementation of mechanical resonators for optimized inertial electromagnetic microgenerators," pp. 653–658, 2008.

[67] I. Ayala Garcia, D. Zhu, J. Tudor, and S. Beeby, "Autonomous Tunable Energy Harvester," vol. 2, pp. 3–6, 2009.

[68] E. Bouendeu, a Greiner, P. J. Smith, and J. G. Korvink, "an Efficient Low Cost Electromagnetic Vibration Harvester of Harvesters," *Pmems2009*, pp. 320–323, 2009.

[69] B. Dick, M. Fralick, H. Jazo, M. Kerber, J. Brewer, R. Waters, and S. Member, "Optimization of kinetic energy harvester for low amplitude vibration," pp. 1840–1843, 2009.

[70] N. Fondevilla, C. Serre, a. Perez-Rodriguez, J. R. Morante, J. Montserrat, and J. Esteve, "Design and fabrication of Si technology miicrogenerators for vibrational energy scavenging," *2009 Spanish Conf. Electron Devices*, vol. 00, no. C, pp. 262–265, 2009.

[71] Z. Hadas, C. Ondrusek, and V. Singule, "Increasing SENSITIVITY of vibration energy harvester," *Proc. SPIE*, vol. 7362, pp. 736203–736203–8, 2009.

[72] G. Hatipoglu and H. Urey, "Procedia Chemistry FR4-based electromagnetic energy harvester for wireless tyre sensor nodes," *PROCHE*, vol. 1, no. 1, pp. 1211–1214, 2009.

[73] B. Mack, K. Kratt, M. Stürmer, and U. Wallrabe, "Electromagnetic micro generator array consisting of 3D micro coils opposing a magnetic PDMS membrane," *TRANSDUCERS 2009 - 15th Int. Conf. Solid-State Sensors, Actuators Microsystems*, pp. 1397–1400, 2009.

[74] D. Marioli, E. Sardini, and M. Serpelloni, "Electromagnetic Generators Employing Planar Inductors for Autonomous Sensor Applications," *Procedia Chem.*, vol. 1, no. 1, pp. 469–472, 2009.

[75] T. Paper, "A micro electromagnetic low level vibration energy harvester based on MEMS technology," pp. 941–951, 2009.

[76] N. Wang, D. P. Arnold, and I. M. Group, "Fully Batch-Fabricated Mems Magnetic Vibrational Energy Harvesters," pp. 348–351, 2009.

[77] P. Wang, X. Dai, X. Zhao, and G. Ding, “a Micro Electromagnetic Vibration Energy Harvester With Sandwiched Structure and Air Channel for High Energy Conversion Efficiency,” *Design*, pp. 4–7, 2009.

[78] V. P. Generator, Z. Wang, B. Wang, M. Wang, H. Zhang, and W. Huang, “MODEL ONLY, and Experimental Study of Permanent Magnet,” vol. 20, no. 3, pp. 1110–1113, 2010.

[79] J. C. Park, D. H. Bang, and J. Y. Park, “Micro-fabricated electromagnetic power generator to scavenge low ambient vibration,” *IEEE Trans. Magn.*, vol. 46, no. 6, pp. 1937–1942, 2010.

[80] B. Yang and C. Lee, “Non-resonant electromagnetic wideband energy harvesting mechanism for low frequency vibrations,” *Microsyst. Technol.*, vol. 16, pp. 961–966, 2010.

[81] I. Sari, T. Balkan, and H. Külah, “An electromagnetic micro power generator for low-frequency environmental vibrations based on the frequency upconversion technique,” *J. Microelectromechanical Syst.*, vol. 19, no. 1, pp. 14–27, 2010.

[82] S. Turkyilmaz, and A. Muhtaroglu, “Design and Prototyping of Second Generation,” pp. 3–6, 2010.

[83] D. Zhu, S. Roberts, M. J. Tudor, and S. P. Beeby, “Design and experimental characterization of a tunable vibration-based electromagnetic micro-generator,” *Sensors Actuators, A Phys.*, vol. 158, no. 2, pp. 284–293, 2010.

[84] E. T. Topal, “Coupled Electromagnetic – Dynamic FEM Simulation of a High Frequency MEMS Energy Harvester Electromagnetic Energy Harvester using,” 2011.

[85] T. Galchev, H. Kim, and K. Najafi, “Diff. Micro power generator for harvesting low-frequency and nonperiodic vibrations,” *J. Microelectromechanical Syst.*, vol. 20, no. 4, pp. 852–866, 2011.

[86] Q. Yuan, S. Member, and X. Sun, “**Design and Microfabrication of Integrated Magnetic,” pp. 1855–1858, 2011.

[87] X. Xing, G. M. Yang, M. Liu, J. Lou, O. Obi, and N. X. Sun, “*’For piezo, see end Para', High power density vibration energy harvester with high permeability magnetic material,” *J. Appl. Phys.*, vol. 109, pp. 1–3, 2011.

[88] E. Bouendeu, A. Greiner, P. J. Smith, and J. G. Korvink, “A Low-Cost Electromagnetic

Generator for Vibration Energy Harvesting," vol. 11, no. 1, pp. 107–113, 2011.

[89] R. Dayal, S. Dwari, and L. Parsa, "A new design for vibration-based electromagnetic energy harvesting systems using coil inductance of microgenerator," *IEEE Trans. Ind. Appl.*, vol. 47, no. 2, pp. 820–830, 2011.

[90] C. Cepnik and U. Wallrabe, "A flat high performance micro energy harvester based on a serpentine coil with a single winding," *2011 16th Int. Solid-State Sensors, Actuators Microsystems Conf. Transducers'11*, pp. 661–664, 2011.

[91] E. Bouendeu, A. Greiner, P. J. Smith, and J. G. Korvink, "Design synthesis of electromagnetic vibration-driven energy generators using a variational formulation," *J. Microelectromechanical Syst.*, vol. 20, no. 2, pp. 466–475, 2011.

[92] A. R. M. Foisal, B. C. Lee, and G. S. Chung, "Fabrication and performance optimization of an AA size electromagnetic energy harvester using magnetic spring," *Proc. IEEE Sensors*, pp. 1125–1128, 2011.

[93] C. P. Jong and Y. P. Jae, "A Bulk Micromachined Electromagnetic Micro-Power Generator for an Ambient Vibration-energy-harvesting System," *J. Korean Phys. Soc.*, vol. 58, no. 5, p. 1468, 2011.

[94] A. Arbor, "Harvesting Traffic-Induced Bridge Vibrations," University of Michigan , Michigan 48109-2122 , USA," pp. 1661–1664, 2011.

[95] E. Sardini and M. Serpelloni, "Sensors and Actuators A : Physical An efficient electromagnetic power harvesting device for low-frequency applications," *Sensors Actuators A. Phys.*, vol. 172, no. 2, pp. 475–482, 2011.

[96] Q. Zhang, S. J. Chen, L. Baumgartel, a. Lin, and E. S. Kim, "Microelectromagnetic energy harvester with integrated magnets," *2011 16th Int. Solid-State Sensors, Actuators Microsystems Conf. Transducers'11*, pp. 1657–1660, 2011.

[97] P. Wang, W. Li, and L. Che, "Design and fabrication of a micro electromagnetic vibration energy harvester," *J. Semicond.*, vol. 32, no. 10, p. 104009, 2011.

[98] F. Khan, F. Sassani, and B. Stoeber, "Copper foil-type vibration-based electromagnetic energy harvester," *ASME Int. Mech. Eng. Congr. Expo. Proc.*, vol. 10, pp. 371–380, 2010.

[99] A. Muhtaro, "Improved Second Generation Electromagnetic MEMS Energy Scavenger," pp. 8–11, 2011.

[100] S. E. Jo, M. S. Kim, and Y. J. Kim, "Electromagnetic human vibration energy harvester

comprising planar coils," *Electron. Lett.*, vol. 48, no. 14, p. 874, 2012.

[101] P. Wang, X. Dai, X. Zhao, Z. Wang, and Z. Yang, "Development of microelectromechanical systems electromagnetic vibration energy scavengers with a nonlinear electroplated nickel spring," *Micro Nano Lett.*, vol. 7, pp. 1173–1175, 2012.

[102] K. Tao, G. Ding, P. Wang, Z. Yang, and Y. Wang, "Fully integrated micro electromagnetic vibration energy harvesters with micro-patterning of bonded magnets," *Proc. IEEE Int. Conf. Micro Electro Mech. Syst.*, pp. 1237–1240, 2012.

[103] I. M. Group, "MEMS Electrodynamic Vibrational Energy Harvesters using Multi-Pole Magnetic Architectures," vol. 0, pp. 6–9, 2012.

[104] H. Liu, B. W. Soon, N. Wang, C. J. Tay, C. Quan, and C. Lee, "Feasibility study of a 3D vibration-driven electromagnetic MEMS energy harvester with multiple vibration modes," *J. Micromechanics Microengineering*, vol. 22, p. 125020, 2012.

[105] J. Chen, D. Chen, T. Yuan, and X. Chen, "A multi-frequency sandwich type electromagnetic vibration energy harvester," *Appl. Phys. Lett.*, vol. 100, no. May, 2012.

[106] A. R. M. Foisal and G.-S. Chung, "Design, Fabrication and characterization of a low frequency electromagnetic energy harvester," *J. Semicond.*, vol. 33, no. 7, p. 074001, 2012.

[107] S. Miki, T. Fujita, T. Kotoge, Y. G. Jiang, M. Uehara, K. Kanda, K. Higuchi, and K. Maenaka, "Electromagnetic energy harvester by using buried NdFeB," *Proc. IEEE Int. Conf. Micro Electro Mech. Syst.*, no. February, pp. 1221–1224, 2012.

[108] S. Roundy and E. Takahashi, "A cost-effecitve planar electromagnetic energy harvesting transducer," *Proc. PowerMEMS 2012*, pp. 10–13, 2012.

[109] Y. Tanaka, T. Fujita, T. Kotoge, K. Yamaguchi, K. Sonoda, K. Kanda, and K. Maenaka, "Design optimization of electromagnetic MEMS energy harvester with serpentine coil," *Proc. - 2013 IEEE Int. Conf. Green Comput. Commun. IEEE Internet Things IEEE Cyber, Phys. Soc. Comput. GreenCom-iThings-CPSCom 2013*, pp. 1656–1658, 2013.

[110] K. Ashraf, M. H. Khir, J. O. Dennis, and Z. Baharudin, "Sensors and Actuators A : Physical Improved energy harvesting from low frequency vibrations by resonance amplification at multiple frequencies," *Sensors Actuators A. Phys.*, vol. 195, pp. 123–132, 2013.

[111] D. Bang and J. Park, "Bulk Micromachined Vibration Driven Electromagnetic Energy

Harvesters for Self-sustainable Wireless Sensor Node Applications," vol. 8, no. 6, pp. 1320–1327, 2013.

[112] H. Liu, Y. Qian, and C. Lee, "A multi-frequency vibration-based MEMS electromagnetic energy harvesting device," *Sensors Actuators, A Phys.*, vol. 204, pp. 37–43, 2013.

[113] H. Liu, Y. Qian, N. Wang, S. Member, and C. Lee, "An In-Plane Approximated Nonlinear MEMS Electromagnetic Energy Harvester," pp. 1–10, 2013.

[114] Q. Zhang and E. S. Kim, "Energy harvesters with high electromagnetic conversion efficiency through magnet and coil arrays," *Proc. IEEE Int. Conf. Micro Electro Mech. Syst.*, pp. 110–113, 2013.

[115] M. Han, Q. Yuan, X. Sun, and H. Zhang, "Design and Fabrication of Integrated Magnetic MEMS Energy Harvester for Low," vol. 23, no. 1, pp. 204–212, 2014.

[116] S.-J. Chen, J.-Y. Wu, and S.-Y. Liu, "Electromagnetic energy harvester with an in-phase vibration bandwidth broadening technique," *2014 IEEE 27th Int. Conf. Micro Electro Mech. Syst.*, pp. 382–384, 2014.

[117] M. Han, W. Liu, B. Meng, X.-S. Zhang, X. Sun, and H. Zhang, "Springless cubic harvester for converting three dimensional vibration energy," *2014 IEEE 27th Int. Conf. Micro Electro Mech. Syst.*, pp. 425–428, 2014.

[118] H. Liu, K. How Koh, and C. Lee, "Ultra-wide frequency broadening mechanism for micro-scale electromagnetic energy harvester," *Appl. Phys. Lett.*, vol. 104, p. 053901, 2014.

[119] T. Shirai, Y. Wakasa, T. Nakagawa, K. Nomura, and H. Yagyu, "ELECTROMAGNETIC ENERGY HARVESTER WITH HIGH EFFICIENCY USING MICRO-MACHINING SI SPRINGS x ( t )," *27TH Int. Conf. MEMS*, pp. 378–381, 2014.

[120] K. Yamaguchi, T. Fujita, Y. Tanaka, N. Takehira, K. Sonoda, K. Kanda, and K. Maenaka, "MEMS Batch Fabrication of the Bipolar Micro Magnet Array for Electromagnetic Vibration Harvester," *J. Phys. Conf. Ser.*, vol. 557, p. 012033, 2014.

[121] Q. Zhang and E. S. Kim, "Micromachined Energy-Harvester Stack With Vertical Integration of Magnets," pp. 1–11, 2014.

[122] M. Bendame, E. Abdel-rahman, and M. Soliman, *w=sqrt (k/m) - Electromagnetic Impact Vibration Energy Harvesters*. 2015.

[123] Q. Zhang, Y. Wang, L. Zhao, and E. S. Kim, "Integration of microfabricated low

resistance and thousand-turn coils for vibration energy harvesting," *J. Micromechanics Microengineering*, vol. 26, no. 2, p. 025019, 2016.

[124] C. W. Dyck, J. J. Allen, and R. J. Huber, "Parallel-Plate Electrostatic Dual-Mass Oscillator," no. 505.

[125] B. H. Russ and P. S. K. Gupta, "Development Of a CAD Model Simplification Framework for Finite Element Analysis," 2012.

[126] W. Wang, J. Jia, and J. Li, "Slide film damping in microelectromechanical system devices," *Proc. Inst. Mech. Eng. Part N J. Nanoeng. Nanosyst.*, vol. 227, no. 4, pp. 162–170, 2013.

# Appendix A

## INNER MASS COMPUTATIONS

- Inner Mass:

Using,

Mass= Density x Volume &

Volume=Length x Width x Thickness

Volume of Magnets = 8[mm] x 5[mm] x 0.02[mm] = 0.8[$mm^3$] = $8^{E-10}$ [$m^3$]

Mass = 0.00000588[kg]

Volume of Ni Plate = 8[mm] x 5[mm] x 0.02[mm] = 0.8[$mm^3$] = $8^{E-10}$ [$m^3$]

Mass = 0.00000712[kg]

Total Mass = 0.000013[kg]

- Inner Spring Constant:

Using,

$$\omega_n = \sqrt{\frac{K}{m}}$$

$K_{inner}$ = 1.283[N/m] @ f = 50[Hz]

- Inner Spring Larger Length:

Using,

$$K = \frac{2*E*t*w^3}{L^3}$$

L = 2.75[mm]

## OUTER MASS COMPUTATIONS

- For frequency of Using dual mass design approach:

$$\frac{\omega_{inner\_mass}}{\omega_{outer\_mass}} = \frac{f_{inner\_mass}}{f_{outer\_mass}} = 0.8$$

$f_{outer}$ = 62.5[Hz] @ $f_{inner}$ = 50[Hz] & $\omega = 2*\pi*f$

- Outer Spring Constant:

Using,

$\omega_n = \sqrt{\frac{K}{m}}$

$K_{outer}$ = 4.0095[N/m]

- Outer Spring Larger Length:

Using:

$K = \frac{2*E*t*w^3}{L^3}$

L = *1.9002*[m]

NOTE-1: In Comsol, width of outer spring was kept 10µm instead of 15µm to get in plane motion

- For outer mass computation, using dual mass design approach:

$\mu = \frac{m_{inner}}{m_{outer}} = 0.5$

$m_{outer}$ = 0.00026[kg] @ $m_{inner}$ = 0.000013[kg]

- Mass distribution in equal proportion in four parts:

Using,

$Density = \frac{mass}{volume}$

Equivalent volume of Nickel Mass (0.00026 kg) = $2.9213E^{-9}[m^3]$

Vertical Length = 2*[0.046mm+0.046mm+00.046mm+0.015mm+0.015mm] (combined length of springs on top and bottom) + 5[mm] (height of magnets) + 6[mm] (width of top and bottom mass = 3mm each kept constant)
= *11.336*[mm] = 0.011336[m]

For Left and right mass Dimensions:

Using,

Volume=Length x Width x Thickness

Using values above: Volume = $7.3033E^{-10}[m^3]$, Length = 0.011336[m], Thickness = $0.2E^5$[m]

Width of left horizontal mass = width of right horizontal mass = 0.003221[m] = *3.221*[mm]

For Top and Bottom mass Dimensions:

Remaining Volume= $\frac{2.9213E^{-9}}{2}$ = $1.4606\ E^{-9}[m^3]$

One side Volume= $\frac{1.4606E^{-9}}{2}$ = $7.3033E^{-10}[m^3]$

Using,
Volume=Length x Width x Thickness
Using these values above:
Volume = $7.3033E^{-10}[m^3]$, Width = *0.003* (kept constant) [m] & Thickness = $0.2E^{5}$[m]
Length of top horizontal Mass = Length of top vertical mass = 0.00121722[m] = 12.1722[mm]
NOTE-2: Smaller lengths were designed to get internal mass frequency of 50[Hz] and outer
mass frequency of 62.5[Hz]

**Coil Calculation:**

Width = 3[µm] = 0.000003[m]
L = $6.25E^{-4}$[m] x $8E^{-3}$[m]

- $L = \frac{6.25E^{-4} \text{ x } 8E^{-3}}{3^{-6}}$ = 0.8333[m] for single coil

Total length = 0.8333 x 8 = 6.668[m]

- $R = \rho \frac{l}{A} = 98[k\Omega]$ at A = $6.125E^{-7}$[µm]

- No of Turns:

**#Matlab code for No of Turns**

```
width = 0.625*10^-3;
height = 8*10^-3;
area = width * height;
wireLengthLimit = 1;
wireWidth  = 3*10^-5;
gap = 3*10^-5;

no_Turn = -1;
wireLength = 0;

while (area>0 && wireLength<wireLengthLimit)

   no_Turn = no_Turn + 1;

   width = width - (2*gap) - (2*wireWidth);
   height = height - (2*gap) - (2*wireWidth);

   area = width * height;

   wireLength = wireLength + (2*width + 2*height - gap);
end
no_Turn
```

# Appendix B

## Analytical Modelling

An electromagnetic harvester is considered as the mass-spring system with a proof mass *m,* which is suspended by the spring of constant *K* and that spring is held by some external frame. So when the vibrations take place, the mass (magnets) moves and its relative motion w.r.t coil placed nearby induces the voltage. Air acts as a damper medium.

The governing equation for power harvesting is presented by William & Yates [43] of a system can be expressed as:

$$P = \frac{m*\xi_\tau*Y^2*(\frac{\omega}{\omega_n})^3*\omega^3}{[1-(\frac{\omega}{\omega_n})^2]^2+[2*\xi\tau*(\frac{\omega}{\omega_n})]^2}$$

When the system works at resonance, we get the maximum output. So it is necessary to design the device with the natural frequency equal to that of the external vibration.

$$P = \frac{m*\xi\tau*Y^2*\omega_n^3}{4*\xi^2}$$

Y = Excitation amplitude

$\omega_n$ = Natural Frequency

$\xi_\tau$ = Total damping in the system comprising of electrical and mechanical damping, expressed in the next portion.

From above equation, we can see that the Power is proportional to the cube of natural frequency and square of excitation amplitude.

**Damping:**

Damping is an important parameter while designing a MEMS device. It is one of the basic parameter that controls the selectiveness of device especially if we want to focus any particular application. Since in the current design, a wideband of frequencies is required, so a high damping factor is necessary. [45] Its effect is considered in the harmonic analysis of design, mentioned in the chapter of Results.

Other widely used methods to increase the bandwidth include the use of multiple array of different magnetic masses of different dimensions [23] and magnetic field tuning methodology [25]. But

the increase of damping method works best, especially when there are plentiful vibrations of multiple frequencies.

Damping is of two types that mainly take place, Parasitic and Electrical damping. Parasitic damping is caused mainly caused by the surrounding medium, air in our case and few of its effect is due to the acceleration. Whereas Electrical Damping is caused due to the internal resistance of the coils.

An important point during designing of a harvester is the matching of resonant frequency of harvester to that of the source of vibration and the maximum possible deflection is desirable to get the maximum rate of change of flux. And thus by varying the electrical impedance of load, we can control the damping and thus adjusting the frequency selectivity of the harvester.

Mechanical damping can be computed by using the formula [126]:

$$C = \frac{\mu * A}{h}$$

And using this value of C in the below equation gives us the mechanical damping:

$$\xi_m = \frac{C}{2 * m * \omega_n}$$

Where ω can also be used in terms of spring constant, K by using:

$$\omega_n = \sqrt{\frac{K}{m}}$$

Electrical Damping is calculated as follows:

$$\xi_e = \frac{(B*l)^2}{2 * m * \omega_n * R}$$

Where,

C = Damping co-efficient

μ = effective viscosity of fluid

A = Shear Area

h = Gap between two surfaces where damping is to be considered

m = mass of device (Calculated in Appendix)

$\omega_n$ = 2*π*f = Natural Frequency in Radians

B = Magnetic Field Strength

l = length of coil

B = Magnetic field strength

R = Resistance of the coil (Calculated in Appendix)

**Rayleigh Damping:**

Also termed as Alpha-Beta damping is a practical damping model and can be estimated from experiments. Also unlike other models, it can be used in both time dependent and frequency dependent (harmonic) analysis. It is used when there are different frequency responses. Since dual mass design approach is used, so in the simulations, Rayleigh damping is taken into account.

Option for Rayleigh damping is found in the structural Mechanics module. In this damping two damping coefficients are mentioned.

Rayleigh Damping = C = αM + βK

α = mass proportional Rayleigh damping coefficient

β = stiffness proportional Rayleigh damping coefficient

M = system structural mass matrix

K = system structural stiffness matrix

NOTE: α & β should be positive

Rayleigh damping coefficients can also be expressed in terms of $f_1$ and $f_2$ as:

$$\alpha = 4*\pi*f_1*f_2 \frac{\xi_1 f_2 - \xi_2 f_1}{f_2^2 - f_1^2}$$

$$\beta = \frac{\xi_2 f_2 - \xi_1 f_1}{\pi(f_2^2 - f_1^2)}$$

α & β = 0.0240757 is used in the simulations and this value was found by using the *Design of Experiment Technique* (DOE), which uses Response Surface Methodology algorithm.

# Appendix C

**Expressions used in COMSOL Multiphysics®:**

| **Expression** | **Description** |
|---|---|
| Nc*intCoilA(mfnc.Bz) | Flux in Coil A (replace A by B,C,D for other coils) |
| fluxA + fluxB + fluxC + fluxD | Single layer flux |
| -d(totalFlux2, TIME) | Total induced voltage |
| comp1.cir.v_4*comp1.cir.C2_i | Power absorbed by load |

- Material Properties used in Comsol for Modal Studies:

| Property/Material | Unit | Nickel | NdFeB |
|---|---|---|---|
| Density | $Kg/m^3$ | 8900 | 7350 |
| Young's Modulus | Pa | $200E^9$ | $10E^{11}$ |
| Poisson's Ratio | 1 | 0.31 | 0.24 |

- Material Properties used for Magnetic Study:

Resistivity of Aluminum used = 2.65[μΩ-cm]

Relative permeability of Air = 1